

The function of a newly identified retinal homeobox-containing gene, *Xenopus RxL* in retinal development

Dissertation

zur Erlangung des akademischen Grades
doctor rerum naturalium (Dr. rer. nat.)

vorgelegt der
Naturwissenschaftlichen Fakultät I
Biowissenschaften
der Martin-Luther-Universität Halle-Wittenberg



von Huiyuan Wu
M.Sc. of Microbial Pharmacy
geb. am 06.04.1973 in Inner Mongolia, P.R.China

Gutachter:

1. Prof. Dr. Thomas Hollemann
2. Prof. Dr. Elmar Wahle
3. Prof. Dr. Michael Kuhl

verteidigt am 29.08.2008

urn:nbn:de:gbv:3-000014661

[<http://nbn-resolving.de/urn/resolver.pl?urn=nbn%3Ade%3Agbv%3A3-000014661>]

To my parents

给我的父母

Table of Contents

Table of Contents	I
List of Figures	V
List of Tables	VI
Abbreviation	VII
Abstract	XI
1 Introduction	1
1.1 <i>Xenopus laevis</i> as model system for developmental biology	1
1.2 Retina- the perception of light	1
1.3 Neural induction - the prelude of eye formation	3
1.4 The early patterning of vertebrate eye	6
1.4.1 The eye field specification in the anterior neural plate	6
1.4.2 The early morphogenesis of the eye	7
1.5 The cell-specification of retina cells	10
1.5.1 The extrinsic cues for retinal cell specification	10
1.5.2 The intrinsic clues for retinal cells specification	11
1.5.3 The intrinsic signals involved in photoreceptor cell specification	12
1.6 <i>Rx</i> genes in eye development	13
1.7 Aim of this thesis	15
2 Materials	16
2.1 The experimental Animal - <i>Xenopus laevis</i>	16
2.2 Bacteria	16
2.3 Chemicals	16
2.4 Buffers, solutions and media	19
2.4.1 Embryos preparation	19
2.4.2 Whole-mount <i>In situ</i> hybridization	20
2.4.3 Vibratome sectioning	21
2.4.4 Mini-preparation of plasmid DNA	21
2.4.5 Gel electrophoresis	22
2.4.6 SDS-polyacrylamide gel electrophoresis (SDS-PAGE)	22
2.4.7 Immunostaining	22
2.4.8 TdT-mediated dUTP digoxigenin nick end-labeling (TUNEL) assay	22
2.4.9 Media	23

2.5	Antibodies	23
2.6	Enzymes	24
2.7	Kits	24
2.8	Oligonucleotides	25
2.8.1	Oligonucleotides for PCR	25
2.8.2	Antisense Morpholino Oligonucleotides (MO)	25
2.8.3	Special delivery morpholino complimentary oligomers (carrier oligomers)	26
2.9	Vectors and Constructs	26
2.9.1	Vectors	26
2.9.2	Constructs	27
2.10	Equipments	29
3	Methods	32
3.1	Genetic methods	32
3.1.1	Construction of Phylogeny of Rx homeoproteins	32
3.1.2	Cloning	32
3.1.3	Preparation of electrocompetent bacteria	34
3.1.4	Electroporation	34
3.1.5	Colony PCR	34
3.1.6	Plasmid preparation	35
3.1.7	Preparation of sequencing samples	35
3.1.8	<i>In vitro</i> synthesis of sense RNAs	36
3.1.9	<i>In vitro</i> synthesis of anti-sense RNAs	36
3.1.10	Extraction of the total RNA from staged embryos	36
3.1.11	Extraction of the total RNA from adult frog tissues	37
3.1.12	Reverse transcriptase-polymerase chain reactions (RT-PCR)	37
3.2	<i>In vitro</i> transcription-translation assay	38
3.3	Handling and manipulation of <i>Xenopus</i> embryos	39
3.3.1	Preparation of embryos from <i>Xenopus laevis</i>	39
3.3.2	Microinjection	39
3.3.3	Lipofection	39
3.4	Analysis Methods	40
3.4.1	Whole-mount <i>in situ</i> hybridization (WMISH)	40
3.4.2	Whole-mount immunostaining of PH3	41
3.4.3	TdT-mediated dUTP digoxigenin nick end-labeling (TUNEL) assay	42
3.4.4	Immunostainig on sections	42
3.5	Histological Methods	43
3.5.1	Vibratome section	43

3.5.2	Cryostat section	43
3.5.3	Plastic section	44
4	Results	45
4.1	Cloning of a novel retina homeobox-containing gene from <i>Xenopus laevis</i> , <i>XRxL</i>	45
4.2	<i>XRxL</i> belongs to the “vertebrate Rx-Like” subgroup of the <i>Rx</i> genes	47
4.3	Temporal and spatial expression of <i>XRxL</i>	50
4.4	<i>XRxL</i> -specific morpholinos inhibit the translation of endogenous <i>XRxL</i> <i>in vitro</i>	51
4.5	Specific inactivation of <i>XRxL</i> function impairs photoreceptor formation	52
4.6	Suppression of <i>XRxL</i> function does not affect the initiation of eye formation	54
4.7	Suppression of <i>XRxL</i> led to reduced expression of photoreceptor markers	56
4.8	RxL-MO microinjection causes apoptosis in the eye area	58
4.9	The temporally inducible <i>RxL</i> construct, <i>RxL-GR</i>	60
4.10	Retina progenitor cells are not competent to <i>XRxL</i> until late neurular stage	61
4.11	<i>XRxL</i> overexpression induces additional photoreceptor formation	63
4.12	<i>XRxL</i> overexpression did not affect the proliferation of overall retinal progenitor cells	64
4.13	<i>XRxL</i> functions as a transcriptional activator	67
4.14	OAR domain does not function as the activation domain of <i>XRxL</i>	69
4.15	Targeted overexpression of <i>XRxL</i> in retinal progenitor cells biased the photoreceptor fate	71
4.16	RxL-VP16 and RxL-ΔOAR also promote photoreceptor cell fate	72
4.17	Targeted repression of <i>XRxL</i> function in RPC inhibits photoreceptor fate	73
4.18	<i>XRxL</i> lipofected photoreceptors are both rods and cones	74
5	Discussion	76
5.1	<i>Xenopus RxL</i> is a new member of the group of vertebrate “ <i>Rx-like</i> ” genes	76
5.1.1	Vertebrate <i>Rx</i> genes of different groups are expressed in different patterns	76
5.1.2	Vertebrate <i>Rx</i> genes of different groups play different roles in eye development	77
5.1.3	The “ <i>Rx-Q50</i> ” group genes might be orthologs of the “ <i>Rx-like</i> ” group genes	78
5.1.4	The invertebrate <i>Rx</i> genes	79
5.2	<i>XRxL</i> directs the retinal cell fate determination	80
5.2.1	<i>XRxL</i> may cooperate with the cell cycle mechanism to coordinate retinal cell fate determination	80
5.2.2	<i>XRxL</i> is involved in the cell fate determination at very early stage	82

5.2.3	<i>XRxL</i> promotes both rod and cone fates	82
5.3	<i>XRxL</i> functions as a transcriptional activator	83
5.4	The role of <i>XRxL</i> in the cascade of regulating photoreceptor cell specification	85
5.4.1	<i>XRxL</i> acts downstream <i>XRx1</i> during eye development	85
5.4.2	<i>XRxL</i> may cooperate with <i>Otx</i> family members during the photoreceptor differentiation	85
5.4.3	<i>XRxL</i> and NeuroD may reside in the same pathway to generate photoreceptor cells	86
5.4.4	Other genes specifically promoting the rod photoreceptor cell fate	87
5.5	Photoreceptor degeneration and <i>XRxL</i>	88
6	Summary	89
7	Bibliography	91
8	Appendix	105
	Acknowledgments	106
	Affidavit	
	Curriculum Vitae	
	List of Publications	

List of Figures

Figure 1.1 The organization of the vertebrate retina.	2
Figure 1.2 Model of the mechanism by which the Dishevelled protein stabilizes β -catenin in the dorsal proportion of the amphibian eggs.	3
Figure 1.3 Model of the coordination of transcription factors in eye field induction.	7
Figure 1.4 Schematic overview of vertebrate eye development.	9
Figure 1.5 Genetic conservation and divergence of retinal development between <i>Drosophila</i> and vertebrates.	14
Figure 2.1 pGEM-T Vector circle map.	26
Figure 2.2 pCS2+ vector graphic map.	27
Figure 4.1 The newly identified member of vertebrate <i>Rx</i> gene family, <i>Xenopus RxL</i> .	47
Figure 4.2 Amino acid sequences alignment of conserved domains of predicted <i>Rx</i> proteins.	48
Figure 4.3 The phylogenic cycle of the all known <i>Rx/Rax</i> homeoproteins.	49
Figure 4.4 The temporal and spatial expression of <i>RxL</i> during development of <i>Xenopus laevis</i> .	50
Figure 4.5 Expression level of <i>RxL</i> in the embryonic stages and the adult tissues of <i>Xenopus laevis</i> .	51
Figure 4.6 <i>RxL</i> -MOs specifically inhibited the translation of endogenous <i>RxL</i> <i>in vitro</i> .	52
Figure 4.7 Interference of photoreceptor formation caused by microinjection of <i>RxL</i> -MOs.	53
Figure 4.8 Effects of <i>RxL</i> loss-of-function on early eye development in <i>Xenopus laevis</i> .	55
Figure 4.9 <i>RxL</i> -MO microinjection led to reduced expression areas of the early-expressed eye marker genes at tadpole stage.	56
Figure 4.10 Effects of <i>RxL</i> -MO microinjection on the expression of retinal differentiation marker genes.	57
Figure 4.11 <i>RxL</i> -MO microinjection inhibited the cell proliferation specifically in the eye area.	59

Figure 4.12 Increased apoptotic retinal cells caused by suppression of <i>XRxL</i> function.	60
Figure 4.13 Schematic diagrams of the structure and working mechanism of inducible RxL-GR.	61
Figure 4.14 Effect of <i>RxL</i> gain-of-function on early eye development in <i>Xenopus laevis</i> .	62
Figure 4.15 Additional photoreceptor formation induced by <i>XRxL</i> overexpression.	64
Figure 4.16 Slightly increased cells proliferation at tadpole stage caused by <i>RxL</i> gain-of-function.	65
Figure 4.17 RxL-GR activation caused slightly increased number of apoptotic cells in retinas.	66
Figure 4.18 Microinjection of <i>RxL-VP16</i> , instead of <i>RxL-EngR</i> , induced an eye phenotype similar to that of overexpression of wild-type <i>RxL</i> .	68
Figure 4.19 Effects of microinjection of <i>RxL-VP16</i> and <i>RxL-EngR</i> on the expression of photoreceptor-specific gene <i>Rho</i> .	69
Figure 4.20 Microinjection of <i>RxL-ΔOAR</i> led to an eye phenotype similar to that caused by microinjection of wild-type <i>RxL</i> .	70
Figure 4.21 Microinjection of <i>RxL-ΔOAR</i> RNA caused additional expression of <i>Rho</i> in the INL.	70
Figure 4.22 Schematic diagram of the procedure to analyze the lipofected retinas.	71
Figure 4.23 Overexpression of wild-type <i>RxL</i> , <i>RxL-VP16</i> and <i>RxL-ΔOAR</i> in retinoblasts increased the proportion of photoreceptors.	72
Figure 4.24 Lipofection of RxL-MO in retinoblasts decreased the proportion of photoreceptors.	74
Figure 4.25 Lipofection of <i>RxL-VP16</i> in retinoblasts increased the proportion of rods at the expense of cone photoreceptor cells.	75

List of Tables

Table 4.1 Quantification of eye phenotypes upon microinjection of RxL-MOs	53
Table 8.1 The Genbank accession numbers of nucleotide sequences of all known Rx-type gene from different species	105

Abbreviation

Amino acids

A	Alanine
C	Cysteine
D	Aspartic acid
E	Glutamate
F	Phenylalanine
G	Glycine
H	Histidine
I	Isoleucine
K	Lysine
L	Leucine
M	Methionine
N	Asparagine
P	Proline
Q	Glutamine
R	Arginine
S	Serine
T	Threonine
V	Valine
W	Tryptophan
Y	Tyrosine
aa	amino acid
Amp	ampicillin
AP	alkaline phosphatase
APB	alkaline phosphatase buffer
A-P	anterior-posterior
<i>Arr</i>	<i>Arrestin</i>
ash	achaete scute homologue
ath	atonal homologue

BCIP	5-Bromo-4-chloro-3-indolyl-phosphate
BCNE center	blastula Chordin and Noggin expression center
bHLH	basic helix-loop-helix
BMB	Boehringer blocking reagent
BMP	bone morphogenetic protein
BSA	Bovine Serum Albumin
cDNA	complementary DNA
CHAPS	3-(3-cholamidopropyl)dimethylammonio-1-Propansulphate
CMZ	ciliary marginal zone
CNS	central nervous system
CNTF	ciliary neurotropic factor
cRax	chicken Rax
cyc	cyclops
DAPI	4',6'-Diamidin-2'-phenylindol-dihydrochloride
°C	degree centigrade
DEPC	diethylpyrocarbonate
Dex	dexamethasone
dH ₂ O	distilled water
ddH ₂ O	double distilled water
Dig	Digoxigenin
Dkk	Dickkopf
DMF	Dimethyl formamide
DMSO	dimethyl sulfoxide
DNA	deoxyribonucleic acid
Dsh	Dishevelled
DTT	dithiothreitol
D-V	dorsal-ventral
<i>E.coli</i>	<i>Escherichia coli</i>
EDTA	Ethylenediaminetetraacetic acid
EFTFs	eye field transcription factors
FGF	fibroblast growth factors
FGFR	FGF receptor
EGTA	Ethylene glycol-bis(2-amino-ethylether-N,N,N',N')-tetra-acetic acid
e.g.	exempli gratia

EngR	the repressor domain of <i>Drosophila engrailed</i>
et al.	et alii
GCL	ganglion cell layer
GR	glucocorticoid receptor
h	hours
HEPES	4-(2-Hydroxyethyl)-1-piperazin
Hh	hedgehog
HCG	human chorionic gonadotropin
i.e.	id est
INL	inner nuclear layer
kb	kilobase
l	liter
L	liter
LB	Luria-Bertani
LIF	leukaemia inhibitory factor
m	milli
μ	micro
M	molar (mol/l)
MAB	maleic acid buffer
MBS	Modified Barth's Saline
MEM	MOPS/EGTA/magnesium sulfate
MEMFA	MOPS/EGTA/magnesium sulfate/formaldehyde
min	minutes
MO	antisense morpholino oligonucleotides
MOPS	4-morpholinopropanosulfonic acid
NBT	Nitro blue tetrazolium chloride
n	nano
<i>n</i>	number
Ngn	neurogenin
NR	neural retina
OD	optical density
ONL	outer nuclear layer
ORF	open reading frame
OS	optic stalk

p	pico
PBS	phosphate-buffered saline
%	percent
PVP	polyvinylpyrrolidone
RA	retinoic acid
PAGE	polyacrylamide gel electrophoresis
RGC	retinal ganglion cell
<i>Rho</i>	<i>Rhodopsin</i>
RNA	ribonucleic acid
RPC	retinal progenitor cell
RSC	retinal stem cells
RPE	retinal pigmented epithelium
RT-PCR	reverse transcriptase-polymerase chain reaction
Rx	retinal homeobox
s.e.m.	standard error of the mean
sec	seconds
SDS	sodium dodecyl sulfate
sFRPs	secreted Frizzled-related proteins
Shh	sonic hedgehog
SSC	standard saline citrate buffer
st.	stage
TdT	terminal deoxynucleotidyl transferase
Tet	tetracycline
TGF	transforming growth factor
TUNEL	TdT-mediated dUTP digoxigenin nick end-labeling
twhh	triggy-winkle hedgehog
U	unit
vs.	versus
v/v	volume per volume
WMISH	whole-mount in situ hybridization
XBF2	<i>Xenopus</i> brain factor 2
Xfz3	<i>Xenopus</i> Frizzled 3
zRx	zebrafish Rx

Abstract

Members of the *Rx* (retinal homeobox) gene family play vital roles during eye development in vertebrates. In this thesis, a new *Rx*-type gene, *XRxL*, was identified from *Xenopus*. According to a phylogenetic analysis, all-known *Rx*-type genes could be grouped into four categories, including the “invertebrate *Rx*” group, which contains all *Rx* genes from invertebrates, the “classical vertebrate *Rx*” group, the “vertebrate *Rx-Q50*” group, and the “vertebrate *Rx-like*” group to which *XRxL* belongs.

The earliest expression of *XRxL* can be detected in the presumptive eye area at late neurula stage by WMISH. Suppression of *XRxL* function *in vivo* by microinjection of *RxL*-specific antisense morpholino oligonucleotides impaired the formation of the photoreceptor layer and reduced the expression of photoreceptor specific genes. Overexpression of *XRxL* induced ectopic expression of photoreceptor specific genes, but did not promote the proliferation of retinal progenitor cells significantly. Targeted overexpression of *XRxL* in developing retinoblasts *in vivo* led to the increased fraction of photoreceptor cells at the expense of amacrine and bipolar cells. Moreover, *XRxL* was found to promote both rod and cone photoreceptors, with a preference for rods. Our *in vivo* experiments also revealed that *XRxL* acts as a transcription activator.

Taken together, *XRxL*, unlike *XRxI*, is required for the determination of retinal cell types, especially photoreceptor cells, rather than to promote the proliferation of retinal progenitor cells.

1 Introduction

1.1 *Xenopus laevis* as model system for developmental biology

The South African clawed frog, *Xenopus laevis* has long been a favorite organism for studying development because of its large egg size, external development, and ability of the embryos to easily heal after microsurgery. Many mysteries of vertebrate development have been uncovered by using this organism with classical experimental approaches, such as fate mapping, transplantation experiments and explant cultures. In recent decades, molecular biology methods were also applied to investigate the vertebrate development with this model organism, so that the mechanism of many important embryogenic events could be further pursued on the molecular level. With *Xenopus* embryos, gain-of-function experiments can be quickly and easily performed by microinjection of *in vitro* synthesized RNA, DNA or proteins as early as immediately after fertilization. Inhibition of certain gene function can be achieved by injecting antisense morpholino oligonucleotides (MOs) or dominant negative constructs. In the case of extracellularly expressed proteins, their functions could also be silenced by injection of antibodies into the blastocoel cavity. Animal cap explants resemble mammalian embryonic stem cells with respect to their pluripotency. They can give rise to derivatives of all three germ layers *in vitro*, when exposed to appropriate signaling factors, and thereby provide a strong tool to study the molecular basis of embryonic induction and cell lineage specification. Lipofection of the gene-expression plasmids in specific precursor cells makes it possible to trace the effects of these genes on cell fate specification. Moreover, transgenic frogs could also be massively generated by restriction endonuclease-mediated integration (REMI) of DNA into demembrated sperm nuclei, followed by transplantation of the nuclei into unfertilized eggs (Kroll and Amaya, 1996), or by coinjection of DNA and *ISceI* Meganuclease in fertilized eggs (Pan et al., 2006a).

1.2 Retina- the perception of light

Vision is probably the most important sense for many vertebrates. It initiates from the reception of various wavelengths of light by photoreceptor cells lining the back of retina. The signal of light is converted into a biochemical signal, relayed through interneurons (i.e. horizontal, bipolar and amacrine cells) and then activates retinal ganglion cells, whose axons are bundled together to form the optic nerve (Figure 1.1). The optic nerve connects the retina and a region of the brain

called the optic tectum (in amphibians and birds) or the lateral geniculate nucleus (in mammals), leading to the formation of images in the brain.

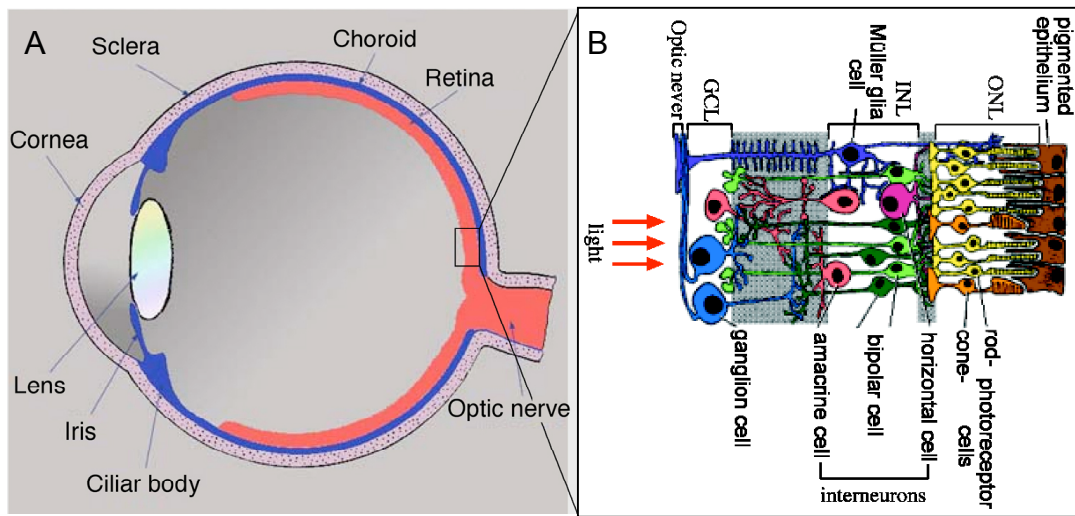


Figure 1.1 The organization of the vertebrate retina. (A) Schematic drawing of the anatomy of the vertebrate camera eye. (B) The insight view of the organization of the retina. Photoreceptors convert light signals to biochemical signals, which are relayed through interneurons and reach the ganglion cell. GCL, ganglion cell layer; INL, inner nuclear layer; ONL, outer nuclear layer. (After Ashery-Padan et al, 2001).

The prevalence of retinal diseases involving loss of retinal cells following congenital defects, traumatic and degenerative damage has inspired researches in potential regenerative therapies (Otani et al., 2004; Smith, 2004). The strategy has been that a full understanding of developmental mechanisms underlying retinal development will lead to methods for manipulating various stem cell types to repair tissue structure and replace lost function. During the past decades, intense studies have addressed to the mechanism of retinal morphogenesis and cell-fate specification.

The retina of *Xenopus laevis* represents an excellent model in these studies due to the high accessibility of the externally developing embryos, rapid eye formation and relative ease in the introduction of foreign genes by microinjection or lipofection. On the other hand, the retina is also a good model for studying cell fate determination and differentiation in the central nervous system (CNS), since it evaginates directly from the neural tube and forms a relatively simple structure with a limited number of neuronal cell types organized in a stereotypical laminar pattern.

1.3 Neural induction - the prelude of eye formation

Since the eye is a highly specialized derivative of the CNS, eye development is closely associated with neural induction, although the first morphological sign of eye formation, the evagination of the developing forebrain, occurs much later. In 1963, studies on explanted presumptive neuroectoderm from frog blastulas showed that these explants underwent neural induction in the absence of mesoderm and endoderm and gave rise to anterior brain, olfactory placodes and eye structures (Nieuwkoop, 1963). The molecular basis of neural induction was gradually uncovered by recent works, which revealed that the initiation of neural induction has been triggered during fertilization, which determines the dorsal-ventral (D-V) polarity of the embryo (Gilbert, 2003).

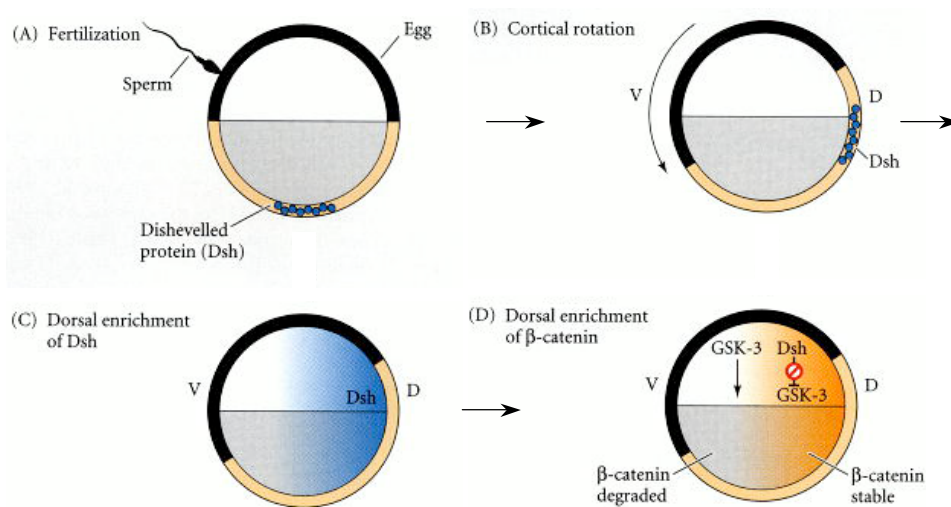


Figure 1.2 Model of the mechanism by which the Dishevelled protein stabilizes β -catenin in the dorsal proportion of the amphibian eggs. (A) Dishevelled protein (Dsh) arrested by other proteins are localized at the vegetal pole of the unfertilized egg. (B) Upon fertilization, Dsh proteins are translocated dorsally due to the cortical rotation. (C) Dsh is released from its vesicles and is distributed in the further dorsal side in the 1-cell embryo. (D) Dsh binds to and blocks the action of GSK-3, thereby preventing the degradation of β -catenin on the dorsal side of the embryo, leading to the enrichment of β -catenin at the dorsal side. V, ventral; D, dorsal. (After Gilbert, 2003).

The cortical rotation caused by the entry of the sperm into the egg translocates Dishevelled protein (Dsh) from the vegetal cortex of the unfertilized egg to the presumptive dorsal side of the embryo (Miller et al., 1999). The released Dsh protein binds to and blocks the action of GSK-3 (glycogen synthase kinase 3), which degrades β -catenin, leading to the accumulation of nuclear β -catenin in the dorsal side and provides the earliest D-V asymmetry (Figure 1.2) (Schneider et

al., 1996; Schohl and Fagotto, 2002). This early β -catenin signal triggers the formation of two signaling centers of the blastula: one is the Nieuwkoop center, involved in dorsal endoderm development, and another is the BCNE center (blastula Chordin and Noggin expression center), involved in neural specification (De Robertis and Kuroda, 2004). The β -catenin signal induces the expression of secreted BMP (bone morphogenetic protein) antagonists such as Chordin and Noggin in cells located in the BCNE center (Wessely et al., 2001). At gastrula stage, the dorsal lip forms opposite to the sperm entry point, known as Spemann-Mangold Organizer continuously expresses Chordin and Noggin as well as other BMP antagonists, like Follistatin and ADMP (anti dorsalizing morphogenetic protein). It has been demonstrated that Noggin, Chordin and Follistatin each prevents BMP2/4 from binding to their respective receptors in the ectoderm and mesoderm near the organizer (Iemura et al., 1998; Piccolo et al., 1996; Zimmerman et al., 1996). All ectodermal cells, which receive this signal, will give rise to forebrain, most of mid- and hindbrain, and floor plate, while mesodermal cells will give rise to notochord during later development (Kuroda et al., 2004). The inhibition of BMP-signaling by the organizer therefore provides the force for ectodermal cells to maintain their “default” fate of neuron and blocks the induction of epidermis promoted by secreted BMPs (Hemmati-Brivanlou and Melton, 1994).

Dsh is a component of the canonical Wnt signaling pathway (Gilbert, 2003). Its translocation caused by the entry of sperm indicates that Wnt signaling might be involved in the D-V patterning earlier than BMP signaling. *Wnt11* mRNA seems to be the most likely candidate for this dorsal determinant (Heasman, 2006). *Wnt11* mRNA localizes to the vegetal cortex during oogenesis (Ku and Melton, 1993) and becomes more abundant on the ventral side compared to the dorsal side at the 32-cell stage (Tao et al., 2005). Loss-of-function experiments showed that maternal *Wnt11* is necessary and sufficient for specification of embryonic D-V axis (Tao et al., 2005). However, at late blastula stages, Wnt signaling eventually suppresses the generation of neural cells (for review see Logan and Nusse, 2004). Injection of the *Wnt8* inhibitor *cerberus* mRNA into a vegetal ventral *Xenopus* blastomere at the 32-cell stage led to the formation of ectopic head structure (Bouwmeester et al., 1996), and the simultaneous repression of BMP and canonical Wnt signals in *Xenopus* also led to head induction (Glinka et al., 1997). Glinka and colleagues therefore proposed a two-inhibitor model for regional specific induction with anti-BMPs alone inducing trunk structure and anti-BMPs together with anti-Wnts inducing heads (Glinka et al., 1997). Cerberus was later found to be a triple antagonist for BMPs, Nodal-related proteins and *Wnt8* (Piccolo et al., 1999). Two other proteins, Frzb and Dkk (Dickkopf) were discovered to be expressed in the involuting endoderm and prevent Wnt signaling (Glinka et al., 1998; Wang et al., 1997). More recently, a screen for cDNAs encoding secreted proteins in

Xenopus gastrula resulted in a surprising 24% isolates encoding sFRPs (secreted Frizzled-related proteins), which constitute a large family of Wnt antagonists that bind Wnt proteins in the extracellular space and prevent them from signaling (De Robertis and Kuroda, 2004).

Fibroblast growth factors (FGFs) appear to be critical for cells to respond to Wnt signaling (Domingos et al., 2001). In addition, it has been also recently found that the dissociation of animal cap cells actually activates FGF signaling and inhibits the BMP signal transducer Smad1 by MAP kinase phosphorylation of its inhibitory sites (Kuroda et al., 2005). This challenges the idea that there is no specific signal activating neural fate and neural fate is a kind of “default fate” of “naïve” ectodermal cells. Proneural roles of FGF were further demonstrated by *in vivo* studies, which revealed that the proneural genes *Sox2* and neural cell-adhesion molecule (*Ncam*) expression both depend on low level of FGF signaling at the blastula stage, but is independent of BMP antagonists (Delaune et al., 2005).

Besides, retinoic acid (RA) has been found to form a gradient with the highest levels at the posterior end of the neural plate (Gilbert, 2003). Along with FGFs and Wnts, RA simultaneously induces neurogenesis and sets up the anteroposterior pattern of the CNS. Afterwards, RA up-regulates a series of posterior genes like *Krox20*, *En*, *Wnt1*, *Pax2* and *Hox* genes, as well as down-regulates a set of anterior genes such as *Otx2*, *XAG-1*, *Emx1/2* and *XINK-2*, thereby generating the basis for patterning the posterior hindbrain and anterior spinal cord (reviewed by Maden, 2002).

Thus, the signals discussed above induce the dorsal ectodermal cells to choose the neural fate instead of epidermal fate. Other genes are required to transform the ectoderm into neural tissue. *Neurogenin* (*Ngn*) is expressed in ectoderm in the absence of BMP signals and appears to be the key protein involved in activating the neural differentiation (Ma et al., 1996). Neurogenin subsequently activates the gene for NeuroD, another basic helix-loop-helix (bHLH) protein, which further activates the genes for structural neural-specific proteins (Lee et al., 1995). In addition, Noggin and Cerberus can induce the transcription factor XBF2 (*Xenopus* brain factor 2) that converts ectoderm into neural tissue (Mariani and Harland, 1998), and Goosecoid, a transcription factor involved in organizer function, activates *Otx2*, a gene that is critical for brain formation (Blitz and Cho, 1995). Thus, the neural plate is formed upon the coordination of these determinants. However, the derivation of eyes from the anterior neural plate involves more complex mechanisms and interactions, in which these signaling factors repeatedly play roles during the whole process of eye development (Yang, 2004).

1.4 The early patterning of vertebrate eye

Neuralized ectodermal explants (animal caps) of *Xenopus* embryos at blastula stage give rise to anterior neural structures including eyes. Since inductive influences of mesoderm and endoderm are absent in this context, these results demonstrated that the molecular mechanisms directing retinal specification must be downstream or parallel to neural induction and be an inherent feature of the developing the anterior neural plate (Chow and Lang, 2001). Several transcription factors that pattern the anterior neural plate such as Pax6, Rx1, Six3 and Hesx1 are essential for the initiation of eye development. However, the precise molecular mechanisms that control their expression are not well understood. There is evidence that Wnt signals may trigger the expression of these factors, since the misexpression of a Wnt receptor, *Frizzled3* (*Xfz3*) results in the ectopic expression of *Pax6*, *Rx* and *Otx2* and leads to ectopic eye formation (Rasmussen et al., 2001). More recently, it was demonstrated that Wnt4 is required for early eye development, acting through the β -catenin-independent, noncanonical pathway (Maurus et al., 2005).

The early eye development in vertebrates can be divided into a series of four steps according to the temporal sequence: (i) induction: eye field specification within the anterior neural plate, (ii) splitting: generation of two eye primordia from a single eye field, (iii) specification: retinal genesis from optic vesicle to optic cup, and (iv) lens induction.

1.4.1 The eye field specification in the anterior neural plate

Accumulating evidence shows that the specification of the eye anlagen from the anterior neural plate requires a set of transcription factors which have been summarized as eye field transcription factors (EFTFs). These EFTFs, including ET, Rx1 (Rax in mouse), Pax6, Six3, Lhx2, tll and Optx2 (also known as Six6), are essential for eye formation. The targeted or spontaneous mutation of *Pax6*, *Rx1*, *Lhx2*, *Tll*, *Six3* or *Six6* in mouse led to abnormal or no eyes in the respective animals (Hill et al., 1991; Lagutin et al., 2003; Li et al., 2002; Mathers et al., 1997; Porter et al., 1997; Tucker et al., 2001; Yu et al., 2000). These EFTFs are not only necessary, but in some contexts are also sufficient for eye formation. Overexpression of *Pax6*, *Six3*, *Rx1* and *Optx2* homologs can expand or induce eye tissues in the nervous system of vertebrates (Andreazzoli et al., 1999; Bernier et al., 2000; Chow et al., 1999; Chuang and Raymond, 2001; Loosli et al., 1999; Oliver et al., 1996; Zuber et al., 1999). Moreover, microinjection of a cocktail of *Otx2*, *Pax6*, *Rx1*, *ET*, *Six3*, *tll* and *Optx2* RNAs into one blastomere of two-cell stage *Xenopus* embryos generates secondary eye fields and ectopic eyes outside the nervous system (Zuber et al., 2003). The same study also shows that *Otx2*, *via* the inhibition of Noggin, induced the earliest expressed EFTF, *ET*. This observation challenged the idea that *Otx2* does not participate in early

eye specification (Chow and Lang, 2001), but demonstrated that *Otx2* provides an environment that primes the anterior neuroectoderm for eye field formation.

Although *Otx2* expression is eventually restricted to the anterior end of the embryo as gastrulation proceeds, double *in situ* hybridization analysis in *Xenopus* shows that *Otx2* transcripts are not present within the eye field as defined by *Rx1* expression at the beginning of neurulation (Andreazzoli et al., 1999; Zuber et al., 2003). The overlapping and dynamic expression patterns of EFTFs specify the eye anlagen in the anterior neural plate, and also indicate the coordinated function of these factors. Induction experiments in animal caps further revealed the circuitry of the EFTF network, in which *ET*, positioned at the front of the circuit induces the expression of *Rx1*, *Lhx2* and *tll* (Figure 1.3). In this model, *Rx1* functions upstream *Pax6*, *Six3* and *Lhx2*, which is consistent with the results from studies on *Rx1*^{-/-}, *Pax6*^{-/-}, *Lhx2*^{-/-} and *Six3*^{-/-} mice (Bernier et al., 2000; Grindley et al., 1995; Lagutin et al., 2003; Porter et al., 1997; Zhang et al., 2000).

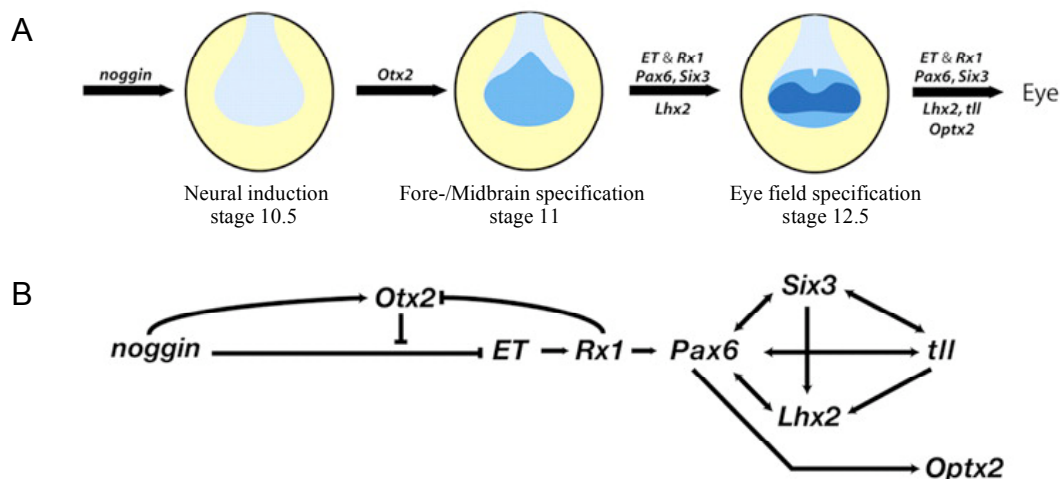


Figure 1.3 Model of the coordination of transcription factors in eye field induction. (A) Schematic diagram showing that *noggin* is involved in the specification of the neural plate (light blue), within which *Otx2* expression demarcates the presumptive fore-/midbrain area (blue). While *ET* and *Rx1* repress the expression of *Otx2*, and along with *Pax6*, *Six3* and *Lhx2* induce the specification of the eye field (dark blue). *Optx2* and *tll* are involved in the eye development after the initiation of the eye field. (B) Schematic drawing of the network of factors leading to the specification of eye field from the anterior neural plate. (After Zuber et al., 2003).

1.4.2 The early morphogenesis of the eye

After induction of the eye field from the anterior neural plate, the EFTFs are continuously essential for the morphogenesis of the eye. One of the main functions of the EFTFs is to maintain cells of the eye anlage in a proliferative state, so that these cells continue to produce additional

cells, which is one precondition for eye morphogenesis. In addition, the product of the *cyc* (*cyclops*) gene, which is expressed in prechordal mesoderm, triggers Hedgehog (Hh) signaling during neurulation. This leads to a suppression of *Pax6* and *ET* expression in the anterior ectodermal midline, the future ventral forebrain. The suppression results in the formation of two distinct domains that demarcate the prospective eyes (Chow and Lang, 2001). The folding of this ectodermal sheet and the migration of cells within this sheet gives rise to the formation of optic vesicles on both sides of the ventral diencephalon, leading to the first morphological sign of eye development (Figure 1.4 A). At this stage, the molecular bias already exists in these cells along the dorsal-ventral (D-V) and anterior-posterior (A-P) axes, thus harbours the molecular plan to establish the future D-V and A-P polarity of the eye. *Pax2*, which is promoted by Hh signals derived from the anterior ventral midline (Ekker et al., 1995; Hammerschmidt et al., 1996; Macdonald et al., 1995), is expressed in the ventral optic vesicle and suppresses dorsally localized *Pax6*. Actually, the boundary between presumptive optic stalk and neural retina in the optical vesicle results from the reciprocal transcriptional repression between *Pax6* and *Pax2* (Schwarz et al., 2000). At the same time, the winged-helix transcription factors *BF-1/Foxg1* and *BF-2/Foxd2* are restricted to the anterior half and the posterior half of the optic vesicle respectively, and probably regulate each other in the same manner as *Pax2* and *Pax6* (Hatini et al., 1994; Huh et al., 1999).

The subsequent close contact between the optic vesicle and the overlying surface ectoderm (lens placode) is required for both neural retina and lens development (Figure 1.4B). It has been shown that neural retina would not develop if the surface ectoderm was removed (Chow and Lang, 2001). FGF was demonstrated to function as one of the neural retina inducing factors emanating from the surface ectoderm, because neural retina development can be rescued in optic vesicle explants cultured without overlying surface ectoderm by the exogenous supplement of FGF signals (Hyer et al., 1998; Nguyen and Arnheiter, 2000). Moreover, *Lhx2* plays an essential role in the transition of optic vesicle to optic cup (Porter et al., 1997), and *Chx10*, whose expression occurs in response to inductive signals from presumptive lens ectoderm, appears to regulate cell proliferation of the neural retina at these stages (Burmeister et al., 1996; Nguyen and Arnheiter, 2000). As soon as the optic cup is formed, *BMP4* is expressed in the dorsal retina and promotes *Tbx5* activity, which in turn suppresses the expression of *Vax1/2* and *Pax2* so that they are restricted to the ventral retina, and thereby reinforces the D-V axial pattern in the developing eye (Koshiba-Takeuchi et al., 2000; Zhang and Yang, 2001). In addition, RA and FGF signals account for the D-V pattern formation of the eye. RA is more abundant in the ventral retina than in the dorsal retina, suggesting that high RA levels may specify a ventral character in the eye

(Dräger et al., 2001). In addition, activation of FGF signaling has a strong ventralizing effect on the *Xenopus* eye (Lupo et al., 2005).

The interaction between the optic vesicle and surface ectoderm triggers a complex cascade leading to lens specification, in which *Pax6* is required cell-autonomously at the onset of lens development. The subsequent involvement of BMP and FGF signals helps to maintain *Pax6* expression in the lens placode, which is essential to activate *Six3* and *FoxE3* expression in the surface epithelium and thereby to regulate the proliferation and differentiation of lens cells. *Pax6* also lies upstream of *Prox1* and *Sox2*, which later play roles in lens fibre cell differentiation (reviewed by Chow and Lang, 2001).

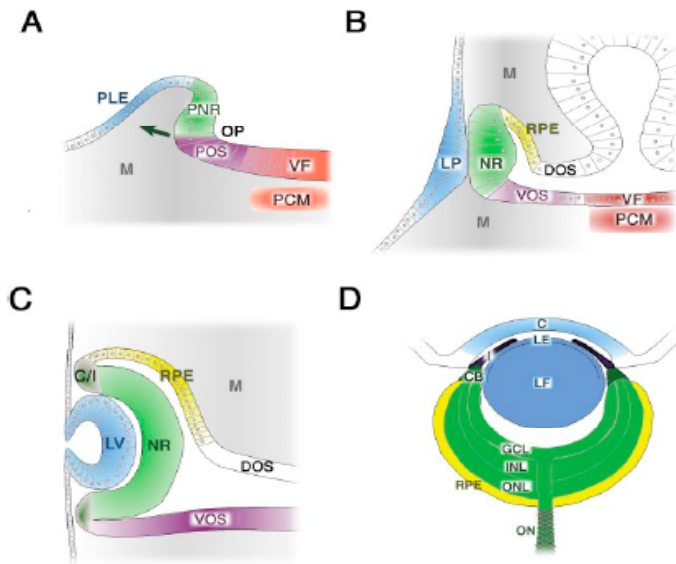


Figure 1.4 Schematic overview of vertebrate eye development. (A) The evagination (indicated by arrow) of the optic vesicles from the ventral diencephalon results in the formation of the optic pits on each side of the embryo (OP). The optic vesicle region can be divided into dorso-distal region (green), which contains the prospective neural retina (PNR) and retinal pigmented epithelium (RPE, not shown), and the proximo-ventral region, which gives rise to the

presumptive ventral optic stalk (POS); PLE, presumptive lens ectoderm; M, mesenchyme; VF, ventral forebrain; PCM, prechordal mesoderm. (B) Continued growth of the optic vesicle leads to the close contact between the lens placode (LP) and the prospective neural retina (NR), which induces the important inductive signals exchanging between each other: RPE, presumptive retinal pigmented epithelium; VOS, ventral optic stalk; DOS, dorsal optic stalk. (C) Invagination of the optic vesicle results in formation of the lens vesicle (LV) and neural retina (NR) and establishes the overall structure of the eye. The point at which the neural retina and RPE meet gives rise to components of the ciliary body and iris (C/I). (D) Mature eye: C, cornea; LE, lens epithelium; LF, lens fiber cells; I, iris; CB, ciliary body; GCL, ganglion cell layer; INL, inner nuclear layer; ONL, outer nuclear layer; ON, optic nerve; (After Chow and Lang, 2001).

The invagination of optic vesicle results in the formation of a bilayered optic cup, which houses the lens vesicle. The inner layer of the optic cup will give rise to the neural retina (NR) and the outer layer will form the retinal-pigmented epithelium (RPE). The extension of this bilayered structure along the lateral-midline axis at the ventral extremity forms the optic stalk (OS). Thus, the overall structure of the eye is established by now (Figure 1.4C). The so-called ciliary marginal zone (CMZ), a special area localized in the most periphery of NR, is worth to mention, where retinal stem cells reside through the entire life of the frog (Amato et al., 2004; Harris and Perron, 1998).

1.5 The cell-specification of retina cells

The vertebrate retina acts as a signal transducer, converting absorbed photons into neural signals by an exquisite cooperation of basically six neuronal cell types and of one type of glial cell, which are all localized in neural retina (NR). These seven types of retinal cells assemble the clear lamination of retina, with ganglion cells located in the inner-most ganglion cell layer (GCL), bipolar, horizontal and amacrine interneurons together with Müller glia in the inner nuclear layer (INL), and cone and rod photoreceptors in the outer nuclear layer (ONL) (Figure 1.1B, Figure 1.4D). All these seven types of retinal cells are generated from a common population of multipotent retinal progenitor cells (RPCs) residing in the optic cup. The differentiation of these retinal cells is initiated in the central part of the optic cup's inner layer and progresses concentrically in a wave-like fashion from the center toward the peripheral edges of the retina (Hu and Easter, 1999; Prada et al., 1991). The different types of retinal cells are generated in an order conserved in many vertebrate species, with ganglion cells and horizontal cells first, followed in overlapping phases by cone-photoreceptor, amacrine cells, rod photoreceptors, bipolar cells, and finally, Müller glia (reviewed by Cepko et al., 1996; Harris, 1997; Marquardt and Gruss, 2002; Young, 1985). A widely accepted model suggests that RPCs pass through an intricate schedule of fate determination, which makes RPCs sequentially generate different cell types under the influence of extrinsic signals (Livesey and Cepko, 2001).

1.5.1 The extrinsic cues for retinal cell specification

Several secreted factors are implicated in guiding RPCs towards different cell fates. For instance, Shh (Sonic hedgehog) molecules, secreted by the first postmitotic retinal neurons, retinal ganglion cells (RGCs), provide a neurogenic wave spreading from the central retina towards the peripheral retina, which drives retinal cell differentiation. Behind the wave front, an increasing number of RGCs differentiate and in turn begin to express Shh, which serves as a feedback signal

modulating the further production of RGCs from the same progenitor pool (McCabe et al., 1999; Zhang and Yang, 2001). In addition, the application of the TGF β family member, Activin A in a rat E18 retinal culture increased the number of rod photoreceptor cells (Davis et al., 2000). Zebrafish embryos treated with RA showed precocious development of rod photoreceptors, while cone photoreceptor maturation was inhibited (Hyatt et al., 1996). Moreover, members of the ciliary neurotrophic factor (CNTF)/leukaemia inhibitory factor (LIF) family can drive cells, which normally would fate to rods, to express features of the bipolar neuron phenotype and fail to express rod markers (Ezzeddine et al., 1997). However, heterochronic transplantation has shown that early and late retinal progenitor cells have distinct differentiation capacities when placed in a similar environment (Yang, 2004). Therefore, besides the activity of extrinsic signals influencing cell fate, cell-intrinsic signals must mediate the changes to be responsive to particular extracellular signals.

1.5.2 The intrinsic clues for retinal cells specification

Recent studies indicated that RPCs might have intrinsically programmed lineages. That is, progenitor cells pass through a series of intrinsically determined competence states, during each of which the progenitor cells are able to give rise to a limited subset of retinal cell types (Cepko et al., 1996). Several genes expressed in both progenitors and postmitotic cells, including *Notch*, *Hes-1*, *Pax6*, *Rx/Rax*, *Prox-1*, *Optx-2*, *Chx-10*, *p27Xic1* and *NeuronD*, were proposed to function as such intrinsic cues (reviewed by Livesey and Cepko, 2001). A conditional knock-out of *Pax6* in the peripheral mammalian retina led to a retinal tissue with only non-glycinergic amacrine cells, suggesting that *Pax6* plays a role in maintaining multipotency of retinal progenitors (Ashery-Padan and Gruss, 2001). In *Pax6* deficient RPCs, the bHLH factors like *Ngn2*, *Mash1* and *Math5* all failed to be activated, but *NeuroD*, which promotes the amacrine cell fate, is still activated in the *Pax6* deficient context (Marquardt et al., 2001). *Math5* normally expressed in a sub-population of RPCs is able to activate the POU domain transcription factor *Brn3b*, thereby driving these progenitors towards the ganglion fate. *Mash1* and *Ngn2* are activated in two strictly non-overlapping RPC populations that both generate bipolar and photoreceptor cells. Therefore, the function of *Pax6* on retinal cell type determination may be mediated by activities of these bHLH genes (Marquardt and Gruss, 2002). More recently, it was proposed that during retinal cell specification, homeodomain genes regulate retinal layer specificity but cannot determine the neuronal fate, while bHLH transcription factors determine neurons within the specified layers (Hatakeyama and Kageyama, 2004). Some evidence supports this idea. For instance, although *Chx10* is required for bipolar cell development, misexpression of *Chx10* alone only leads to

increased number of Müller glia or undifferentiated cells in the INL, none of which are mature bipolar cells (Hatakeyama et al., 2001). In addition, *Pax6* or *Six3* alone can generate only undifferentiated cells in the INL, while co-expression of *NeuroD* and *Pax6* or *Math3* and *Six3* significantly increases amacrine cell formation (Inoue et al., 2002). On the other hand, co-expression of *Math3* and *Pax6* produces horizontal cell fate more preferentially than amacrine cell (Inoue et al., 2002). Therefore, it is likely that within the homeodomain factor-specified layer, certain bHLH genes regulate the specification of neuronal subtypes (Hatakeyama and Kageyama, 2004).

The lateral inhibition mediated by Notch signaling pathway is demonstrated to play a crucial role in regulating the cell fate determination during retinogenesis (reviewed by Hatakeyama and Kageyama, 2004; Cayouette et al., 2006). Activation of Notch signaling alone induces expression of bHLH repressors such as *Hes1* and *Hes5*, which in turn repress bHLH activator and inhibit neuronal differentiation. When Notch signaling is inactivated, the bHLH repressors are off and allow bHLH activator to induce neuronal-specific gene expression (Hatakeyama and Kageyama, 2004). Recently, it has been revealed that higher Notch activity permits progenitor cells to remain proliferative and undifferentiated, and simultaneously allows them to pass through the competence waves, whereas the low or absent Notch activity releases these progenitors from cycling and leads to differentiation (Jadhav et al., 2006a).

Another homeobox gene, *Rx1* is necessary for the multipotency of the retinal progenitor cells (Casarosa et al., 2003; Casarosa et al., 1997; Mathers and Jamrich, 2000). Misexpression of *Rx1* promotes generation of Müller glia cells (Furukawa et al., 2000; Wang and Harris, 2005), similar to the gliogenic activities reported for Notch, *Hes1* and *Hes5* (Furukawa et al., 2000; Hojo et al., 2000). *Pax6*, *Six3* and *Rx1* are known to promote the proliferation of retinal progenitors. Thus, they appear to be required for eye development at two levels: maintenance of retinal progenitors and promotion of specific retinal cell types, depending on the developmental stage.

1.5.3 The intrinsic signals involved in photoreceptor cell specification

Photoreceptor cells are comprised of cone and rod photoreceptors. Cone photoreceptors are responsible for color vision in bright light, while rods are sensitive in dim light but do not discern color. However, these two different photoreceptors are generated in different phases during retinogenesis. Cones are generated much earlier than rods, which represent the last-born retinal neurons.

Several secreted factors have been shown to influence positively and negatively postmitotic rod differentiation *in vitro*, including *Shh*, *RA* and *EGF* (reviewed by Levine et al., 2000). *In vivo*

studies also support the function of these cell-extrinsic factors on photoreceptor differentiation. For example, in zebrafish, treatment of embryos with antisense oligonucleotides against *Hh* (*Shh* and *twhh* (*tiggy-winkle hedgehog*)) could slow or arrest the progression of the photoreceptor differentiation wave derived from the RPE Hh signaling (Stenkamp et al., 2000). Expression of a dominant negative form of FGFR (FGF receptor) in developing *Xenopus* embryos led to a 50% loss of both photoreceptor and amacrine cells, accompanied by a 3.5-fold increase of Müller glia (McFarlane et al., 1998). However, few genes have been reported to influence the photoreceptor cell type determination intrinsically. Overexpression of *NeuroD* induces selective overproduction of photoreceptor cells in chicken, mouse and *Xenopus* (Inoue et al., 2002; Wang and Harris, 2005; Yan and Wang, 1998). *Crx*, an Otx-like homeobox protein, can bind to the *Rhodopsin* promoter and transactivate its expression, along with a number of other photoreceptor specific genes (Chen et al., 1997). *Crx* is required for the maturation of photoreceptor cells in rodent (Furukawa et al., 1997b; Livesey et al., 2000), but in zebrafish, it plays an early role in promoting the mitotic cells to choose photoreceptor fate (Liu et al., 2001). In *Xenopus*, *Otx5b*, a gene highly-related to *Crx*, is expressed in both bipolar and photoreceptor cells and selectively biases photoreceptor fate, whereas its homologous gene *XOtx2* promotes bipolar fate by suppressing *XOtx5b* function (Vicgian et al., 2003). Recently, a retinal homeobox gene, *RaxL*, first identified in chicken (*cRaxL*), was demonstrated to play a role in the initiation of photoreceptor differentiation (Chen and Cepko, 2002).

Genes involved in subtype specification of photoreceptors are even more rarely identified. Alexiades and Cepko showed that amacrine cells, horizontal cells, and rods are progeny of one subpopulation of progenitors expressing *VC1.1* epitope, whereas the *VC1.1* negative progenitors give rise to cones. *Nrl*, a basic/leucine zipper transcription factor, is required for rod photoreceptor differentiation (Mears et al., 2001) and *Nrl*-null retinas show a transformation of rods into cone-like cells. *Nr2e3*, a rod photoreceptor specific nuclear receptor, has been shown to repress transcription of multiple cone-specific genes (Chen et al., 2005).

1.6 *Rx* genes in eye development

Rx (Retinal homeobox) is encoded by a subfamily of *paired*-like homeobox genes. Members of the *Rx* family have been described to play pivotal roles in eye development of several vertebrate species. In *Xenopus*, *Rx1* is initially expressed in the anterior neural plate, and then most abundantly in the optical vesicle as neurulation proceeds. During early tadpole stages, it is expressed throughout the neural retina, but by stage 40, *XRx1* is most strongly expressed in the

CMZ. This expression pattern is remarkably conserved among vertebrates (Mathers et al., 1997). Inactivation of *Rx1* in mouse and *Xenopus* led to loss of optic vesicle formation and impaired the development of ventral forebrain structures (Mathers et al., 1997; Andreazzoli et al., 1999). Misexpression of *Rx1* in *Xenopus* embryos resulted in the extension of ectopic RPE along the optic nerve region and in a hyperproliferation of the neural retina (Mathers et al., 1997). These observations are consistent with experiments showing that *XRx1* misexpression in *Xenopus* could expand endogenous *Pax6*, *Six3*, and *Otx2* expression, which resulted in enlarged eye fields (Andreazzoli et al., 1999). These results suggest that *Rx1* controls the initial specification of retinal cells and their subsequent proliferation.

Many of EFTFs were originally identified as homologs of genes required for eye formation in *Drosophila melanogaster*. For instance, *Pax6* is a homolog of *Drosophila eyeless (ey)* and *twin of eyeless (toy)* (Quiring et al., 1994), and *Six3* and *Optx2* are homologs of *Drosophila sine oculis (so)*. These transcription factors share largely conserved roles in retinal development between *Drosophila* and vertebrates (Figure 1.5). Interestingly, *Rx* gene is not required for insect eye formation, but seems to play an upstream role of *Pax6* in vertebrates (Bailey et al., 2004).

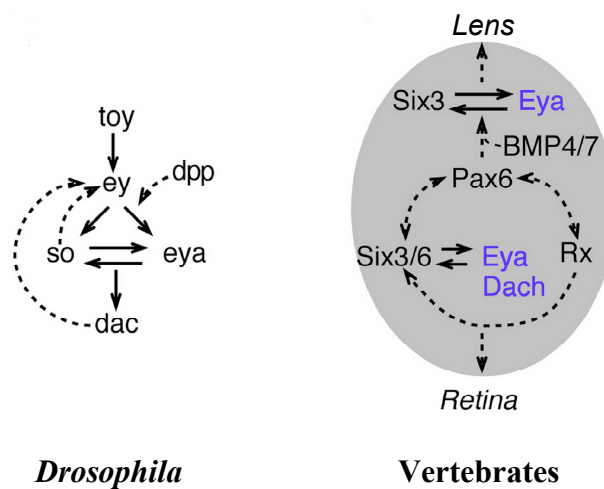


Figure 1.5 Genetic conservation and divergence of retinal development between *Drosophila* and vertebrates. Schematic diagram showing the network of transcription factors in regulation of the eye development in *Drosophila* (left) and vertebrates (right). *Pax6* is the homolog of *Drosophila eyeless (ey)* and *twin of eyeless (toy)*, *Six3* and *Six6 (Optx2)* are homologous to *sine oculis (so)*, *Eya* and *Dach* are homologous to *eye absent (eya)* and *dachshund (dac)* respectively.

Various paralogs of the *Rx* gene exist in each vertebrate species examined except rodents and cavefish, which has only one *Rx* gene identified so far. In zebrafish (Chuang et al., 1999; Mathers et al., 1997) and medaka fish, three *Rx* paralogs have been isolated from each of the species. Interestingly, zebrafish *Rx3* (Rojas-Muñoz et al., 2005) and medaka fish *Rx3* (Deschet et al., 1999; Loosli et al., 2001) showed higher similarity with *Xenopus Rx1* and mouse *Rx1* (or *Rax* genes as called in mouse and chicken) concerning their expression pattern and function than their paralogous genes zebrafish *Rx1* and *Rx2* and medaka fish *Rx2*. Two *Rx* genes, *cRax* and *cRaxL* were also identified in chicken. During neurogenesis, chicken *Rax* is expressed in the prospective retina and in the ventral forebrain, which is similar to mouse *Rx1* (Ohuchi et al., 1999). *cRaxL*, however, is expressed in neural ectoderm later than *cRax* and is highly restricted to the photoreceptor layer during the initial stages of photoreceptor differentiation (Chen and Cepko, 2002). Recently, a second *Rx* gene, *QRx*, was identified in human, which is expressed in both the outer and the inner nuclear layers of the retina, and was demonstrated to be involved in the modulation of photoreceptor gene expression (Wang et al., 2004). Taken together, it seems that paralogs of *Rx* genes in vertebrate function at different time points during eye development.

1.7 Aim of this thesis

Studies on *Rx* genes showed that some of them are already expressed from early neurula stages onwards, but others are expressed in the developing retina. Thus, while earlier-expressed *Rx* genes are required for the specification of eye field and maintain the proliferation of the RSCs, later-expressed *Rx* genes seem to be essential for retinal cell fate determination. The retina of *Xenopus* has long been an excellent model to study eye development. However, only one type of *Rx* was identified from *Xenopus* at the beginning of this project. We therefore asked if other *Rx* gene exists in *Xenopus*. If so, what would be its function - is it involved in the RSCs proliferation or the later retinal cell differentiation? If it mainly plays a role in the later cell differentiation, which retinal cell types, or even subtypes would it promote?

2 Materials

2.1 The experimental Animal - *Xenopus laevis*

The South African clawed frog *Xenopus laevis* is an amphibian of the order *Anura* and has a natural geographic range along the African Rift Valley, south of the Sahara Desert. Pigmented and albino frogs were obtained from a commercial supplier (NASCO, USA) and held in aquaria (water temperature 19 °C).

2.2 Bacteria

E. coli XL1-Blue (Stratagene GmbH, Heidelberg), *recA1*, *endA1*, *gyrA96*, *thi-1*, *hsdR17*, *supE44*, *relA1*, *lac[F' proAB, lacI^qΔM15, Tn10(Tet^r)]^c.*

2.3 Chemicals

Acetic acid	Roth
Acetic anhydride	Sigma
Agarose	Roth
Albumin, Bovine Serum (BSA)	Sigma
Albumin Fraction V	Roth
Ammonium Persulfate	Serva
Ampicillin sodium salt	AppliChem
Blocking reagent	Roche
Boric acid	Roth
5-Bromo-4-chloro-3-indolyl-phosphate (BCIP)	Fermentas
Bromphenol blue sodium salt	Merck
Calcium chloride, dihydrate	AppliChem
Calcium sulfate	Roth
CHAPS	Roth
Chloroform	Merck
L-Cysteinhydrochloride	Roth
10 mM dNTP mix	Fermentas
DAPI	Roth
Dexamethasone	Sigma

Diethylpyrocarbonate (DEPC)	Sigma
Digoxigenin-11-dUTP (10 mM)	Roche
Digoxigenin-11-UTP (10 mM)	Roche
DIG RNA Labeling Mix	Roche
Dimethyl formamide (DMF)	Roth
Dimethyl sulfoxide (DMSO)	Roth
Dithiothreitol (DTT)	Sigma
DNA Ladder, O'GeneRuler™ 1kb	Fermentas
Entellan	Merck
Eosin	Merck
Ethanol (≥99.8%)	Roth
Ethylenediaminetetraacetic acid (EDTA)	Sigma
Ethylene glycol-bis(2-amino-ethylether -N,N,N',N')-tetra-acetic acid (EGTA)	Sigma
Ethidium Bromide	Q-Biogene
Ficoll 400	Serva
FluorSave™ Reagent	Calbiochem
Formaldehyde	Roth
Formamid	Roth
Gelatin	Roth
Glutaraldehyde (25%)	Roth
Glycerol	Roth
Hemotoxyelin (Solution, Gill No.3)	Sigma
Heparin	Roth
HEPES	Roth
Horse Serum (HS)	Gibco
Human chorionic gonadotropin (HCG)	Sigma
Hydrogen chloride	Merck
Hydrogen peroxide (30%)	Roth
Isopropanol	Roth
LB Broth Base	Invitrogene
LB Agar	Invitrogene
Lithium chloride	Roth
Magnesium chloride	Roth
Magnesium sulfate, heptahydrate	Aldrich-Sigma
Maleic acid	Roth

β -Mercaptoethanol	Sigma
Methanol	Roth
L-[³⁵ S]-Methionon	Amersham Bioscience
MOPS	Q-Biogene
Mowiol	Calbiochem
Nitro blue tetrazolium chloride (NBT)	Fermentas
Nile blue chloride	Fluka
NTP set (100 mM for each separately)	Fermentas
PageRuler™ Prestained Protein Ladder	Fermentas
Paraformaldehyde	Roth
Polyvinylpyrrolidone (PVP-40)	Sigma
Potassium hexacyano-ferrate (III) (K ₃ Fe(CN) ₆)	Sigma
Potassium hexacyano-ferrate (II), trihydrate (K ₄ Fe(CN) ₆ •3H ₂ O)	Sigma
Potassium chloride	Roth
Potassium hydrogenphosphate	Roth
ProteinaseK	Merck
Red-Gal (5-Bromo-6-chloro-3- indolyl- β -D-galactopyranoside)	Sigma
RNase OUT™ Ribonuclease Inhibitor	Invitrogen
RNase A	Fermentas
RNase T1	Sigma
Rose-Gal (6-Chloro-3-indolyl- β - -D-galactopyranoside)	AppliChem
Sodium acetate	Roth
Sodium azide	Roth
Sodium bicarbonate (Cell Culture Tested)	Sigma
Sodium chloride	Roth
Sodium citrate	Fluka
Sodium dihydrogenphosphate	Merck
Sodium dodecyl sulfate (SDS)	Roth
Sodium hydrogenphosphate, dodecahydrate	Merck
Sodium hydroxide	Roth
Sucrose	Roth
Tetracycline	Sigma
Tetramethylethyldiamin (TEMED)	Fluka

Tissue-Tek® O.C.T.™ Compound	Sakura Finetek
Torula RNA	Sigma
Triethanolamine	Roth
Tris(hydroxymethyl)-aminomethane (Tris)	Roth
Triton X-100	Ferak
TRIzol® Regent	Invitrogene
Tween-20	Roth
X-Gal (5-Bromo-4-chloro-3-indolyl -β-D-galactoside)	Q-Biogene
Xylene	Sigma
Xylencyanol	Roth

2.4 Buffers, solutions and media

2.4.1 Embryos preparation

Human chorionic gonadotropin (HCG)

10,000 U/vial HCG (Sigma) was suspended in 5 ml ddH₂O to make a stock solution of 2000 U/ml. Aliquoted in fractions of 1ml, and stored at -20 °C.

5x MBS (Modified Barth's Saline)

440 mM NaCl, 12 mM NaHCO₃, 5 mM KCl, 4.1 mM MgSO₄, 50 mM Hepes in dH₂O, pH adjusted to 7.4 and then supplemented with 2.05mM CaCl₂. The solution was filtrated with 0.2 μm filters (Sartorius, Germany) and stored at room temperature. Upon requirement, the stock solution was diluted to 1x MBS or 0.1x MBS.

L-Cystein hydrochloride solution (2 %)

2% L-Cystein hydrochloride, pH adjusted to 7.8 – 8.0.

Nile blue solution

1 L phosphate buffer containing 50 mM Na₂HPO₄ and 50 mM NaH₂PO₄ was warmed up to 60°C. 0.01% (w/v) Nile blue chloride was dissolved in it with stirring overnight. After filtration, the Nile blue solution was ready to use.

10x MEM (MOPS/EGTA/Magnesium sulfate buffer)

1 M MOPS, 20 mM EGTA, 10 mM MgSO₄ in dH₂O. The solution was filtrated with 0.2 μm filters and stored at room temperature.

MEMFA (MOPS/EGTA/Magnesium sulfate/formaldehyde buffer)

3.7% formaldehyde in 1x MEM, prepared before use.

10x PBS (phosphate-buffered saline)

1.37 M NaCl, 27 mM KCl, 80 mM Na₂HPO₄ and 18 mM KH₂PO₄ in dH₂O, pH 7.4. Autoclaved.

X-Gal stock solution

40 mg/ml X-Gal (5-Bromo-4-chloro-3-indolyl- β -D-galactoside) in DMSO, stored in dark at -20°C.

Red-Gal (or Rose-Gal) stock solution

25 mg/ml Red-Gal (5-Bromo-6-chloro-3-indolyl- β -D-galactopyranoside) or Rose-Gal (6-Chloro-3-indolyl- β -D-galactopyranoside) in DMSO, stored in dark at -20°C.

X-Gal staining solution

5 mM $K_3Fe(CN)_6$, 5 mM $K_4Fe(CN)_6$, 5 mM $MgCl_2$, and 1 mg/ml X-Gal in PBS.

Red-Gal (or Rose-Gal) staining solution

5 mM $K_3Fe(CN)_6$, 5 mM $K_4Fe(CN)_6$, 5 mM $MgCl_2$, and 0.05 mg/ml Red-Gal (or Rose-Gal) in PBS.

500x Dexamethasone solution

5 mM dexamethasone in ethanol, stored at -20°C in the dark.

2.4.2 Whole-mount *In situ* hybridization**DEPC (Diethylpyrocarbonat) H₂O**

0.1% (v/v) DEPC in ddH₂O was incubated at 37°C for 2 hr and autoclaved.

PTw

0.1% Tween-20 in PBS.

PTw/MEMFA

4% (v/v) formaldehyde in PTw

Triethanolamine solution

0.1M Triethanolamine-hydrochloride in dH₂O, pH adjusted to 7.5.

100x Denhart's solution

2 % BSA, 2 % PVP and 2 % Ficoll 400 in dH₂O, stored at -20°C.

Torula RNA (10 mg/ml)

10 mg/ml Torula RNA in DEPC H₂O was dissolved at 37°C with shaking over night. After centrifugation at 6000 rpm for 10 min, the supernatant was aliquoted and stored at -20°C.

20x SSC (standard saline citrate buffer)

3 M NaCl and 0.3 M Na Citrate in dH₂O, pH 7.2-7.4.

Hybridization mix

50% deionized formamid*, 1 mg/ml Torula-RNA, 10 μ g/ml Heparin, 1x Denhardt's, 0.1% Tween-20, 0.1% CHAPS, and 10 mM EDTA in 5x SSC, stored at -20°C.

* To deionize formamid: Add 50 g of mixed bead resin (BioRad) to 500 ml formamid, mix on magnetic stirrer for 2 h and filter on Whatman paper.

NBT solution

100 mg/mL NBT in 70% DMF, stored at -20°C.

BCIP solution

50 mg/mL in 100% DMF, stored at -20°C.

Ethanol series

100%, 75% and 50% (v/v) ethanol in dH₂O respectively; 25% ethanol in PTw.

Methanol series

100%, 75%, 50% and 25% (v/v) methanol in dH₂O respectively.

5x MAB (maleic acid buffer)

500 mM maleic acid, 750 mM NaCl in dH₂O, pH 7.5, autoclaved.

Boehringer Blocking Reagent (BMB) stock solution

10 % BMB was dissolved 1x MAB at 60°C, autoclaved and stored at -20°C.

MAB/BMB

2% BMB in 1x MAB

MAB/BMB/HS

2% BMB, 20% heat-treated horse serum in 1x MAB

APB (Alkaline phosphatase buffer)

100 mM Tris-HCl, pH 9.0, 50 mM MgCl₂, 100 mM NaCl and 0.1% Tween-20 in dH₂O.

Color reaction solution

175 µg/ml NBT and 175 µg/ml BCIP in APB.

TE buffer (Tris/EDTA buffer)

10 mM Tris-HCl (pH 7.5) with 1 mM EDTA.

RNase A stock solution

10 mg/ml of RNase A dissolved in TE buffer, heated at 100°C for 10 min, and stored at -20°C.

Bleaching solution

50% (v/v) formamid and 1% H₂O₂ in 5x SSC.

2.4.3 Vibratome sectioning**Gelatin-Albumin**

0.44% (w/v) Gelatine, 13.5% (w/v) Albumin (Sigma) and 18% (w/v) Sucrose in PBS, stirred at 60°C till well dissolved and centrifuged 6000 rpm for 10 min. Stored at -20°C.

Moviol mounting solution

25% (v/v) moviol was dissolved in PBS (takes about 16 hours to dissolve) and then ½ PBS volume of glycerol was added to the dissolved moviol with stirring. The solution was centrifuged at 6,000 rpm for 10 min and the supernatant was aliquoted and stored at -20°C.

2.4.4 Mini-preparation of plasmid DNA**TELT buffer**

2.5 M LiCl, 62.5 mM EDTA and 0.4% (v/v) Triton X-100 in 50 mM Tris-HCl (pH 7.5), stored at 4°C.

Lysozyme solution

10 mg/ml Lysozyme in dH₂O, prepared before use.

2.4.5 Gel electrophoresis**10x TBE buffer (Tris/boric acid/EDTA buffer)**

0.89 M Tris, 0.89 M boric acid and 20 mM EDTA in dH₂O.

Glycerol loading buffer

10 mM EDTA, 30% glycerol (v/v), 0.025 % Bromphenol blue and 0.025 % Xylencyanol in 10 mM Tris-HCl, pH 7.5.

2.4.6 SDS-polyacrylamide gel electrophoresis (SDS-PAGE)**Ammonium persulfate stock solution**

10% (w/v) ammonium persulfate in dH₂O and stored at -20°C.

Tris-glycin electrophoresis buffer

25 mM Tris base, 250 mM glycine and 0.1% SDS in dH₂O, pH 8.3.

2x SDS gel loading buffer

200 mM DTT, 4% (w/v) SDS, 0.2% bromophenol blue and 20% (v/v) glycerol in 100 mM Tris-HCl, pH 6.8. Aliquots were stored at -20°C.

2.4.7 Immunostaining**4% Paraformaldehyde (PFA)**

4% Paraformaldehyde in PBS, stirred and heated to 60-65°C till the solution became clear, pH adjust to 7.2. Aliquots were stored at -20°C.

Permeabilization and blocking solution

20 mg/ml bovine serum albumin (BSA, Roth) and 0.5% (v/v) Triton X-100 in PBS.

Antibody buffer

10 mg/ml BSA and 0.05% Triton X-100 in PBS.

PBS-TB

0.05% (v/v) Tween-20 and 0.2% BMB in PBS.

PBS-TBN

0.05% (v/v) Tween-20, 0.2% BMB and 0.3 M NaCl in PBS.

2.4.8 TdT-mediated dUTP digoxigenin nick end-labeling (TUNEL) assay**PBT_w**

0.2% Tween in PBS.

PBS/EDTA

1 mM EDTA in PBS.

PBT

2 mg/ml BSA and 0.1% Triton X-100 in PBS.

2.4.9 Media**Luria-Bertani (LB) medium:**

20 g LB Broth Base was dissolved into 1 L dH₂O and autoclaved for 20 min at 121°C, stored at 4°C.

Luria-Bertani (LB)-Ampicillin (Amp) agar plate:

32 g LB Agar was dissolved in 1 L dH₂O and autoclaved for 20 min at 121°C. After the medium was cooled down to around 50°C, ampicillin solution (100 mg/ml in dH₂O) was added with a final concentration of 100 µg/ml and plates were poured in a sterile hood.

Luria-Bertani (LB)-Tetracycline (Tet) agar plate:

32 g LB Agar was dissolved in 1 L dH₂O and autoclaved for 20 min at 121°C. After the medium was cooled down to around 50°C, tetracycline solution (5 mg/ml in 100% Ethanol) was added with a final concentration of 12.5 µg/ml and plates were poured in a sterile hood.

2.5 Antibodies**Anti-Digoxigenin/AP** (Roche Diagnostics)

Fab fragment of polyclonal antibodies from sheep specifically recognizing digoxigenin and digoxin, conjugated with alkaline phosphatase.

Anti-phospho-histone H3 (Upstate Biotechnology)

A polyclonal antibody generated from rabbit with synthetic phospho-peptide derived from the sequence of human Histone H3 as the immunogen.

Anti-rabbit/AP (Sigma-Aldrich)

An alkaline phosphatase (AP)-conjugated goat affinity purified antibody to rabbit IgG (whole molecule).

Anti-calbindin D-28K Rabbit pAb (Calbiochem & Oncogene)

Rabbit polyclonal antibody generated with purified bovine cerebellum calbindin D-28K protein as immunogen.

Anti-calbindin D-28K mouse mAb (Swant)

A mouse IgG produced by hybridization of mouse myeloma cells with spleen cells from mice immunized with calbindin D-28K purified from chick gut.

Cy3-goat-anti-mouse IgG conjugate (Invitrogen)

A polyclonal antibody raised in goat against the whole mouse IgG molecule and purified with antigen-affinity-chromatography, conjugated with Cy3.

2.6 Enzymes

Restriction enzymes with supplied buffers	Fermentas
Terminal Deoxynucleotidyl Transferase (TdT, 20 U/μl) with supplied buffer	Fermentas
RNase A	Sigma-Aldrich
RNase T1	Sigma-Aldrich
Proteinase K	Merck
<i>T4</i> DNA-Ligase (3 U/μl) with supplied buffer	Fermentas
SP6 RNA-Polymerase (50 U/μl) with supplied buffer	Stratagene
T3 RNA-Polymerase (50 U/μl) with supplied buffer	Stratagene
T7 RNA-Polymerase (50 U/μl) with supplied buffer	Stratagene
<i>Taq</i> DNA-Polymerase (5 U/μl) with supplied buffer	Fermentas
<i>Pfu</i> DNA-Polymerase (2.5 U/μl) with supplied buffer	Fermentas
Deoxyribonuclease I (DNaseI, RNase-free) (1U/μl)	Fermentas

2.7 Kits

The following kits were used in this study, according to manufacturers' instructions:

Big Dye Terminator Cycle Sequencing Kit	Applied Biosystems
mMESSAGE mMACHINE™ SP6	Ambion
pGEM®-T Vector System	Promega
QIAGEN® PCR Purification Kit	Qiagen
QIAGEN® Plasmid Midi Kit	Qiagen
QIAEX® Gel Extraction Kit	Qiagen
RNeasy Mini Kit	Qiagen GmbH, Hilden
RevertAid™H Minus First Strand cDNA Synthesis Kit	Fermentas
TnT®-Coupled Reticulocyte Lysate System	Promega
Technovit 7100	Heraeus Kulzer

2.8 Oligonucleotides

2.8.1 Oligonucleotides for PCR

The oligonucleotides were ordered from Sigma-Aldrich and dissolved in ddH₂O to get a 100 μM stock solution. In the following sequences, f represents forward primer, and r represents reverse primer, “seq” indicates the primer is used for sequencing. The restriction enzyme recognized sites are underlined.

RxL-EcoRI-f	5'-GCGGAATTCAATGTTTCTAGACAAATGTGAAGG-3'
RxL-XhoI-r	5'-CCGCTCGAGTCAGATTGGCTGCCATGTTTTATCTATCG-3'
RxL-fusion-XhoI-r	5'-CCGCTCGAGGATTGGCTGCCATGTTTTATCTATCG-3'
RxL-ΔOAR-r1	5'-TTTATCTATTTCTCTAAGGGAAATTTGTCCGCAA-3'
RxL-ΔOAR-XhoI-r2	5'-CCGCTCGAGGATTGGCTGCCATGTTTTATCTATTTCTCTC-3'
RxL-A9T-EcoRI-f	5'-GCGGAATTCAATGTTTCTTGACAAATGTGAAGGAG-3'
GR-XhoI-f	5'-CGGCTCGAGACCTCTGAAAATCCTGG-3'
GR-XbaI-r	5'-CGCTCTAGATCACTTTTGATGAAACAGAAGTTTTTTG-3'
VP16-XhoI-f	5'-CCGCTCGAGGCCCGCCGACCGATGT-3'
VP16-XbaI-r	5'-GCTCTAGATCACCCACCGTACTCGTCAA-3'
VP16-M173T-r	5'-CAAACCTCGAAGTCGGCCATATCCAGAGCGCCGTAG-3'
VP16-M173T-f	5'-CTACGGCGCTCTGGATATGGCCGACTTCGAGTTTG-5'
XMitf-M-f	5'-AAAGCTTCGGTGGATTACATTCGC-3'
XMitf-M-r	5'-CTAACAGTGATCATTTTCTTCCATGCTG-3'
RxL-234-f	5'-TCGAGTTCAGGTTTGGTTCC-3'
RxL-547-r	5'-GAGCACTGCTGAGAGGGTTGG-3'
H4-f	5'-CGGGATAACATTCAGGGTATCACT-3'
H4-r	5'-ATCCATGGCGGTAAGTGTCTTCCT-3'
SP6-seq	5'-TTTAGGTGACACTATAGAATAC-3'
T7-seq (pGEM-T)*	5'-TAATACGACTCACTATAGGGCGA-3'
T7-seq (pCS2+)**	5'-TCTACGTAATACGACTCACTATAG-3'
T3-seq	5'-ATTAACCCTCACTAAAGGGA-3'
RxL-EngR-seq-f	5'-AGTTGCACCAACAGCAACTG-3'
RxL-EngR-seq-r	5'-TCCTCCTCCTTGATGGTCAG-3'

*, **: T7 primers for pGEM-T and pCS2+ vectors respectively.

2.8.2 Antisense Morpholino Oligonucleotides (MO)

Morpholino Oligonucleotides were obtained from Gene Tools (USA) and were dissolved in RNase-free H₂O to make the stock concentration of 1mM.

Standard control MO (Cont-MO)	5'-CCTCTTACCTCAGTTACAATTTATA-3'
XRxL specific MO1 (RxL-MO1)	5'-CTAGAAACATCCCTTGTGCTGACAG-3'
XRxL specific MO1 (RxL-MO2)	5'-TGTCTTCTGAACTGCACTTAGCTG-3'

2.8.3 Special delivery morpholino complimentary oligomers (carrier oligomers)

Cont-MO-SD	5'-AAAAAAAAAATATAAATTGTAAGTGA-3'
RxL-MO1-SD	5'-AAAAAAAAAACTGTCAGCACAAGGGA-3'
RxL-MO2-SD	5'-AAAAAAAAAAACAGCTAAGTGCAGTTC-3'

2.9 Vectors and Constructs

2.9.1 Vectors

pGEM-T (Promega)

This vector contains a 3' terminal thymidine overhang in both ends and is convenient for the cloning of PCR products. The PCR fragments with a 3'-terminal deoxythymidine could be directly cloned into pGEM-T vector. It contains T7 and SP6 RNA polymerase promoters flanking a multiple cloning region within the α -peptide coding region of β -galactosidase (Figure 2.1). This vector was used to construct plasmids generating anti-sense RNA probes.

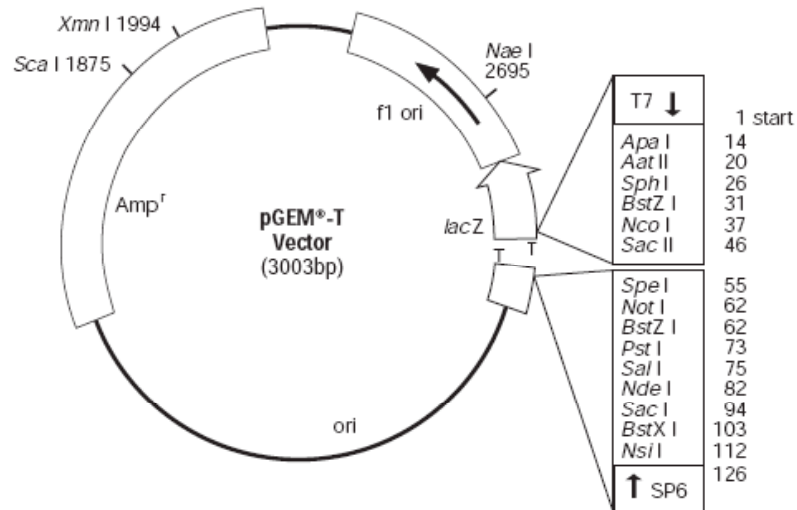


Figure 2.1 pGEM-T Vector circle map. The vector is a linear molecular with a 3' terminal thymidine at each end, which resides internally in a lacZ cassette and flanks with the multiple-cloning sides (Promega, USA).

pCS2+ (Mental Health Research Institute, University of Michigan)

This multipurpose expression vector contains a strong enhancer/promoter (simian CMV IE94) followed by a polylinker (polylinker I) and the SV40 late polyadenylation site. The SP6 promoter allows *in vitro* RNA synthesis of sequence cloned into polylinker I. The second polylinker (polylinker II) provides several possible sites to linearize the vector for SP6 RNA transcription. This vector was used in generation of constructs for *in vitro* synthesis of sense mRNA or for lipofection. The graphic map is shown in Figure 2.2.

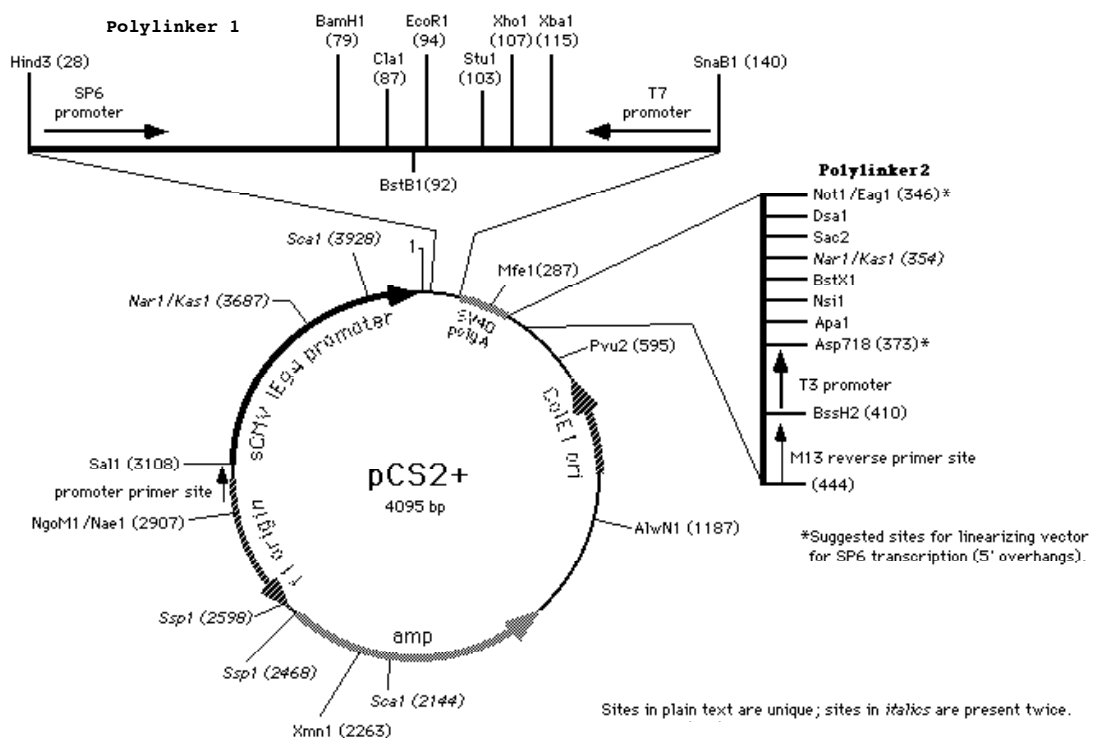


Figure 2.2 pCS2+ vector graphic map. The interested genes were cloned into polylinker 1 to make the constructs. After linearized with a restriction enzyme in polylinker 2, the constructs could be used as the template for *in vitro* synthesis of the sense RNA (Turner and Weintraub, 1994).

2.9.2 Constructs

The antisense probes generated from the following indicated constructs are all specific for *Xenopus* transcripts.

XR_xL/pBlueScript SK(-)

A full-length cDNA clone of XR_xL in pBlueScript SK(-) was purchased from National Institute of Basic Biology, Japan, referred as to XR_xL/pBlueScript SK(-). The clone number is XL073a16. In this study, XR_xL ORF was subcloned from this construct to pCS2+ vector. XR_xL/pBlueScript

SK(-) was linearized with *EcoRI* and *in vitro* transcribed with T7 to synthesize *RxL* antisense probe for whole-mount *in situ* hybridization.

Otx5b/pBlueScript SK(-)

A cDNA clone of *XOtx5b* in pBlueScript SK was a kind gift from Prof. Robert Vignali (Vignali et al., 2000). This construct was linearized with *NotI* and *in vitro* transcribed with T7 to synthesize *XOtx5b* antisense probe for whole-mount *in situ* hybridization.

EngR/pCS2_Myc-NLS (Holleman et al., 1998)

The repressor domain of *Drosophila engrailed* (EngR) was cloned from this construct to generate RxL-EngR/pCS2+.

MyoDGR/pSP64T (Hollenberg et al., 1993; Kolm and Sive, 1995)

The human glucocorticoid receptor ligand binding domain (GR) was cloned from this construct to generate RxL-GR/pCS2+.

hSRF-VP16/pCS2+ (Hines et al., 1999)

The region encoding the activator domain of VP16 protein was cloned from this construct to generate RxL-VP16/pCS2+.

Pax6/pCS2+ (Hirsch and Harris, 1997)

This construct was linearized with *NotI* and *in vitro* transcribed with T7 to synthesize *Pax6* antisense probe for whole-mount *in situ* hybridization.

Rhodopsin/pGEM-T (Saha and Grainger, 1993)

This construct was linearized with *NotI* and *in vitro* transcribed with T7 to synthesize *Rhodopsin* antisense probe for whole-mount *in situ* hybridization.

Rx1/pGEM3 (Casarosa et al., 1997)

This construct was linearized with *XhoI* and *in vitro* transcribed with SP6 to synthesize *Rx1* antisense probe for whole-mount *in situ* hybridization.

Six3/pGEM-T (Zhou et al., 2000)

This construct was linearized with *NotI* and *in vitro* transcribed with T7 to synthesize *Six3* antisense probe for whole-mount *in situ* hybridization.

Arrestin/pGEM-T (Korf et al., 1989)

This construct was linearized with *NcoI* and *in vitro* transcribed with SP6 to synthesize *Arrestin* antisense probe for whole-mount *in situ* hybridization.

eGFP/pCS2+

This construct was used in lipofection.

2.10 Equipments

Microliter pipettes

Pipetman P10	Gilson S.A.S., France
Pipetman P20	Gilson S.A.S., France
Pipetman P200	Gilson S.A.S., France
Pipetman P1000	Gilson S.A.S., France

PCR Thermocycler

Tpersonal Thermocycler	Biometra, Germany
TGRADIENT Thermocycler	Biometra, Germany

Centrifuge

Biofuge pico	Heraeus, Germany
SIGMA 2K15	Sigma laborzentrifugen, Germany
Sorvall RC-5B	Thermo Scientific, USA

Spectrophotometer

NanoDrop® Spectrophotometer ND-100	peQlab Biotechnology, Germany
Bio photometer	eppendorf, Germany

Elektroporator

Electro Square Porator™ ECM830	BTX, Germany
--------------------------------	--------------

Sterile Hood

KS12	Thermo Scientific, USA
------	------------------------

Incubator/Thermoblock/Waterbath

Incubator: Function line	Heraeus Instruments, Germany
Incubator shaker: innova™ 4300	New Brunswick Scientific, USA
Incubator shaker: innova™ 4230	New Brunswick Scientific, USA
Water bath DIN 40050-IP20	Memert, Germany
Thermomixer: Thermomixer 5437	eppendorf, Germany
Thermomixer: HTMR-131	HLC-Haep Labor Consult, Germany

Shaker

Rocky 100	Labortechnik Fröbel, EU
RM5V-30	CAT. M. Zipperer, Germany

Histological equipments

Vibratom Leica VT1000 S	Leica Microsystem, Germany
Microtom Leica RM2066	Leica Microsystem, Germany
Microm HM500 OM	Microm, Germany
Super Frost® plus microscope slides	Menzel-Glasäser, Germany
Cover slides (24x 60mm)	Menzel-Glasäser, Germany

Electrophoresis

Electrophoresis power supply E844	Consort, Belgium
Power Pack P25	Biometra, Germany
Bio-Rad Gel Doc 2000	Bio-Rad Laboratories, USA

Microinjection

Microinjector: PV820 Pneumatic Picopump	Helmut Saur, Germany
Needle-puller: PN-30	Narishige, Japan

Microscope

Zeiss Stemi 2000	Carl Zeiss, Germany
Olympus SZX12	Olympus Microscopy, Japan
Leica DMR	Leica Microsystem, Germany
Nikon Eclipse E600	Nikon, Japan

UV supply for Microscope

ebq 100	LEJ Leistungselektronik, Germany
---------	----------------------------------

Camera

iNTAS MS 500	iNTAS, Germany
Vosskühler CCD-1300QLN	Vosskühler, Germany

Computer

Personal Computer	ASUS, Taiwan
Macintosh iBook G4/OS 9.0/X	Apple, USA

Software

Analyze 68K Mac Molly® Tetra V3.10	Soft Gene, Germany
BLAST(http://www.ncbi.nlm.nih.gov/BLAST/)	National Institute for Health, USA (Altschul et al., 1997)
DNASTAR lasergene® V4.03	DNASTAR, USA

Freehand 9/10

Macromedia Central Europe, Germany

Genetyx Application

Software Development, Japan

Microsoft® Office 2004/XP

Microsoft, USA

Photoshop 7.0/PS

Adobe Systems, USA

Primer3 (<http://frodo.wi.mit.edu/>)

Whitehead Institute for Biomedical Research,
USA (Steve Rozen and Helen J. Skaletsky,
2000)

QCapture Pro 5.1

QImaging, USA

3 Methods

3.1 Genetic methods

3.1.1 Construction of Phylogeny of Rx homeoproteins

The nucleotide sequences of all known *Rx*-type genes were obtained from Genbank, and deduced to amino acid sequences by using Editseq (DNASTAR, USA). The deduced amino acid sequences were aligned with MegAlign (DNASTAR, USA). Based on the amino acid sequences of the homeobox and the OAR domain of all *Rx*-type genes, the phylogenetic tree was constructed with Geneious (Biomatters, New Zealand).

3.1.2 Cloning

For cloning the desired genes, PCRs were carried out in a 50 μ l reaction mix containing 5 μ l 10x buffer (supplied with enzyme), 10-30 ng DNA template, 0.25 μ M each of forward and reverse primers, 0.5 mM each of dNTPs and 1 μ l *Pfu* DNA polymerase. The thermocycle program was performed with activating the enzyme and denaturing the DNA template at 95°C for 2 min, followed by 26 cycles of DNA denaturation at 95°C for 45 sec, annealing at 55-60°C for 45 sec and extension at 72°C for 1-3 min according to the length of the PCR product (1kb/2min as recommended by the manufacturer), and the final extension at 72°C for 10 min.

XR_xL-full-length/pCS2+

The *XR_xL* cDNA, *XR_xL* ORF flanked by partial 5'- and 3'-UTRs was obtained by digestion of *XR_xL*/pBlueScript SK(-) with *EcoRI* and *XhoI*. The obtained fragment was subcloned into the pCS2+ vector. This generated construct was used as a template plasmid in TNT assay (see below).

XR_xL/pCS2+

The open reading frame (ORF) of *XR_xL* was amplified with the forward primer RxL-EcoRI-f and the reverse primer RxL-XhoI-r (contains stop codon) using *XR_xL*/pBlueScript SK(-) as the template. The PCR product was digested with *EcoRI* and *XhoI* and ligated in the *EcoRI/XhoI* digested pCS2+ vector. This construct was linearized with *NotI* and *in vitro* transcribed with SP6 to synthesize sense RNA for overexpression. This construct was also directly used for lipofection.

RxL- Δ OAR/pCS2+

The fragment of *XR_xL* ORF N-terminal to the OAR domain was amplified with the forward primer RxL-EcoRI-f and the reverse primer RxL- Δ OAR-r1 using *XR_xL*/pCS2+ as the template, and further amplified by nested PCR with the forward primer RxL-EcoRI-f and the reverse primer RxL- Δ OAR-XhoI-r2 (contains the sequence C-terminal to OAR domain) to get the *XR_xL* lacking

sole OAR domain. To add a stop codon at the 3'-terminus, the nested PCR product was used as a template and amplified with the primers RxL-EcoRI-f and RxL-XhoI-r. The resulting PCR product, *XRxL* ORF lacking OAR and containing a stop codon at the 3'-terminus, was digested with *EcoRI* and *XhoI* and cloned into pCS2+ vector to generate the construct RxL-ΔOAR/pCS2+. This construct was linearized with *NotI* and *in vitro* transcribed with SP6 to synthesize the sense RNA for overexpression. This construct was also directly used for lipofection.

RxL-fusion/pCS2+

The ORF of *XRxL* was amplified with the forward primer RxL-EcoRI-f and the reverse primer RxL-fusion-XhoI-r (without the stop codon) with *XRxL*/pCS2+ as the template. The PCR product was digested with *EcoRI* and *XhoI* and ligated into pCS2+ vector. This construct contains *XRxL* ORF without a stop codon and was used to generate RxL-fusion chimeric constructs where the restriction enzyme *XbaI* was avoided (see below, i.e. RxL-EngR/pCS2+).

RxL(XbaI)-fusion/pCS2+

The ORF of *XRxL* was amplified with the forward primer RxL-A9T-EcoRI-f and the reverse primer RxL-fusion-XhoI-r (without stop codon) using *XRxL*/pCS2+ as the template. The PCR product was digested with *EcoRI* and *XhoI* and ligated into the pCS2+ vector. In this construct, the *XbaI* recognised site was muted without changing the encoded amino acid. It contains *XRxL* ORF without a stop code and was used to construct RxL-fusion chimeric constructs (see below).

RxL-GR/pCS2+

The glucocorticoid receptor ligand-binding domain (GR) was amplified with the forward primer GR-XhoI-f and the reverse primer GR-XbaI-r using MyoDGR/pSP64T as the template. The PCR product was digested with *XhoI* and *XbaI* and ligated into *XhoI/XbaI* digested RxL(XbaI)-fusion/pCS2+ plasmid to generate the desired construct. This construct was linearized with *NotI* and transcribed with SP6 to synthesize the sense RNA.

RxL-VP16/pCS2+

The DNA region encoding the activator domain of VP16 was amplified with the forward primer VP16-XhoI-f and the reverse primer VP16-XbaI-r using hSRF-VP16/pCS2+ as the template. The *XhoI/XbaI* digested PCR product was cloned into the pCS2+ vector. The obtained plasmid was digested with *EcoRI* and *XhoI* and ligated with the *EcoRI/XhoI* digested PCR fragment of *XRxL* ORF (without stop codon). This construct was linearized with *NotI* and transcribed with SP6 to synthesize the sense RNA. This construct was also directly used for lipofection.

RxL-EngR/pCS2+

The DNA fragment of the repressor domain of *Drosophila engrailed* was obtained by digestion of EngR/pCS2_Myc-NLS with *XhoI* and *SnaBI*. This fragment was ligated into the *XhoI/SnaBI* digested RxL-fusion/pCS2+ plasmid. This generated construct was linearized with *NotI* and transcribed with SP6 for the sense RNA synthesis.

XMitf/pGEM-T

The gene *XMitf* was amplified from the cDNA library with the forward primer XMitf-f and the reverse primer XMitf-r as described (Kumasaka et al., 2004) and directly subcloned into pGEM-T vector. This construct was linearized with *NcoI* and transcribed with SP6 to synthesize the antisense probe for whole-mount *in situ* hybridization.

3.1.3 Preparation of electrocompetent bacteria

A single colony of *E. coli* XL-1 Blue was picked from a LB plate containing tetracycline, inoculated in 3 ml LB medium without antibiotics, and cultured overnight at 37°C with a rotary speed of 220 rpm. This 3 ml bacteria culture were then inoculated to 300 ml LB medium without antibiotics in a 1 L flask, and cultured at 37°C with a rotary speed of 220 rpm for about 3 hr until the OD reached approximate 0.5. The culture was intensively cooled down on ice. Meanwhile, the centrifuge cups, pipets and 1.5 ml eppendorf tubes supposed to be used in the preparation were all pre-cooled at 4°C.

The bacteria were transferred to a pre-cooled centrifuge cup and precipitated by centrifuge at 6,000 rpm for 15 min at 4°C. The supernatant was discarded and the pellet was gently resuspended in the chilled 10% glycerol (autoclaved) and collected again by centrifuge at 6,000 rpm for 20 min. The washing step with the chilled 10% glycerol was repeated three more times and the pellet was finally resuspended in 2 ml 10% glycerol. The bacteria were aliquoted in 50 µl per eppendorf tube on ice and immediately transferred to the liquid Nitrogen. Aliquots were stored at -80°C.

3.1.4 Electroporation

1 µl circular plasmid or 2 µl ligated plasmid was added to 50 µl electrocompetent bacteria (just melted on ice) and gently mixed by tapping. After incubation on ice for 5 min, the cell-DNA mixture was transferred to a chilled 1 mm electroporation cuvette (Equibio, UK) and applied on the electroporator (Electro Square PoratorTM ECM830, BTX). The sample was pulsed once (500 V for 8 msec) and immediately filled with 450 µl chilled LB medium. After being gently mixed by pipeting, the bacteria were kept on ice. This 500 µl bacteria was transferred to a 1.5 ml eppendorf tube and incubated at 37°C for 30 min. A 50 µl aliquot and the rest were spread on LB-Amp plates respectively, and incubated overnight at 37°C.

3.1.5 Colony PCR

A single colony was picked with an autoclaved toothpick from a LB-Amp plate and scratched on a fresh LB-Amp plate. The rest bacteria on the toothpick were rinsed in 10 µl ddH₂O. This 10 µl bacteria suspension was heated at 95°C for 10 min to lyse the bacteria, and 8 µl of it was used as the template for the colony PCR. A standard 25 µl colony PCR reaction contained 8 µl of the

template, 1.5 mM MgCl₂, 2.5 µl *Taq* polymerase buffer (supplied with enzyme, without MgCl₂), 1 µM forward primer and reverse primer respectively, 0.1 mM dNTPs and 0.1 µl *Taq* polymerase (5 u/µl, Fermentas).

The PCR reaction was run under a thermocycle program with activating the enzyme and denaturing the DNA template at 95°C for 2min, followed by 26 to 30 cycles of DNA denaturation at 95°C for 45 sec, annealing at 55-58°C for 45 sec and extension at 72°C for 45 sec to 2 min according to the length of the PCR product (1kb/1min as recommended by the manufacturer), and the final extension at 72°C for 10 min.

The PCR products were analysed on a 1% agarose gel marked with 1kb DNA Ladder (Fermentas).

3.1.6 Plasmid preparation

3.1.6.1 Plasmid mini-preparation (TELT preparation)

The bacteria were grown in 3 ml LB medium containing appropriate antibiotics overnight at 37°C. 1.5 ml of the bacteria culture was collected in an eppendorf tube and centrifuged at full speed for 1 min in a bench centrifuge. The supernatant was removed and the pellet was fully resuspended in 150 µl of TELT solution. 15 µl of 10 mg/ml lysozyme was added in the bacteria suspension, and mixed thoroughly by pipetting. After incubation at room temperature for 5 min, the bacteria lysate was heated at 95 °C for 2 min and then immediately placed on ice for 5 min. The bacteria lysate was centrifuged at full speed for 15 min at room temperature and the pellet was removed with a sterilized toothpick. 100 µl isopropanol was added in the remaining supernatant, mixed gently and incubated in room temperature for 10 min. After a full-speed centrifugation at room temperature for 10 min, the supernatant was discarded and the pellet was washed with 200 µl of 70% ethanol by centrifuging at full-speed for 5 min at room temperature. The supernatant was removed. After the pellet was air-dried, it was dissolved in 30 µl of TE buffer with RNase A (10 µg RNase A per ml TE).

3.1.6.2 Plasmid midi-preparation

When 1 µg/µl or a higher concentration of plasmids was desired, the plasmid was extracted with a QIAGEN® Plasmid Midi Kit according to the manufacturer's manual.

3.1.7 Preparation of sequencing samples

For preparation of the template for sequencing reaction, the plasmid prepared with TELT method was re-precipitated by addition of 7/10 volume of isopropanol. The pellet was washed with 200 µl 70% ethanol and air-dried before resuspended in 20 µl ddH₂O. The concentration was determined with NanoDrop® Spectrophotometer ND-100 (peQlab, Germany).

A 10 µl sequencing PCR reaction contained 200-300 ng of the plasmid template, 1 µl 10 µM primer, 2 µl 5x Big Dye® Terminator sequencing buffer (supplied with the kit), 2 µl sequencing

mix and appropriate volume of ddH₂O. The thermocycle program was performed with activating the enzyme and denaturing the DNA template at 96°C for 2 min, followed by 26 cycles of DNA denaturation at 96°C for 30 sec, annealing at 55°C for 45 sec and extension at 60°C for 4 min.

The sequencing reaction product was then purified as following. 1 µl 3 M sodium acetate, 1 µl 125 mM EDTA and 50 µl of 100% ethanol were added in the reaction mixture and gently mixed. After incubated at room temperature for 5 min, this mixture was centrifuged at full-speed for 15 min in a bench centrifuge. The supernatant was removed and the pellet was washed with 250 µl of 70% ethanol and centrifuged at full-speed for 5 min. The pellet was air-dried and submitted for the nucleotides sequencing assay.

3.1.8 *In vitro* synthesis of sense RNAs

To prepare synthetic capped RNA, the SP6 mMessage-mMachine™ Kit (Ambion) was used according to the manufacturer's protocol. A 20 µl reaction contains 1-1.5 µg linearized plasmid template, 2 µl 10x reaction buffer, 10 µl 2x NTPs/Cap, 2 µl enzyme mix. Transcription was carried out at 37°C for 2.5 hr. The DNA template was removed by addition of 2 U DNaseI followed by incubation at 37°C for 30 min. The mRNA was purified with the RNeasy Mini Kit (Qiagen) according to the manufacturer's protocol and eluted with 20 µl RNase-free H₂O. The concentration of synthesized RNA was determined using the NanoDrop® Spectrophotometer ND-1000 (peQlab, Germany), and the quality was examined on a 1% agarose gel. The synthesized RNA was stored in aliquots at -20°C.

3.1.9 *In vitro* synthesis of anti-sense RNAs

The preparation of digoxigenin-labeled antisense RNA was carried out in a 25 µl reaction mixture containing 1-1.5 µg linearized template plasmid, 5 µl 5x Transcription buffer (Fermentas), 2 µl 0.1 M DTT, 0.5 µl RNase OUT (Invitrogen), 1 µl RNA polymerase (Fermentas), and 4 µl Digoxigenin-Mix (a mix of 10 mM ATP, 10 mM GTP, 10 mM CTP, 6.5 mM UTP, and 3.5 mM Dig-11-UTP, Roche). The reaction mixture was incubated at 37°C for 2.5 hr, and the DNA template was removed by addition of 2 µl DNaseI (Fermentas) and the following incubation at 37°C for 30 min. Antisense RNA probe was purified with the RNeasy Mini Kit (Qiagen) according to the manufacturer's protocol and eluted with 35 µl RNase-free H₂O. The purified RNA probe was stored at -20°C and diluted in hybridization mix according to the intensity of the *in situ* hybridization signal.

3.1.10 Extraction of the total RNA from staged embryos

2-4 embryos were collected in an eppendorf tube and immersed with 400 µl Trizol. After vortex for 3 min, the embryos were completely disrupted with a fine syringe. The embryo lysate was centrifuged at room temperature for 5 min. The supernatant was transferred to a new tube and

then added with 0.2 volume of chloroform. This two-phase mix was vortexed for 30 sec and centrifuged at 4°C for 10 min. The aqueous supernatant (around 200 µl) was transferred to a new tube and re-extracted with an equal volume of chloroform (vortex for 30 sec followed by centrifugation at 4°C for 5 min). The supernatant was transferred to a new tube, mixed with an equal volume of isopropanol, and left to stand at -20°C for 30 min. The precipitated RNA was isolated by centrifugation at maximal speed at 4°C for 30 min. After washed with 400 µl 70% ethanol and air-dried, the pellet was resuspended in RNase free H₂O (20-30 µl). Genomic DNA was removed by applying 1µl DNase I (Fermentas) and the following incubation at 37°C for 30 min. Finally, the RNA was further purified by RNeasy Mini Kit (Qiagen) according to the manufacturer's protocol and eluted in 20-30 µl RNase-free H₂O.

3.1.11 Extraction of the total RNA from adult frog tissues

The tissue samples as well as a mortar and pestle were pre-chilled in liquid Nitrogen. The tissues were then grounded to powder with the pre-chilled mortar and pestle. The tissue (50-100 mg) was homogenized in 1.0 ml of TRIZOL reagent by sequentially passing it 10 or more times through needles (0.8, 0.55, 0.33 diameter) fitted to an RNase-free syringe. 200 µl of chloroform was added to the homogenized lysate, mixed by inverting 15 sec and allowed to stand at room temperature for 2-3min. The sample was then centrifuged for 15 sec at 10,000 rpm at 4°C. The upper aqueous phase which contained the RNA was transferred into a fresh tube. The RNA was precipitated from the aqueous phase by mixing it with 0.5 ml of isopropanol and left to stand at -20°C for 30 min. It was then centrifuged at 10,000 rpm for 10 min at 4°C. The supernatant was discarded and the pellet was washed with 70% ethanol and centrifuged at 10,000 rpm for 5 min at 4°C. The RNA pellet was air-dried and then suspended in 90 µl of DEPC H₂O. Genomic DNA in the RNA sample was digested with 4 µl DNase I (Fermentas) in the supplied buffer at 37°C for 20 min. Finally, the RNA was further purified by RNeasy Mini Kit (Qiagen) according to the manufacturer's protocol and eluted in 20-30 µl RNase-free H₂O.

3.1.12 Reverse transcriptase-polymerase chain reactions (RT-PCR)

The first strand cDNA was synthesized with the RevertAidTM H Minus First Strand cDNA Synthesis Kit (Fermentas) according to the manufacturer's protocol with minor modification. 100 ng of the total RNA from staged embryos or adult tissue was mixed with 1 µl random hexamer primer (0.2 µg/µl) and filled with DEPC H₂O to a volume of 12 µl. After gently mixed and briefly span down, the mixture was incubated at 70°C for 5 min. Afterwards, the mixture was immediately chilled on ice and the drops were collected by brief centrifugation. Being placed on ice, the mixture was further added with 4 µl 5x reaction buffer, 1 µl RibolockTM Ribonuclease Inhibitor (20 u/µl), 2 µl 10 mM dNTP mix and 1µl Reverse Transcriptase (200 u/µl). This

reaction mixture with a final volume of 20 μl was incubated at 25°C for 12 min and then 42°C for 60 min, followed by heating at 70°C for 10 min to stop the reaction.

A standard 12.5 μl of PCR reaction contained 2.5 μl cDNA obtained from RT reaction, 0.7 μl of 25 mM MgCl_2 , 1 μl 10x PCR buffer (supplied with *Taq* polymerase, without MgCl_2), 0.5 μl of specific primer mixture (forward and reverse primers, 7.5 μM for each), 0.05 μl *Taq* polymerase (5 u/ μl , Fermentas), and 7.75 μl ddH₂O. The forward and reverse primers used for detection of *H4* expression were H4-f and H4-r respectively and for *XRxL* were RxL-234-f and RxL-547-r.

PCR program used are shown as follows: pre-denaturation at 94°C for 2 min, 24 (for *H4*) or 32 (for *XRxL*) cycles of denaturation at 94°C for 45 sec, annealing at 56°C (*H4*) or 58°C (*XRxL*) for 45 sec and extension at 72 °C for 45 sec, followed by final extension at 72°C for 10 min.

The PCR products were separated on a 1.7% agarose gel and imaged with Bio-Rad Gel Doc 2000 (Bio-Rad, USA).

3.2 *In vitro* transcription-translation assay

In vitro transcription-translation assay was used to analyze the ability of RxL-MOs to suppress the translation of *XRxL*. It was performed in a 12.5 μl reaction with the TnT®-Coupled Reticulocyte Lysate System (Promega) according to the manufacturer's user manual. The reaction mixture contained 6.25 μl TnT® Rabbit reticulocyte lysate, 0.5 μl TnT® Reaction buffer, 0.25 μl amino acid mixture (1 mM, minus Methionine), 0.25 μl RNase OUT ribonuclease inhibitor (40 u/ μl , Invitrogen), 200 ng of circular *XRxL*/pCS2+ plasmid or *XRxL*-full-length/pCS2+ plasmid as the template, indicated amount (0, 1 or 2 μl) of morpholino nucleotideoligos (1 mM), 0.25 μl TnT® SP6 RNA Polymerase, 0.5 μl L-[³⁵S] Methionin (1,000 Ci/mmol at 10 mCi/ml) and appropriate amount of DEPC-H₂O to fill to a final volume of 12.5 μl . The reaction mixture was incubated at 30°C for 1.5 hr.

After the incubation, an equal volume of 2x SDS gel loading buffer was mixed with the reaction mixture and heated at 95°C for 5 min. Proteins generated from the *in vitro* transcription-translation reaction were then analyzed on a 12% polyacrylamide gel marked with a the Prestained Protein Ladder (Fermentas). The gel was run at 30mA, 200V through the starting gel, and then run at 50mA, 200V. After electrophoresis, the gel was dried at 70°C for 2 hr and then exposed on a Kodak BioMax XAR film (Kodak) in a Kodak X-Omatic cassette (Kodak) overnight. On the next day, the film was developed and the proteins with different molecular weight could be visualized.

3.3 Handling and manipulation of *Xenopus* embryos

3.3.1 Preparation of embryos from *Xenopus laevis*

One day before egg collection, female albino and pigmented *Xenopus laevis* frogs was primed with 50-100 U of human chorionic gonadotropin (HCG). For induction of full ovulation, 500-1000 U HCG was injected into the dorsal lymph sac of frogs 10 hr prior to egg collection. Eggs were fertilized *in vitro* with minced testes in 0.1x MBS, dejellied with of 2% cystein hydrochloride (2% L-cystein hydrochloride, pH 7.8-8.0), and cultured in 0.1x MBS. Albino embryos were stained with Nile Blue solution after dejellied. Embryos were staged according to Nieuwkoop and Faber (Nieuwkoop and Faber, 1967).

3.3.2 Microinjection

The microinjection needles were prepared with borosilicate glass capillaries (Harvard apparatus, UK) using the Narishige PN-30 needle puller (Narishige, Japan). The needles were back-filled using microloaders (Eppendorf). Prior to microinjection, embryos were transferred to 1x MBS and then arranged on a glass slide with a little buffer left. The injection was performed with a pneumatic PicoPump PV820 injector (Helmut Saur Laborbedarf, Germany) on a cooling plate. A volume of 5 nl mixture of desired synthetic RNA or morpholino oligonucleotides (MOs) with the synthetic β -gal RNA was injected in a dorsoanimal blastomere of embryos at the 4-cell stage. After injection, the embryos were cultivated in 1x MBS in Petri dishes for 1 hr and then in 0.1x MBS till the desired stages.

Embryos were fixed in MEMFA at the desired developmental stage for 30 min. After washing three times for 10 min in PBS, embryos were transferred to X-Gal/red-Gal/rose-Gal staining solution until staining was sufficient. Afterwards, the embryos were re-fixed in MEMFA for 1.5 hr. For whole-mount *in situ* hybridization assay, embryos were sufficiently dehydrated with absolute ethanol and stored at -20°C. For PH3 immunostaining and TUNEL assay (see below), embryos were dehydrated with methanol and stored in Dent's solution at -20°C for at least 24 hr prior to use.

3.3.3 Lipofection

The retinoblasts targeted-lipofection was performed with NF stage 17/18 *Xenopus* embryos according to the protocol from Ohnuma et al. (Ohnuma et al., 2002b) with minor modification.

The DNA sample for lipofection was prepared by mixing a DNA plasmid purified with Midi-Prep kit (Qiagen) with DOTAP, a lipofection reagent (Roche). The ratio of DNA and DOTAP is always 1 μ g of DNA to 3 μ l of DOTAP. Thus, for the control group, where only eGFP was lipofected, 2 μ g of eGFP/pCS2+ was mixed with 6 μ l DOTAP. For the experimental group, 2 μ g of the plasmid harboring the interested gene in a pCS2+ vector and 1.5 μ g of eGFP/pCS2+ were

mixed with 10.5 μg DOTAP. DOTAP was kept on ice and added to the plasmid briefly before loading the mixture in a glass needle (same as microinjection).

Because MOs are uncharged, they need to be paired to a complementary DNA (carrier oligomer) to be transfected (Marcus et al., 1996). The carrier oligomer is a 26-mer DNA which is partially complimentary to the MO. A solution (0.5 mM) of partially paired MO (special delivery morpholino, SD-MO) was prepared by mixing 15 μl of 1 mM morpholino solution, 8.05 μl of 1.33 mM carrier oligomer solution and 6.95 μl ddH₂O. For lipofection, 3.6 μl SD-MO (0.5 mM) and 1.5 μg eGFP plasmid were mixed with 11.5 μl DOTAP. DOTAP was added briefly before loading the mixture in a glass needle.

Embryos at NF stage 17/18 were arranged with the anterior side upward in an agarose mold covered with 0.1x MBS in a Petri dish. The tip of a glass needle loaded with lipofection mixture was opened with a fine forceps to release 1-2 nl of liquid with a single pulse of injection. The tip of the needle was introduced into the embryo's retinal area just under the epidermis and 4-10 nl of the lipofection mixture was injected by several pulses. Both retinal areas of each embryo were lipofected.

After injection, embryos were kept in a 0.1x MBS solution until NF stage 41-42. To analysis the cell fate determination, embryos were fixed with 4% paraformaldehyde at room temperature for 2 hr and then embedded for cryostat section.

3.4 Analysis Methods

3.4.1 Whole-mount *in situ* hybridization (WMISH)

The whole-mount *in situ* hybridization was performed according to a three days procedure as described previously (Hollemann et al., 1998).

Day 1:

Embryos were rehydrated through the ethanol series (75%, 50% in dH₂O and 25% in PTw) for 5 min in each step, followed by the intensive 4 times washing with PTw for 5 min. Embryos were then digested with 10 $\mu\text{g}/\text{ml}$ Proteinase K (Sigma) in PTw at room temperature for 10-20 min according to the stage of the embryos. Subsequently, embryos were washed twice with 0.1 M triethanolamine (pH7.5) for 5 min and acetylated by sequentially twice addition of 12.5 μl acetic anhydrite into the 5 ml embryos incubation tube fully-filled with 0.1 M triethanolamine (pH7.5) and incubated at room temperature for 5 min after each addition. After washed twice with PTw for 5 min, embryos were re-fixed with PFA at room temperature for 20 min. Afterwards, embryos were washed 5 times with PTw for 5 min and rinsed with 1ml mixture of equal volumes of PTw and hybridization mix. After a preincubation in 500 μl hybridization mix at 65 °C for 10 min, the embryos were pre-hybridized in 1 ml hybridization mix at 65°C for 6 hr. Embryos were then

hybridized overnight in 1 ml hybridization solution containing the appropriate amount of antisense probe at 65 °C.

Day 2:

The probe/hybridization mix was recovered and stored at -20°C for reuse. The embryos were refilled with 1 ml hybridization mix and incubated at 60°C for 10 min, followed by 3 times washing with 2x SSC at 60 °C for 15 min each time. Unspecifically bound antisense probe was digested by an RNase Mix (20 µg/ml RNase A, 10 U/ml RNase T1 in 2x SSC) at 37°C for 60 min. Embryos washed once with 2x SSC for 10 min at room temperature and then twice with 0.2x SSC at 60°C for 30 min. The procedure afterward was performed under ambient temperature except specified. After washed twice with MAB for 15 min, embryos were blocked in MAB/BMB for 20 min and then in MAB/BMB/HS for 60 min. Embryos were incubated in MAB/BMB/HS containing 1:5000 diluted anti-Digoxigenin/AP (Roche) for 4 hr. After incubation, embryos were washed 3 times with MAB for 10 min and then overnight at 4°C.

Day 3:

Embryos were washed 5 times with MAB for 5 min and then equilibrated twice in the chilled APB for 10 min. After transferred to a pre-cooled color reaction solution (APB containing NBT and BCIP), embryos were incubated on ice in dark until the sufficient staining was reached. The staining reaction was stopped by directly changing the staining solution to methanol. The following twice replacement of fresh methanol helped to reduce the background. Embryos were rehydrated through a methanol series (75%, 50% and 25% methanol) for 5 min in each step and stored in MEMFA at 4°C.

3.4.2 Whole-mount immunostaining of PH3

Whole-mount PH3 assay was performed according to the protocol as described (Dent et al., 1989) with minor modification.

After fixed with MEMFA, embryos were dehydrated through a methanol series (25%, 50%, 75% methanol in dH₂O and 100% methanol) and then transferred to Dent's solution (20% DMSO in methanol, v/v). After Dent's solution were refreshed twice, embryos were stored at -20°C at least overnight before the procedure was continued.

Embryos were rehydrated through a methanol series (100%, 75%, 50% methanol in dH₂O and 25% methanol in PBS, 5 min for each step) followed by 3 times washing with PBS for 5 min. Unspecific binding was blocked by incubation of embryos with 20% horse serum in PBS at room temperature for 4 hr. Embryos were incubated overnight with 1 to 200 diluted anti-phosphohistone H3 (anti-PH3, Upstate Biotechnology, USA) in PBS containing 20% serum and 5% DMSO at 4°C.

On the following day, the antibody solution was recovered, added with 0.02% Azid and stored at 4°C for reuse. To remove the unbound antibody, embryos underwent intensive washing steps:

twice with PBS-TB for 2 hr, once with PBS-TBN for 2 hr, 3 times with PBS-TB for 5 min, and then were kept in PBS-TB overnight at 4°C.

The secondary antibody (anti-rabbit/AP, Sigma-Aldrich) was applied with 1:1000 dilution in PBS containing 20% serum and 5% DMSO. After incubation with the secondary antibody for 5 hr at room temperature, the embryos were intensively washed twice with PBS-TB for 30 min, once with PBS-TBN for 30 min, 3 times with PBS-TB for 5 min and then kept in PBS-TB overnight at 4°C.

The color reaction was performed as in the whole-mount *in situ* hybridization assay. After equilibrated twice with APB, embryos were incubated in a NBT/BCIP color reaction solution at 4°C in dark. It took 2 days to reach an intensive staining.

The color reaction was stopped by transferring embryos to 100% methanol, and the methanol was refreshed few times until the background color could not be washed off anymore. Embryos then rehydrated through a methanol series of 75%, 50% and 25% methanol in dH₂O and were stored in MEMFA at 4°C till subjected to plastic section.

3.4.3 TdT-mediated dUTP digoxigenin nick end-labeling (TUNEL) assay

The TdT-mediated dUTP digoxigenin nick end-labeling (TUNEL) assay was performed according to the protocol from Hensey and Gautier (Hensey and Gautier, 1998) with minor modification. The procedure was done at room temperature except specified.

Embryos stored in Dent's solution at -20°C were rehydrated with the methanol series (100% methanol, 75%, 50% methanol in dH₂O and 25% methanol in PBS, 5 min for each step) and then washed twice with PBS for 5 min. Embryos were further washed twice with PBTw and then twice with PBS. Each washing step lasted for 15 min. After equilibrated with TdT buffer (5x TdT buffer diluted in PBS) for 1 hr, embryos were incubated in 200 µl TdT buffer containing 0.5 µM digoxigenin-11-dUNP (Roche) overnight with the 5 ml glass vials upright on a nutator. To terminate the TdT activity, embryos were incubated twice in PBS/EDTA at 65°C for 1 hr. After washed 4 times with PBS for 1 hr each time and PBT for 15 min, embryos were blocked with 20% horse serum in PBS for 1 hr and then incubated in 20% horse serum in PBS containing a 1:2000 dilution of anti-Digoxigenin/AP (Roche) overnight at 4°C.

To remove the unbound antibody, the embryos were washed 6 times in PBT for 1 hr each time and subsequently washed overnight in PBT at 4°C.

The color reaction was then performed as described for WMISH assay.

3.4.4 Immunostaining on sections

The cryostat sections (see below) were rehydrated 3 times in PBS for 5 min. The embryo sections were permeabilized and blocked with the permeabilization solution for 60 min at room temperature. The sections was applied with the first antibody diluted in the antibody buffer (1:50

dilution for anti-calbindin monoclonal antibody and 1:300 for anti-calbindin polyclonal antibody), covered with coverslips, and incubated overnight at 4°C.

After the sections were intensively washed 5 times with PBS for 5 min, the secondary antibody, Cy3-conjugated anti-mouse was applied with a dilution of 1:500 in PBS. After incubation at room temperature for 1-2 hr in dark, the sections were washed with PBS containing 1:10,000 diluted DAPI for 10 min and then 5 times with PBS (5 min for each time). The sections were mounted with FluorSave™ Reagent and the fluorescence images were documented with a microscope Nikon Eclipse E600 (Nikon, Japan) installed with a camera Vosskühler CCD-1300QLN (Vosskühler, Germany).

3.5 Histological Methods

3.5.1 Vibratome section

Specimens of embryos after whole-mount *in situ* hybridization were transferred to PBS and then infiltrated in gelatin-albumin solution for 20 min. 1.5 ml gelatin-albumin was mixed with 105 µl 25% glutaraldehyde on ice for 1 min and poured into the plastic mold (Polyscience) to make the lower layer. The infiltrated embryos were then transferred on the solidified gelatin-albumin layer. After the solution around the embryos was carefully removed, the upper layer was prepared as the lower layer and filled over the embryos. Sections (30 µm) were cut on a Leica VT1000S vibratome (Leica, Germany) as described previously (Hollemann et al., 1999) and mounted with Mowiol.

3.5.2 Cryostat section

Lipofected embryos were fixed with 4% PFA and then washed with PBS for 3 times 5 min before transferred to 30% sucrose. The tubes were kept straight up until the embryos sank to the bottom of the tubes. The embryos were transferred to a plastic mold (4-6 embryos per mold). After the sucrose solution was removed, Tissue-Tek® O.C.T.™ Compound (Sakura Finetek Europe, Neatherlands) was filled in the mold to immerse the embryos. The embryos in each mold were arranged with dorsal sides upward and aligned with all eyes in one line. The mold was then immediately put on a smooth surface of a dry-ice block. After solidification, the blocks were stored at -80°C until sectioning.

The embryo-embedded blocks were equilibrated for 30 min in the cryostat (Microm HM500 OM, Germany). The embryos were cut transversally in ribbons of 10-12 µl thick sections with the cryostat temperature at -26°C and block temperature at -14°C.

3.5.3 Plastic section

The embryos were embedded in Technovit 7100 (Heraeus Kulzer) according to the manufacturer's protocol. Before the embryos were treated for embedding, the lower layer of the embedding block was prepared. 1.5 ml of the infiltration medium (10 mg/ml Harder I in Technovit 7100, filtrated with 0.2 μ m filter (Sartorius, Germany)) was mixed with 0.1 ml Harder II on ice for 1 min and poured in a disposable plastic tissue embedding mold (Polyscience, USA). It takes roughly 1 hr for solidification.

Embryos were dehydrated with gradually increased concentrations of ethanol solutions until 100% ethanol. The embryos were washed with 100% ethanol for 10 min for two more times followed by preinfiltration medium (a mixture of equal volumes of Technovit 7100 and 100% ethanol) for 2 times 10 min. The embryos were then equilibrated twice with the infiltration medium for 5 min and kept in infiltration medium until embedding.

Embryos were transferred on the solidified lower layer and the solution around the embryos was removed with a pipetman. After the embryos were properly oriented, the upper-layer medium was prepared as the lower-layer and filled over the embryos. After 1 hr, the mold was covered with parafilm and kept overnight at 37°C.

The mold was removed and the block was tailored to fit a single embryo with leaving a 2 mm edge to each side of embryos. The block was fixed on a block-holder with glue and then loaded on the machine. 5-6 μ m thick sections were cut with a Leica RM2255 Microtome (Leica, Germany) and floated on a slide covered with 25% ethanol. After dried on a heating plate at 42°C, the slide was mounted with Entellan (Merck) and covered with cover-slide.

4 Results

4.1 Cloning of a novel retina homeobox-containing gene from *Xenopus laevis*, *XRxL*

Various homologous *Rx* genes have been identified from many vertebrate species, such as zebrafish (dr), medaka fish (ol), mouse (mm), chick (gg), human (hs), and bovine (rn) (Chen and Cepko, 2002; Chuang et al., 1999; Deschet et al., 1999; Furukawa et al., 1997a; Loosli et al., 2001; Mathers et al., 1997; Ohuchi et al., 1999; Wang et al., 2004). Generally, two different paralogous *Rx* genes play different roles during eye development in a certain species, except rodent. In *Xenopus*, however, only one *Rx* paralog, *XRx1*, had been reported at the beginning of this study (Mathers et al., 1997), we therefore tried to identify other retinal homeobox containing genes, by BLAST search of the *Xenopus* ESTs at [http:// xenopus.nibb.ac.jp](http://xenopus.nibb.ac.jp).

One clone containing two amino acids divergent from *XRx1* within the homeobox region (the boxed amino acid residues in Figure 4.2) was identified in a normalized *Xenopus* tailbud (NF stage 25) library and obtained from the National Institute of Basic Biology (Japan), being referred to as *Xenopus Rx-like* (*XRxL*). Genbank accession number is DQ360108. This clone contained an open reading frame (ORF) encoding for a predicted protein of 228 amino acids flanked with partial 3'- and 5'-UTRs. The ORF was amplified by PCR using the designed forward and reverse primers (Oligonucleotides: RxL-EcoRI-f and RxL-XhoI-r) and subcloned into the pCS2+ vector for further study. The nucleotide- and amino acid-sequences of *Xenopus* RxL ORF are shown in Figure 4.1A.

Rx genes belong to the *aristaless*-related *paired-like* homeobox gene family (Meijlink et al., 1999). Members of this subfamily of homeobox protein are primarily defined by four conserved domains (Bopp et al., 1986; Mathers et al., 1997; Strickler et al., 2002): (i) an N-terminal octapeptide (OP), (ii) a paired class homeobox, (iii) an *Rx* domain, and (iv) a C-terminal paired tail or OAR domain. However, in *XRxL*, the N-terminal octapeptide is absent (Figure 4.1B, Figure 4.2), which is similar to the chick homolog, cRaxL. The comparison of the protein sequences similarity between *XRxL* and cRaxL or *XRx1* revealed that *XRxL* shows higher homology with cRaxL than with *XRx1* (Figure 4.1B).

A

AA: M F L D K C E G D L C D L R E D G S
 N: ATG TTT CTA GAC AAA TGT GAA GGA GAT TTG TGT GAC TTG AGG GAA GAC GGC AGC
 Nr: 9 18 27 36 45 54

T P T R G T P E E D N E I P K K K H R R
 ACA CCA ACG CGT GGC ACT CCT GAG GAG GAT AAT GAG ATA CCT AAA AAG AAA CAC CGC AGG
 63 72 81 90 99 108

N R T T F T T Y Q L H E L E R A F E R S
 AAT CGA ACA ACA TTC ACA ACC TAC CAG CTT CAT GAA TTA GAG CGT GCC TTT GAG CGT TCA
 123 132 141 150 159 168

H Y P D V Y S R E E L A M K V S L P E V
 CAC TAT CCT GAT GTA TAC AGT CGA GAA GAG CTA GCT ATG AAG GTC AGC CTG CCA GAG GTT
 183 192 201 210 219 228

R V Q V W F Q N R R A K W R R Q E K L E
 CGA GTT CAG GTT TGG TTC CAG AAT AGA CGA GCA AAA TGG AGG CGG CAA GAG AAA CTG GAG
 243 252 261 270 279 288

S S S S T L H D S P L L S F S R S P R A
 TCT TCC TCT AGC ACA CTA CAT GAT TCC CCA CTA CTA TCT TTC TCA AGA TCC CCA AGA GCT
 303 312 321 330 339 348

T T M G P L S N T L P L E S W L T S P I
 ACA ACT ATG GGG CCT CTG AGC AAT ACT CTT CCT CTG GAA TCC TGG CTC ACT TCA CCA ATC
 363 372 381 390 399 408

S G T T T I H S M P A F M A P S Q A L Q
 TCA GGG ACT ACC ACC ATC CAC AGT ATG CCA GCA TTC ATG GCT CCT TCC CAG GCC CTT CAG
 423 432 441 450 459 468

P T Y P S H T F L N S G P A M T P I Q P
 CCA ACT TAC CCA AGT CAC ACA TTT TTG AAC AGT GGC CCT GCA ATG ACC CCT ATC CAA CCT
 483 492 501 510 519 528

L S S A P Y H Q C M G G F A D K F P L E
 CTC AGC AGT GCT CCT TAT CAT CAG TGT ATG GGG GGA TTT GCG GAC AAA TTT CCC TTA GAG
 543 552 561 570 579 588

E M D Q R S S S I A A L R M K A K E H I
 GAA ATG GAT CAA AGA AGT TCA AGC ATT GCT GCA CTG AGA ATG AAG GCA AAG GAG CAC ATC
 603 612 621 630 639 648

Q T I D K T W Q P I
 CAG ACG ATA GAT AAA ACA TGG CAG CCA ATC TGA
 663 672 681

B

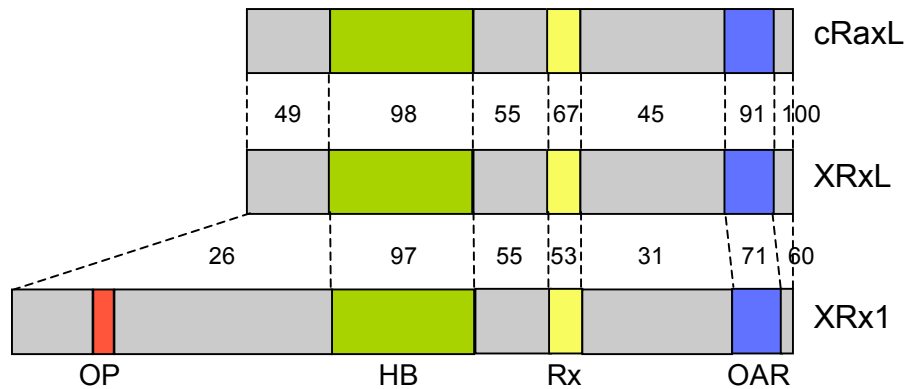


Figure 4.1 The newly identified member of vertebrate *Rx* gene family, *Xenopus RxL*. (A) The nucleotide sequence (N) and the deduced amino acid sequence (AA) of the ORF of *XRxL*. Numbering (Nr) is according to the nucleotide sequence. The conserved homeobox (green), Rx (yellow) and OAR (blue) domains are highlighted. (B) Comparison of the similarity of the predicted protein sequences between cRaxL and XRxL, XRxL and XRx1 respectively. Numbers represent the percentages of similarity between the corresponding domains, determined with MegAlign (DNASTAR, USA). OP, octapeptide; HB, homeobox; Rx, Rx domain; OAR, OAR domain.

4.2 *XRxL* belongs to the “vertebrate Rx-Like” subgroup of the *Rx* genes

The identification of *Xenopus RxL* added one more member to the *Rx* gene family. The known paralogs of *Rx* genes in other species seem to play different roles in eye development. To predict the possible function of *XRxL*, we applied a phylogenetic approach to identify the conservation and divergence based on the primary structures of all reported *Rx* gene-encoded proteins. All *Rx*-type gene sequences were obtained from GenBank and the deduced amino acid sequences were aligned using MegAlign program (DNASTAR, USA). The alignment of the octapeptide, homeobox, Rx domain and OAR domain of *Rx*-type proteins is shown in Figure 4.2. The sequences of the most conserved homeobox and OAR domain were used to construct the phylogenetic cycle (Figure 4.3).

The result clearly shows that all of the 34 *Rx* genes from 27 species could be grouped into four categories: (i) the invertebrate *Rx* genes, (ii) the classical vertebrate *Rx* genes, (iii) the vertebrate *Rx-Q50* genes (QRx), and (iv) the vertebrate *Rx-like* genes.

	octapeptide RxxSIxAl	homeobox	Rx-domain	OAR-domain RxxSIxAL		
Classical vertebrate Rx	hs_rax 31 RUHSTEALIGF pt_rax 31 im_rax 31 mm_rax 31 rn_rax 31 md_rx 31 gg_rax1 31 xl_rx1a 30 xl_rx2a 30 ol_rx3 33 dr_rx3 30 am_rx1 35 dr_rx1 35 dr_rx2 35 ol_rx2 35 xl_rxl 34 oa_rx 36 gg_rax2 34	134 KKHRRNRTFTTYQLHELBRAFEKSHYPDVIYGRLELAGKVNILPEVVRVQVWFRRAKWRQEKLE 134 134 134 134 134 120 128 128 101 104 140 135 133 135 34 36 34	239 LPLESLGPPPL 239 239 239 239 240 214 222 222 190 194 241 229 227 229 128 130 128 116 116 116 116 116 116 482 613 444 178 197 197 234 166 537	318 ADPRNSSIAALRIKAKEH1QA 318 319 314 313 322 289 297 297 267 266 306 301 300 299 200 203 200 156 156 156 187 156 156 727 844 690 254 250 256 491 319 237 759	346 347 342 350 317 322 325 292 292 334 332 327 327 231 228 184 184 184 215 184 184 758 819 282 306 306 528 528 266 826	
Vertebrate Rx-like	am_rx1 35 dr_rx1 35 dr_rx2 35 ol_rx2 35 xl_rxl 34 oa_rx 36 gg_rax2 34	140 135 133 135 34 36 34	241 229 227 229 128 130 128 116 116 116 116 482 613 444 178 197 197 234 166 537	306 301 300 299 200 203 200 156 156 156 187 156 156 727 844 690 254 250 256 491 319 237 759	334 332 327 327 231 228 184 184 184 215 184 184 758 819 282 306 306 528 528 266 826	
Vertebrate Rx-Q50	hs_raxL pt_raxL im_raxL md_raxL bt_qrx cf_rxl	25 25 25 34 25 25	116 116 116 116 116 116	156 156 156 187 156 156	184 184 184 215 184 184	
Invertebrate Rx	aa_rx 117 dm_rx 114 dp_rx 114 hb_rx 27 tc_rc 32 jw_rx 23 sp_rx 58 sk_rx 72 nv_rx 22 ci_rx 102	IDR-YR-S-Q PR-T-D--L PR-T-D--L PR-D--L PR-T-DN--L PR-D--L PS--D--M PS--D--L NI--D--K DET--PSG-SH	395 526 347 89 108 88 265 143 83 555	--VDP--S-- --VDP--S-- --VDP--S-- --GDP--T--G --MDP--S-- --MDP--S-- --MDP--S-- --DP--N--L --L-- --L-- --L-- --R--	--M-TN--S-I-- --M-SN--T-I-- --M-SN--T-I-- --TT--O--MR--VES --L--TT-- --H--T--Q--MR--YVET --S--VT--O--M--LEN --S--VS--M--EIN --E--S--T--LES --SOARDEPRENTANE--SN-S	LEN LDN LDQ VES VEN YVET LEN EIN LES SN-S

Figure 4.2 Amino acid sequences alignment of conserved domains of predicted Rx proteins. Amino acid sequences were deduced from nucleotide sequences of the *Rx/Rax* cDNAs found in Genbank. The accession numbers are shown in Appendix. All the amino acid residues identical with human *Rax1* (*hs_rax*) are represented by dashes. Gaps required for optimal alignment are represented by dots. Members belonging to the same group are highlighted in green (classical vertebrate Rx), yellow (vertebrate Rx-like), orange (vertebrate Rx-Q50) and blue (invertebrate Rx) respectively. The conserved glutamine (Q) fingerprint of mammalian Rx-Q50 members, where glutamate (E) is the substitute of the N-terminal amino acid of each domain in the corresponding Rx-protein. Numbers in bold in *Xenopus* RxL is in bold. Numbers in italic indicate the position of the N-terminal amino acid of each domain in the corresponding Rx-protein. Numbers in bold in the last line represent the total number of amino acids of the corresponding Rx-protein. The similar sequences located in the octapeptide and the OAR-domain are highlighted in gray. In XRxL (*xl_rxl*) homeobox, the two amino acids divergent from the XRx1 (*xl_rx1a*, *xl_rx2a*) homeobox are in boxes. #, represents the sequence QLTLILLSLSQ.

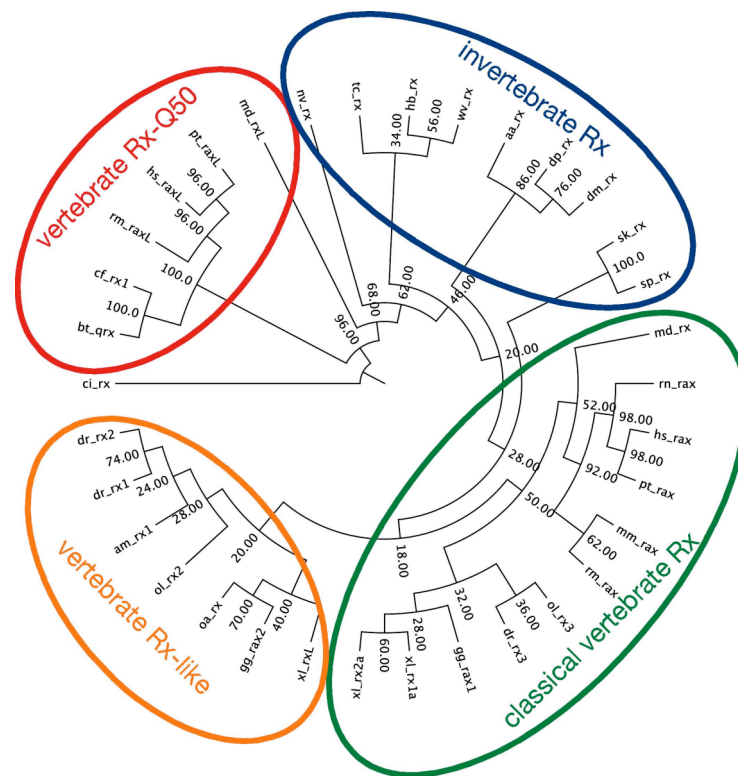


Figure 4.3 The phylogenic cycle of the all known Rx/Rax homeoproteins. The amino acid sequences were deduced from nucleotide sequences of the *Rx/Rax* cDNAs in Genebank (the accession numbers are shown in Appendix). The phylogenic cycle was constructed according to the alignment of the amino acid sequences of homeobox domain and OAR domain. *Xenopus* RxL belongs to the “vertebrate Rx-like” group.

The first group contains all *Rx*-type proteins from invertebrates, which seem to possess only one *Rx* gene in each species. The second group, the “classical vertebrate *Rx*” genes, which are homologous to the first identified *Rx* gene in *Xenopus*, *Rx1*, is highly conserved among all vertebrates. In addition, mammals possess a second *Rx*-type (*QRx*) gene, characterized by the truncated N-terminus, four conserved exchanges within the homeobox (Q/E, A/K, H/N, R/K, Figure 4.2, amino acids in red) and a subtype-wise conserved OAR domain, which together define the third group, the group of “vertebrate *Rx-Q50*”. Lower vertebrates also have a second *Rx*-type protein, which makes up the fourth group, the group of “vertebrate *Rx-like*”. Members of this group also contain a sub-group specific OAR domain, and are often truncated at N-terminus as well, but their homeobox are much more similar to members of the “classical vertebrate *Rx*” group than to *QRx*. Thus, all vertebrates with the exception of murinae (mouse and rat) seem to contain two different *Rx* versions, although *Xenopus* and zebrafish possess two copies of a certain version (i.e. *xl_rx1a* and *xl_rx1b* in *Xenopus laevis* and *dr_rx1* and *dr_rx2* in zebrafish), which most likely results from the partial polyploidy of these animals.

The newly identified *XRxL* gene is defined as a *Xenopus* homologous gene in the group of “vertebrate *Rx-like*” (Figure 4.3). Therefore, it is not surprising that the amino acid sequence of

XR x L shows even higher identity with the chick homolog cRaxL (68%) than with its *Xenopus* paralog XR x 1 (59%), although its homeobox domain is 96.7% homologous to that of XR x 1 (Figure 4.1B).

4.3 Temporal and spatial expression of XR x L

The expression pattern of *RxL* was examined in staged embryos of *Xenopus laevis* by whole-mount *in situ* hybridization (WMISH). A faint, nevertheless spatially restricted expression of *XR x L* was first observed within the emerging eye vesicles at late neurula stage (NF stage 19; Figure 4.4A), much earlier than reported before (Pan et al., 2006b). Expression of *XR x L* increased in subsequent stages within the developing eye and reached highest levels at tadpole stage (NF stage 35; Figure 4.4A-E). From stage 22 to 31, a gradient distribution of *XR x L* expression in the optic vesicle was observed, with a stronger expression in the dorsal side than the ventral side (Figure 4.4B-D). When *XR x L* expression reached highest level at NF stage 35, it was only restricted to the outer nuclear layer (ONL) and the CMZ of the retina (Figure 4.4E,E'). The expression pattern of *XR x L* largely differs from that of *Xenopus Rx1*, which is already strongly expressed within the eye field territory at early neurula stage, NF stage 14, (Mathers et al., 1997) and is expressed all over the retina at tadpole stage with the strongest expression in the CMZ (Figure 4.4 F).

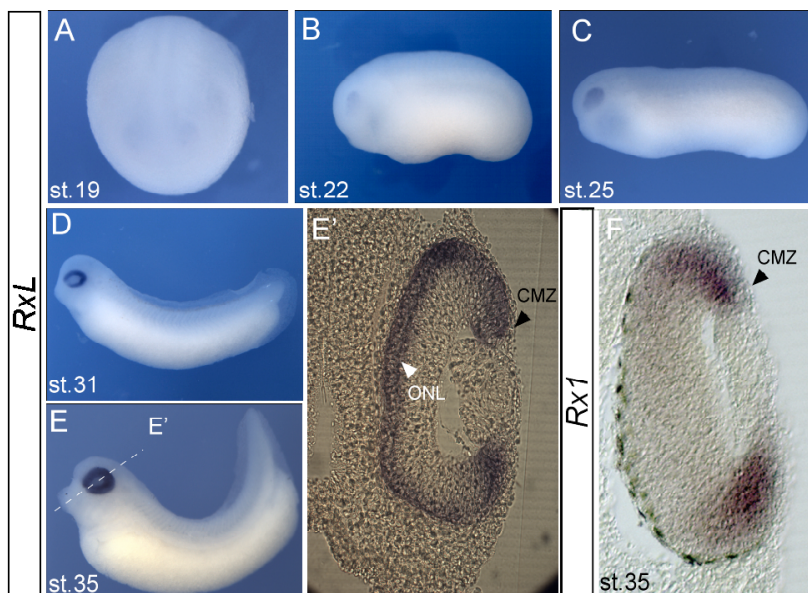


Figure 4.4 The temporal and spatial expression of *RxL* during development of *Xenopus laevis*. (A-F) Whole-mount *in situ* hybridization analysis of staged embryos with a *Xenopus RxL* (A-E') or *Rx1* (F) antisense riboprobe. (A) NF stage 19 neurula, anterior view with dorsal side upward. (B-E) NF stage 22, 25, 31 and 35 embryos respectively, with the anterior side to the left. (E') Transversal section of the embryo shown in E as indicated by white dashes, with dorsal side upward. The section shows that *RxL* expression is restricted to the ONL (white arrowhead) and the CMZ (black arrowhead) at NF stage 35. (F) Transversal section of an NF stage 35 embryo, in which *Rx1* is expressed all over the NR and strongly expressed in the CMZ (black arrowhead). CMZ, ciliary marginal zone; ONL, outer nuclear layer.

(A) NF stage 19 neurula, anterior view with dorsal side upward. (B-E) NF stage 22, 25, 31 and 35 embryos respectively, with the anterior side to the left. (E') Transversal section of the embryo shown in E as indicated by white dashes, with dorsal side upward. The section shows that *RxL* expression is restricted to the ONL (white arrowhead) and the CMZ (black arrowhead) at NF stage 35. (F) Transversal section of an NF stage 35 embryo, in which *Rx1* is expressed all over the NR and strongly expressed in the CMZ (black arrowhead). CMZ, ciliary marginal zone; ONL, outer nuclear layer.

To confirm the temporal expression pattern of *XRxL*, RT-PCR was performed with RNA extracted from the staged embryos. Since there is 52.5% nucleotide sequence identity between *Xenopus RxL* and *RxI* genes, we carefully picked the primers (Oligonucleotides: RxL-234-f and RxL-547-r) in a region where *RxL* nucleotide sequence is largely divergent from that of *RxI* to avoid the cross-amplification between *Xenopus RxL* and *RxI*. The first significant expression of *RxL* was detected at NF stage 19 (Figure 4.5A), confirming the results of WMISH, although very weak expression was detectable at even gastrula stage (NF stage 12.5, Figure 4.5A). *XRxL* expression remained at a weak level until tailbud stage (NF stage 24), but showed a burst at early tadpole stage (NF stage 31), and then peaked at NF stage 35 (Figure 4.5A), when photoreceptor cell differentiation is initiated (Decembrini et al., 2006; Locker et al., 2006). At later stages, e.g. stage 42, *RxL* expression still remained.

RT-PCR was also carried out with RNA extracted from various tissues of the adult frog. The results showed that *XRxL* is expressed in eye, brain, kidney, lung, liver, pancreas, stomach and ovary, and at lower level in heart, intestine and testis, but no expression could be detected in skin and muscle (Figure 4.5B)

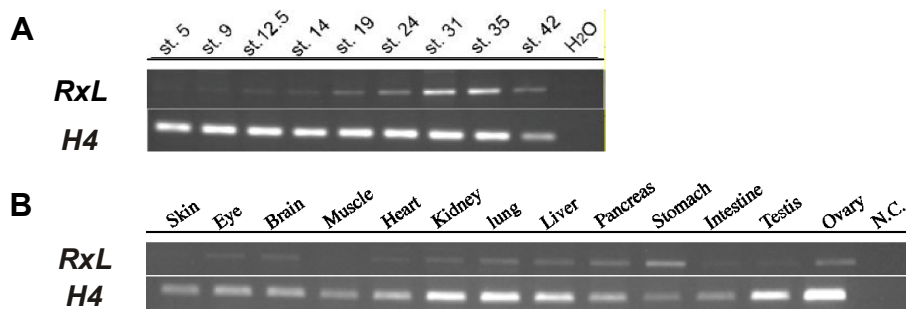


Figure 4.5 Expression level of *RxL* in the embryonic stages and the adult tissues of *Xenopus laevis*. (A-B) Analysis of expression of *RxL* by RT-PCR with total RNA extracted from whole embryos at indicated stages (A) or with total RNA extracted from indicated adult tissues (B). The expression level of *Histone 4* (*H4*) was examined in parallel as a control.

4.4 *XRxL*-specific morpholinos inhibit the translation of endogenous *XRxL* *in vitro*

In order to analyze the function of *XRxL* during eye development, *XRxL*-specific antisense morpholino oligonucleotides (morpholinos, MOs) were used to inhibit the expression of *XRxL* *in vivo*. Two morpholinos were designed, referred to as RxL-MO1 and RxL-MO2. RxL-MO1 specifically targets the region of the last 15 nucleotides of the 5'-UTR and the first 10 nucleotides of the ORF of the *XRxL* transcript, while RxL-MO2 specifically targets the 25 nucleotides in the 5'-UTR of the *XRxL* transcript (Figure 4.6A). To confirm the function of these two morpholinos, an *in vitro* transcription and translation assay was performed using the TnT®-Coupled Reticulocyte Lysate system. Two target plasmids were examined in this experiment. One plasmid,

referred to as RxL-ORF, contained the complete ORF region of *XRxL* gene, which presumptively generates the transcript similar to the injected synthetic RNA; the second plasmid, referred to as RxL-full-length, contained the *XRxL* ORF flanked by 5'- and 3'-UTRs (Figure 4.6B), which is supposed to generate the transcript mimicking endogenous *RxL* mRNA. As expected, RxL-MO1 slightly inhibited the translation of RxL-ORF transcript, while RxL-MO2 did not affect the expression of this transcript (Figure 4.6C). On the other hand, both morpholinos strongly blocked the translation of RxL-full-length transcript, whereas the standard control morpholino (Cont-MO) did not affect the translation of either RxL-ORF or RxL-full-length (Figure 4.6C). These results clearly show that, at least *in vitro*, the translation of endogenous *RxL* could be efficiently and specifically inhibited by either RxL-MO1 or RxL-MO2.

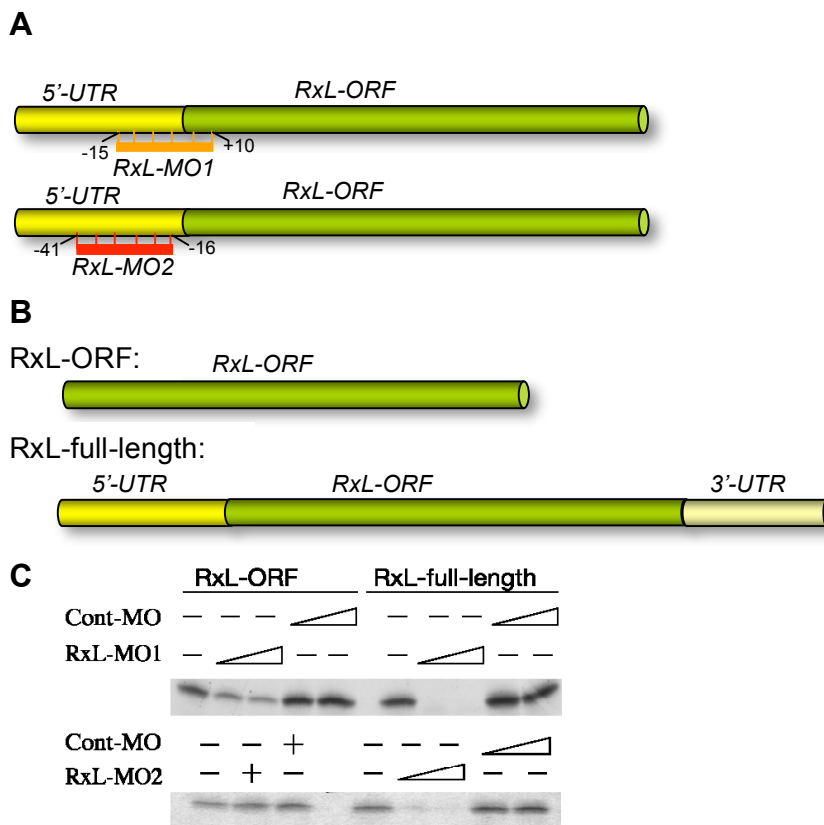


Figure 4.6 RxL-MOs specifically inhibited the translation of endogenous *RxL* *in vitro*. (A) Schematic diagrams showing the respective targets of RxL-MO1 and RxL-MO2. RxL-MO1 targets a sequence spanning the 5'-UTR and the ORF of *RxL*, and RxL-MO2 targets the 5'-UTR of *RxL*. (B) Schematic representation of the target transcripts used in the *in vitro* transcription and translation assay. (C) The specificity of

RxL-MOs examined by the *in vitro* transcription and translation system. RxL-MO1 slightly inhibited the translation of RxL-ORF, while RxL-MO2 had no effect on the translation of RxL-ORF. Both morpholinos blocked the translation of RxL-full-length, whereas control morpholino (Cont-MO) did not affect the translation of either transcript.

4.5 Specific inactivation of *XRxL* function impairs photoreceptor formation

To analyze the effects of *XRxL* deficiency, either 2.5 pmol RxL-MO1 or 1.6 pmol RxL-MO2 and synthetic β -gal RNA were co-injected into one of the dorsoanimal blastomeres of embryos at the 4-cell stage. More than 60% of those embryos showed a reduction in eye size on the injected side

(Table 1, Figure 4.7B,C). Plastic sections of such embryos revealed that in the eye of the RxL-MO injected side, photoreceptor cells were arrayed in the ONL much more loosely than those in the non-injected side (Figure 4.7B-C'', and inserts). In the RxL-MO injected embryos, the optic vesicles are evaginated, in contrast to the effects of *XRxl* loss-of-function, which inhibits the evagination of optic vesicle (Mathers et al., 1997). However, microinjection of Cont-MO did not cause any malformation of the injected eye (Figure 4.7A-A'').

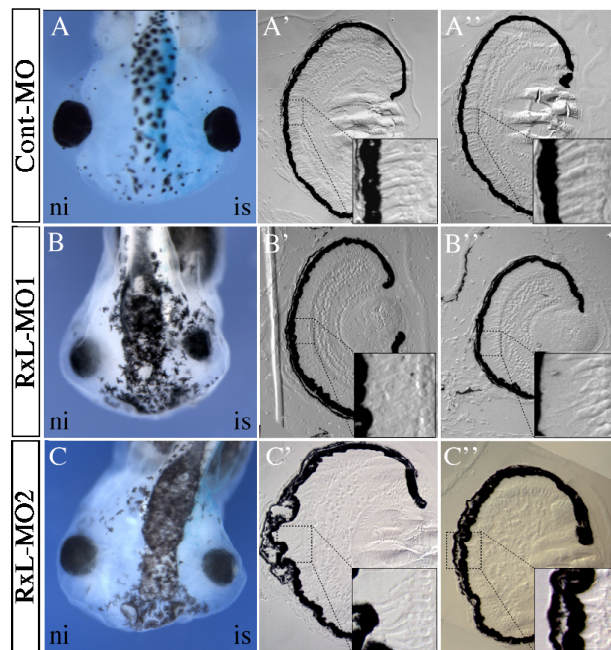


Figure 4.7 Interference of photoreceptor formation caused by microinjection of RxL-MOs. (A-C'') NF stage 44/45 embryos co-injected with β -gal RNA and MO in one of the dorsoanimal blastomeres at the 4-cell stage. (A,B,C) Dorsal views of embryos injected with 2.5 pmol Cont-MO (A), 2.5 pmol RxL-MO1 (B), or 1.6 pmol RxL-MO2 (C), with the injected side to the right. (A',B',C', A'',B'',C'') Transversal sections of the eye on the non-injected side (A',B',C') and the injected side (A'',B'',C'') of embryos shown in A, B, and C respectively. The inserts show the details of the photoreceptor layer of each retina.

Table 4.1. Quantification of eye phenotypes upon microinjection of RxL-MOs

Probes injected (pmol/ embryo)	<i>n</i> *	Normal (%)	Reduced eye size (%)	Enlarged eye size (%)
None (Control)	164		17.1**	
Cont-MO 2.5	52	65.4	19.2	15.4
Cont-MO 1.6	46	78.3	19.6	2.2
RxL-MO1 2.5	105	29.5	64.8	5.7
RxL-MO1 1.6	50	54	40	6
RxL-MO2 2.5	35	22.9	68.6	8.6
RxL-MO2 1.6	26	26.9	65.4	7.7

**n*, the total number of NF stage44/45 embryos injected with the indicated probes.

**This datum represents uninjected wild-type control embryos with eyes in different size, since there is no X-Gal staining on the embryos.

The phenotypes caused by microinjection of RxL-MOs motivated us to further investigate the function of *RxL* during retina development on the molecular level. Since microinjection of both morpholinos gave rise to an identical phenotype, Rx-MO2 was used in the most of the rest of experiments, simplified as RxL-MO, except special indication.

4.6 Suppression of *XRxL* function does not affect the initiation of eye formation

Several transcription factors, summarized as eye field transcription factor (EFTFs), are required for eye formation. In order to understand the role of *RxL* within this network, we investigated the effects of *XRxL* suppression on the expression of *Pax6*, *Rx1* and *Six3*. These transcription factors are strongly expressed in the anterior neural plate and involved in specification of the eye anlagen at early neurula stages (NF stage 14/15) (Chow and Lang, 2001). Embryos were injected with RxL-MO into one of the dorsoanimal blastomeres at the 4-cell stage and then analysed by WMISH for expression of *Pax6*, *Rx1* and *Six3* at various stages. Compared with the control groups (Figure 4.8G, 94.1%, $n=16/17$) for *Pax6*, 92.5%, $n=37/40$ for *Rx1*, and 100%, $n=8/8$ for *Six3*), the expression of *Pax6*, *Rx1* and *Six3* was not affected by RxL-MO injection at early neurula stages (NF stage 14/15) (Figure 4.8A-C,G; 90.6%, $n=29/32$ for *Pax6*; 83.3%, $n=30/36$ for *Rx1*; 81.8%, $n=27/33$ for *Six3*). However, at stage 24, when *RxL* is significantly expressed (Figure 4.4A, Figure 4.5A), the expression of these genes was markedly reduced in the RxL-MO injected side (Figure 4.8D-F,H; 63.4%, $n=26/41$ for *Pax6*; 60%, $n=18/30$ for *Rx1*; 67.4%, $n=31/46$ for *Six3*). These results are in line with the determined expression pattern of *XRxL* (Figure 4.4, Figure 4.5). At NF stage 14/15, when *XRxL* expression is not detectable in the eye area, suppression of its function does not affect early eye field specification. However, at tailbud stages, when *XRxL* is significantly expressed in the eye area, eye morphogenesis is significantly interfered by the suppression of RxL function.

These results indicate that *Xenopus RxL* acts either downstream or in parallel to *Pax6*, *Rx1* and *Six3*, since *XRxL* is obviously not required for the activation of these genes. However, *XRxL* function is required for proper eye vesicle formation at tailbud stages, indicating that *XRxL* is indispensable in the normal eye development after it starts to be significantly expressed.

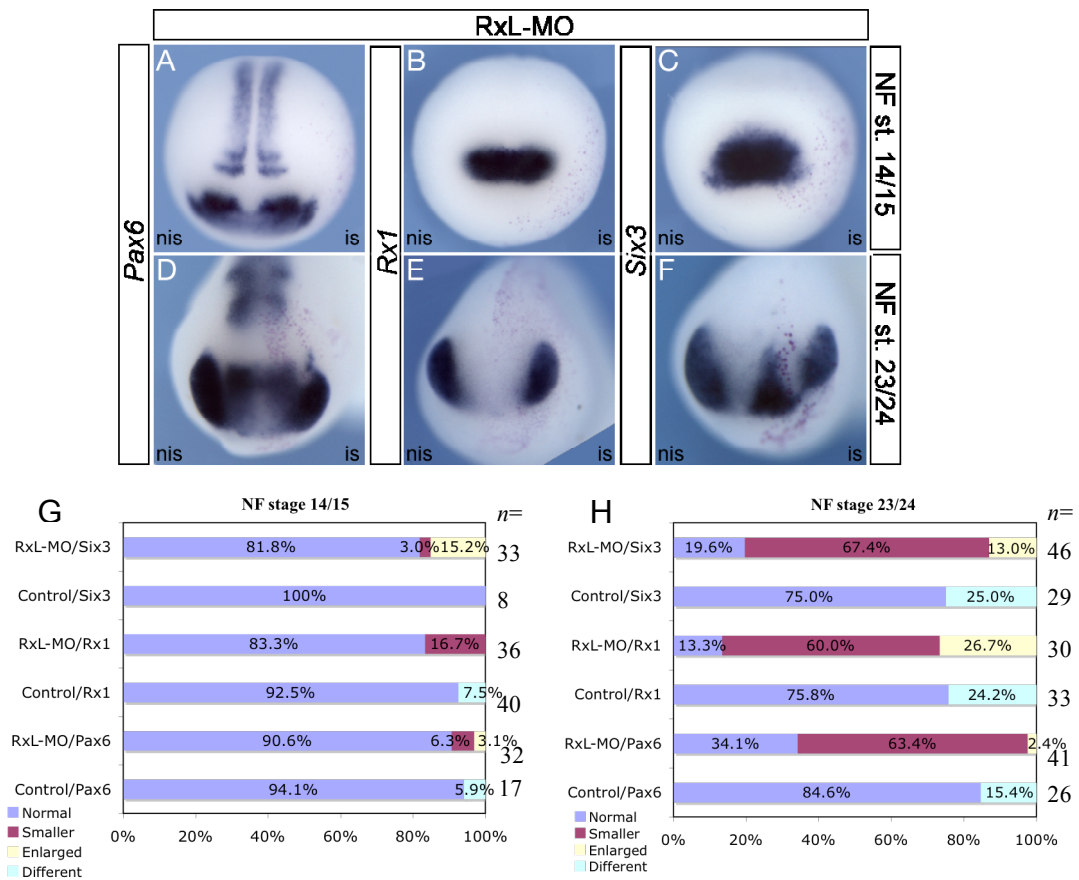


Figure 4.8 Effects of *RxL* loss-of-function on early eye development in *Xenopus laevis*. (A-F) WMISH analysis of staged embryos injected with RxL-MO in one of the dorsoanimal blastomeres at the 4-cell stage. The staining pattern of respective gene (dark blue) on the injected side (“is”, the right side of each embryo shown) was compared with that on the non-injected side (“nis”, left side). (A-C) At neurula stage (NF stage 14/15), expression of *Pax6* (A), *Rx1* (B) and *Six3* (C) was not affected upon inhibition of *RxL*. (D-F) At tailbud stage (NF stage 23/24), the expression of *Pax6* (E), *Rx1* (F) and *Six3* (G) was all seriously reduced in the MO injected sides. (G-H) Statistics of RxL-MO injected embryos showing effects on the expression area of *Pax6*, *Rx1* and *Six3* at NF stage 14/15 (G) and NF stage 23/24 (H) respectively. In control groups, the cases of embryos expressing the marker genes unequally in both sides are represented as “Different”.

The effects of *XRxL* deactivation on these EFTFs expression, sustained at tadpole stage (NF stage 34/35). Most of the RxL-MO injected embryos showed much smaller expression area of these genes (73.1%, $n=19/26$ for *Pax6*; 70%, $n=14/20$ for *Rx1*; 62.5%, $n=15/24$ for *Six3*) in the retina of the injected side, compared to the control side (Figure 4.9). However, the expression intensities of these genes were not significantly reduced (Figure 4.9B,B',D,D',F,F'). In addition, we also examined the effects of *Xenopus RxL* deficiency on the expression of *Otx5b*, which is involved in photoreceptor specification (Vicgian et al., 2003). Similar to the effects on EFTFs analyzed

above, the expression area of *Otx5b* in the retina was reduced on the RxL-MO injected side (66.7%, $n=8/12$), but the intensity remained virtually equal to the control side (Figure 4.9G-H').

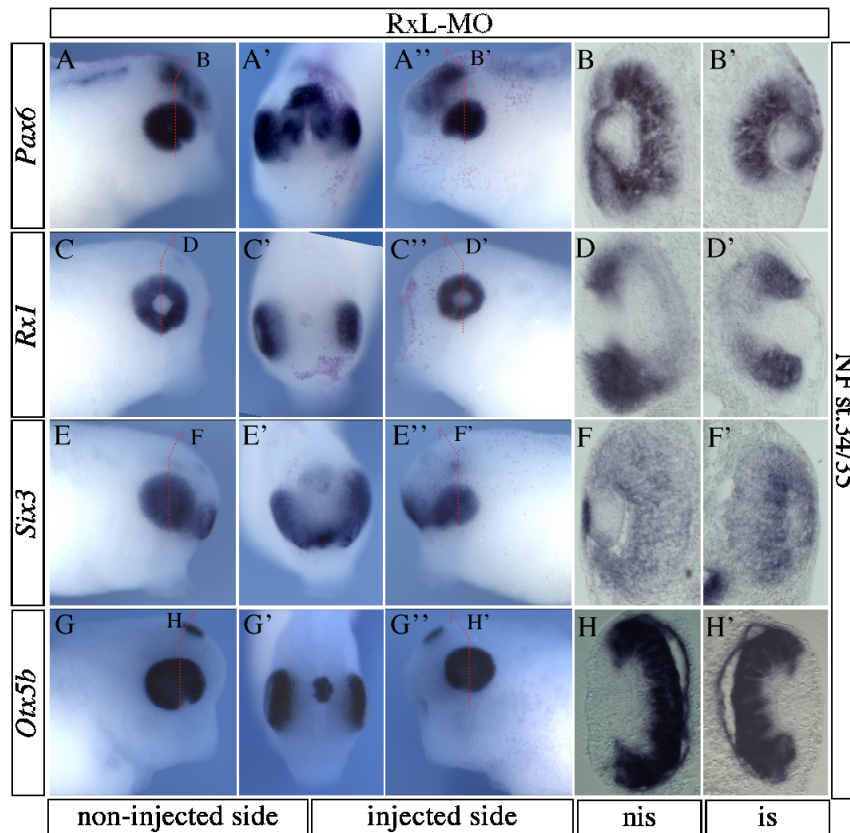


Figure 4.9 RxL-MO microinjection led to reduced expression areas of the early-expressed eye marker genes at tadpole stage. (A-H') WMISH analysis of NF stage 34/35 embryos injected with RxL-MO in one of the dorsoanimal blastomeres at the 4-cell stage. The embryos were examined with antisense riboprobe of *Pax6* (A-B'), *Rx1* (C-D'), *Six3* (E-F'), or *Otx5b* (G-H'). Each embryo is shown lateral

views of non-injected sides (A,C,E,G) or injected sides (A'',C'',E'',G''), and anterior views (A',C',E',G') respectively. (B,B',D,D',F, F',H,H') Transversal sections of eyes of each embryo as indicated by red dashes, with dorsal sides upward. RxL-MO injection led to a reduced expression area of these genes, whereas the intensity of their expression remained almost unchanged compared to the non-injected side. nis, non-injected side; is, injected side.

4.7 Suppression of *XRxL* led to reduced expression of photoreceptor markers

To investigate the impact of *RxL* in respect to retinal cell differentiation, the expression of some late-expressed eye marker genes were further examined in RxL-MO injected embryos. *Rhodopsin* (*Rho*), which marks photoreceptors, can be first detected at stage 33/34 and is abundantly expressed at stage 36/37 (Chang and Harris, 1997). RxL-MO injected embryos were collected at stage 36/37 and analyzed for the expression of *Rho* by WMISH. *Rho* expression is significantly reduced on the RxL-MO injected side, compared to the control side (Figure 4.10A-B'; 62.3%, $n=43/69$), with 5.8% of the embryos lacking *Rho* expression completely (Figure 4.10C-D'). It should be noted, although the expression areas of *Pax6*, *Rx1*, and *Six3* were also reduced due to RxL-MO injection, we never observed the complete loss of expression of any of these genes. To

analyze whether RxL-MO microinjection affects photoreceptor cell development or just impairs *Rho* gene, expression transcripts of another photoreceptor specific gene, *Arrestin* (*Arr*), were detected in RxL-MO injected embryos at the same stage (Korf et al., 1989). It turned out that the expression of *Arr* was also dramatically reduced upon RxL-MO injection (Figure 4.10E-F'; 48.9%, $n=23/47$).

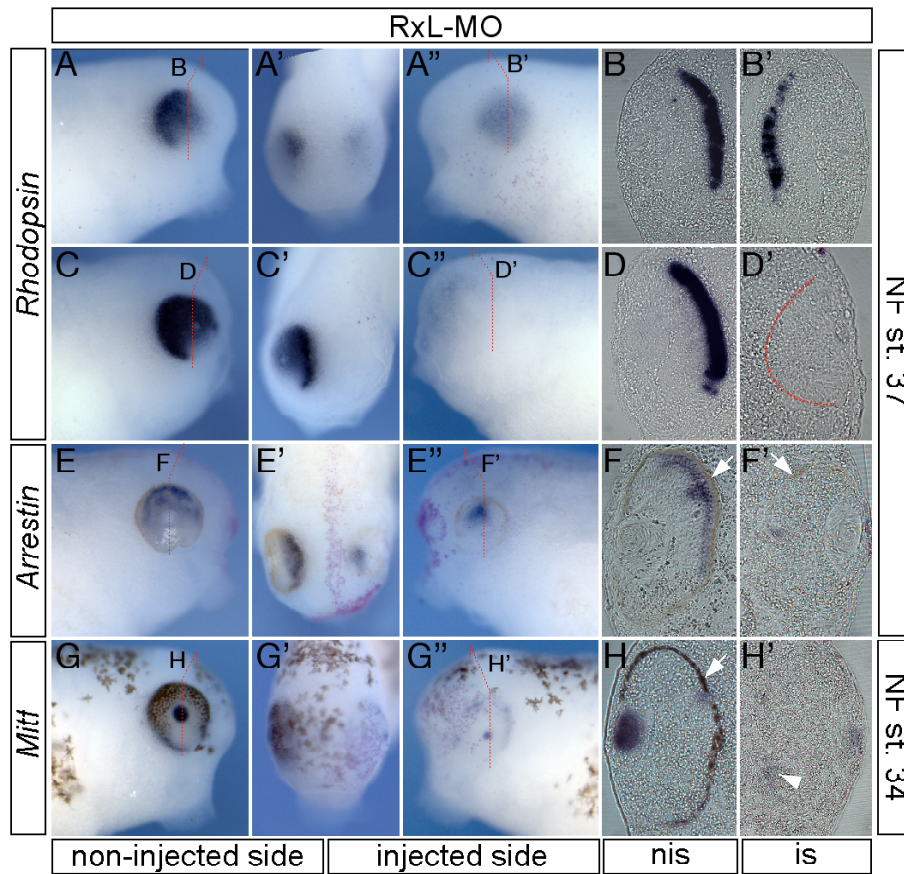


Figure 4.10
Effects of RxL-MO microinjection on the expression of retinal differentiation marker genes. (A-H') WMISH analysis on the staged embryos injected with RxL-MO in one of the dorsoanimal blastomeres at the 4-cell stage. The embryos were probed with Dig-labelled antisense RNA of *Rhodopsin*

(A-D'), *Arrestin* (E-F') or *Mitf* (G-H'). Embryos shown in A-D' are offsprings of albino parents, and therefore the pigmentation is not visible. Embryos shown in E-H' are offsprings of the albino female and the wild-type male, so that the RPE formation is visible at these stages. Each embryo is shown as the lateral view of the non-injected side (A, C, E, G) or the injected side (A'', C'', E'', G''), and the dorsal view (A', C', E', G') respectively. (B, B', D, D', F, F', H, H') Transversal sections of both eyes of each embryo as indicated by red dashes, with dorsal side upward. The red dashes in D' mark the RPE area. RxL-MO injection led to a dramatically reduced expression of *Rhodopsin* (A-B'), and in some cases, a complete loss of its expression (C-D'). Inhibition of XRxL also caused the reduced expression of *Arrestin* (E-F') and impaired RPE formation at this stage (E-F', white arrows). The RPE marker gene, *Mitf* is still expressed in the RxL-MO injected retina (H', arrowhead), although at weaker intensity compared to the control retina (G-H'). nis, non-injected side; is, injected side.

In the MO-injected embryos, the reduced RPE formation was more often observed in the RxL-MO injected side between NF stage 34/35 and NF stage 36/37 (55.2%, $n=32/58$, Figure 4.10E-F', white arrow), compared with embryos injected with Cont-MO (8%, $n=4/50$). However, at NF stage 39, the pigmentation of the RPE in the RxL-MO injected side usually reached a level equal to that in the control side (as shown in Figure 4.7). It seems that the RxL-MO injection led to a delay of RPE development. Therefore, the expression of a RPE marker, *Mitf* was examined in the RxL-MO injected embryos. *Mitf* is strongly expressed in the RPE and the epiphysis at stage 29/30. At stage 37/38, *Mitf* expression is reduced to almost undetectable levels in the RPE and the epiphysis, whereas appears in the lens (Kumasaka et al., 2004). As shown in Figure 4.10G-H'', at NF stage 33/34, *Mitf* was expressed in both the RPE and the lens of the eye in the RxL-MO injected side, but in a much weaker level compared to the control side (Figure 4.10G-H''; 48.4%, $n=15/31$), which may explain the delayed development of the RPE. However, since RPE development was only transiently repressed, the reduced *Mitf* expression might not be a direct consequence of the inhibition of XR_xL function.

4.8 RxL-MO microinjection causes apoptosis in the eye area

Since XR_xL expression was detected in the CMZ (Figure 4.4E') where the retinal proliferating cells reside (Perron et al., 1998), impaired eye formation upon RxL-MO injection may be due to a reduction of proliferating cells during eye development. Phosphorylated histone H3 (PH3) positive cells were examined to identify proliferating cells (Saka and Smith, 2001). It was found that at NF stage 30/31, the number of PH3 positive cells was significantly reduced in the RxL-MO injected side, compared to that in the control side (15.4/section vs. 20.5/section, $p<0.05$, Figure 4.11A,B). Since the numbers of PH3 positive cell in the body are similar between the injected side and the control side, this reduction of proliferating cells in the RxL-MO injected side is mainly due to the significantly reduced proliferating cells in the eye area (6.1/section vs. 9.5/section, $p<0.05$, Figure 4.11A,B). The Cont-MO injection did not cause significant change of the number of proliferating cells either in total (19.4/section vs. 20.5/section) or in the eye area (10.8/section vs. 9.5/section, Figure 4.11A,C). Therefore, RxL-MO microinjection led to a reduction of cell proliferation specifically in the eye area.

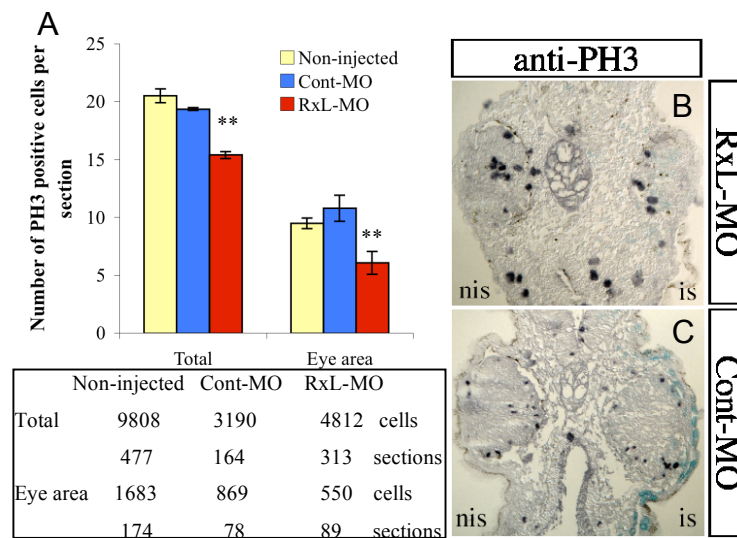


Figure 4.11 RxL-MO microinjection inhibited the cell proliferation specifically in the eye area. (A) Comparison of PH3 positive cell numbers (per section) in total or eye area among the non-injected side (yellow bars), Cont-MO injected side (blue bars), and RxL-MO injected side (red bars) of embryos at NF stage 30/31. The average of PH3 positive cell numbers on per section was

determined in each embryo. For non-injected, $n=5$ embryos; for Cont-MO, $n=2$ embryos; for RxL-MO, $n=3$ embryos. Values are given as means \pm s.e.m. Quantification of the counted cells and sections are shown in the frame. **, $p<0.05$, compared with the non-injected side. (B,C) Transversal sections of the NF stage 30/31 embryos injected with RxL-MO (B) or Cont-MO (C) in one of dorsoanimal blastomeres at the 4-cell stage, with the dorsal sides upward and the injected sides to the right.

The reduced number of proliferating cells could also be the consequence of the decreased survival of cells due to increased apoptosis. TUNEL assay was applied to detect apoptotic cells in whole-mount (Hensey and Gautier, 1998). Embryos injected with Cont-MO or RxL-MO into one of the dorsoanimal blastomeres at the 4-cell stage were subjected to TUNEL assay at NF stage 30/31. Inhibition of *RxL* function indeed increased the number of apoptotic cells approximate three folds (Figure 4.12A,C,D), compared to the retina in the non-injected side (8.6 per retina section vs. 2.6 per retina section). In contrast, injection with Cont-MO led to a number of apoptotic cells in the retina (2.28 per retina section) similar to that in non-injected side (2.6 per retina section, Figure 4.12A, B, D).

Taken together, although *RxL* does not induce eye formation in *Xenopus*, it is necessary for retinal progenitor cells to survive and develop properly. RxL-MO injection increased the number of apoptotic cells in retina, which may account for the reduced eye size within the injected side. In addition, the strongly impaired expression of photoreceptor-specific genes caused by *RxL* loss-of-function indicated that *RxL* might play a role in photoreceptor cell development.

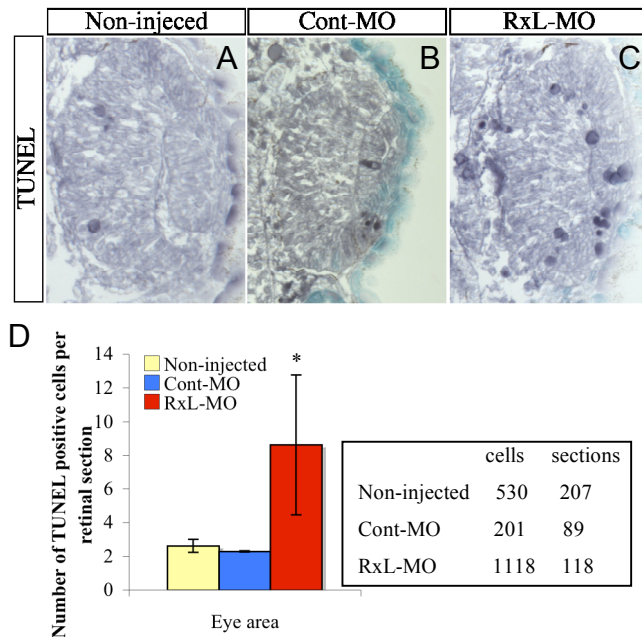


Figure 4.12 Increased apoptotic retinal cells caused by suppression of *XRxL* function. (A-C) Transversal sections of the retina in the non-injected (A), Cont-MO injected (B) or RxL-MO injected (C) side of NF stage 30/31 embryos, with dorsal sides upward. The dark-blue dots represent TUNEL positive cells. (D) Comparison of the number of TUNEL positive cells in eye areas of the non-injected (yellow bar), Cont-MO injected (blue bar) and RxL-MO injected side (red bar) of NF stage 30/31 embryos. The average of TUNEL positive cell number on per section was determined in each retina. For non-injected, $n=5$

retinas; for Cont-MO, $n=2$ retinas; for RxL-MO, $n=3$ retinas. Values are given as means \pm s.e.m. *, $p=0.28$, compared with the non-injected side. Quantification of the counted cells and sections are shown in the frame.

4.9 The temporally inducible *RxL* construct, *RxL-GR*

To further investigate the function of *XRxL* during eye development, gain-of-function experiments were performed. A temporally inducible *RxL* construct, *RxL-GR*, was applied in the gain-of-function experiments, which is the complete *RxL* ORF in-frame fused to the human glucocorticoid receptor ligand-binding domain (GR) (Figure 4.13A). When glucocorticoid receptor ligands are absent, the GR-fusion protein binds to hsp90 (Heat-shock protein 90) in the cytoplasm. Once a ligand is present, it competes with hsp90 for binding to the GR and releases the GR-fusion protein from hsp90, so that the GR-fusion protein, in this case, *RxL-GR*, could enter the nucleus and fulfill its function (Figure 4.13B) (Gammill and Sive, 1997). Thus, induction of the exogenous *RxL* function could be achieved by simply adding synthetic ligand, dexamethazone (Dex) into the embryo-growth medium at desired stages.

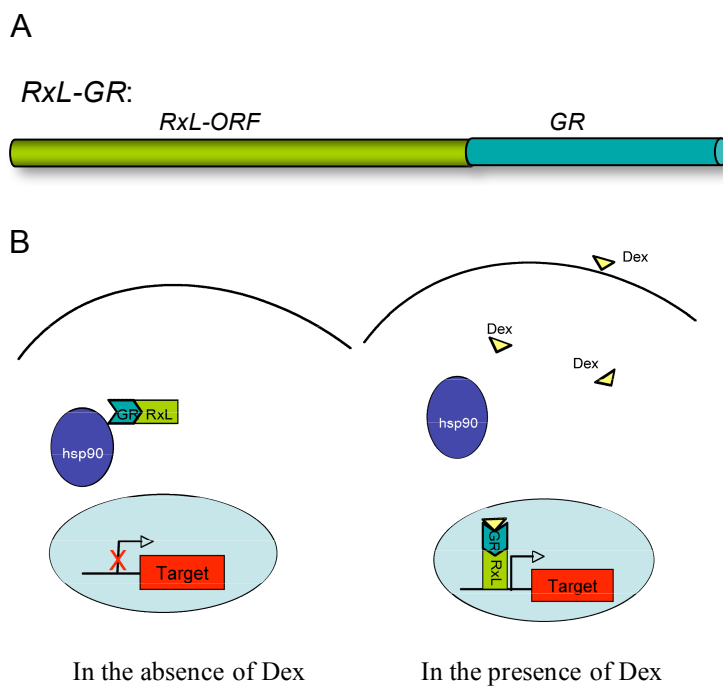


Figure 4.13 Schematic diagrams of the structure and working mechanism of inducible RxL-GR. (A) RxL-GR is constructed by in-frame fusion of *RxL ORF* and glucocorticoid receptor ligand binding domain (*GR*). (B) In the absence of the glucocorticoid receptor ligand, dexamethazone (Dex) (left), RxL-GR binds to hsp90 in the cytoplasm. With the presence of Dex (right), RxL-GR is released from hsp90 and enters into nucleus, where it can activate target genes.

4.10 Retina progenitor cells are not competent to XR_xL until late neurular stage

The expression of *XR_xL* was detected at around NF stage 14 by RT-PCR, and could be first visualized by WMISH at NF stage 19. Therefore embryos injected with synthetic *RxL-GR* RNA in a dorsoanimal blastomere at the 4-cell stage were induced by addition of Dex in the growth-medium at either NF stage 14 or NF stage 16/17. To examine whether *RxL* misexpression induces ectopic expression of early eye-patterning genes, we collected the embryos two stages later after induction and analyzed for the expression of *Rx1* and *Six3* by WMISH. We did not observe ectopic expression of either *Rx1* or *Six3* no matter RxL-GR was induced at early (NF stage 14) or late neurula stage (NF stage 16/17, Figure 4.14A, C). When the injected embryos were induced at NF stage 14, neither *Rx1* nor *Six3* expression was influenced two stages later (Figure 4.14Ab, Af, C). However, when RxL-GR function was induced at NF stage 16/17, extended *Rx1* and *Six3* expression domains were observed in the injected side at stage 19 (Figure 4.14Ad, Ah, C; 47.7% and 41.7% of embryos for *Rx1* and *Six3* respectively). These results indicated that the eye field is not competent to respond to XR_xL until late neurula stages, in line with the results of *XR_xL* loss-of-function (Figure 4.8). Interestingly, when the embryos induced at different stages were analyzed at stage 24, it was found that the early (NF stage 14) induction of RxL-GR activity led to a reduced expression area of *Rx1* and *Six3* (Figure 4.14Bb, Be, D; 90% and 83.9% for *Rx1* and *Six3* respectively), whereas later (NF stage 16/17) induction of RxL-GR function tended to enlarge their expression areas to some degree (Figure 4.14Bc, Bf, D; 43.5% and 30% for *Rx1* and

Six3 respectively). Although the late-induction could also lead to a reduced expression of *Rx1* and *Six3* (Figure 4.14D, 43.5% and 50% of embryos for *Rx1* and *Six3* respectively) in some embryos, the extent of the reduction was much less than that in the early-induced embryos (images not shown). As the control, the embryos injected with *RxL-GR* without Dex treatment mostly remained the expression of *Rx1* and *Six3* unaffected in the injected sides at examined stages (Figure 4.14Aa, Ae, Ac, Ag, Ba, Bd). The frequencies of variant *Rx1* and *Six3* expression in both sides of these embryos were comparable with those in the control embryos (Figure 4.14C, D).

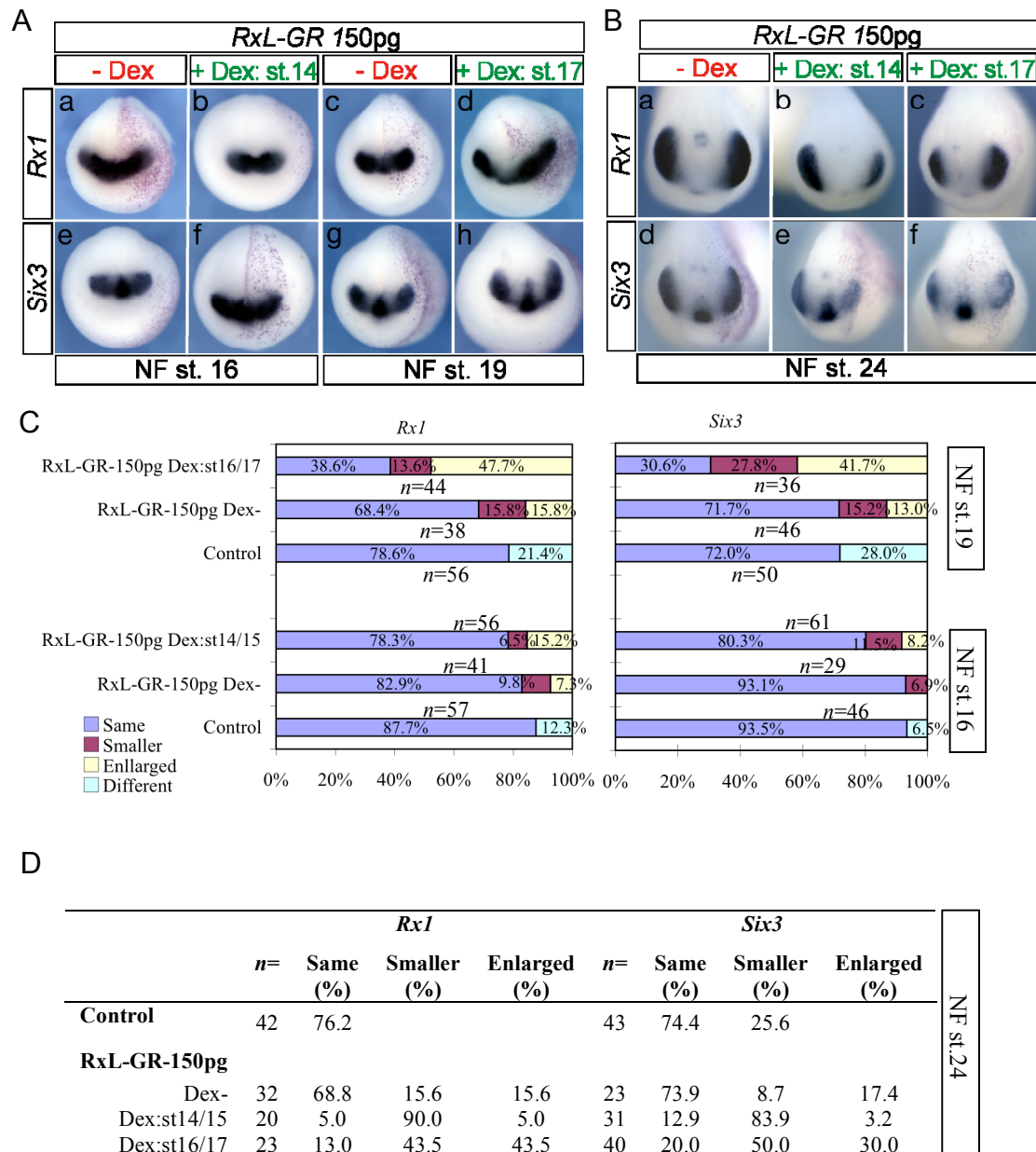


Figure 4.14 Effect of *RxL* gain-of-function on early eye development in *Xenopus*. (A, B) WMISH analysis of the embryos injected with 150pg synthetic *RxL-GR* RNA in one of the dorsoanimal blastomeres at the 4-cell stage, anterior views, with injected sides to the right. (A) Injected embryos were induced with dexamethazone (Dex) at NF stage 14 or stage 17 and analyzed for the expression of *Rx1* (Ab,Ad) and *Six3*

(Af,Ah) at stage 16 (Ab,Af) and stage 19 (Ad,Ah), respectively. As a control, *Rxl* (Aa,Ac) and *Six3* (Ae,Ag) expression patterns of non-induced embryos were also examined at the same stages. RxL-GR induction at NF stage 14 did not affect either *Rxl* or *Six3* expression two stages later (Ab, Af); however, induction at stage 17 led to enlarged expression areas of *Rxl* (Ad) and *Six3* (Ah) two stages later. The non-induced embryos showed unchanged expression of *Rxl* and *Six3* in the injected sides (Aa, Ac, Ae, Ag). (B) Injected embryos were induced with Dex at NF stage 14 (Bb, Be) or NF stage 17 (Bc, Bf) and analyzed for the expression of *Rxl* (Bb, Bc) and *Six3* (Be, Bf) at stage 24. As a control, the expression patterns of *Rxl* (Ba) and *Six3* (Bd) were examined in the non-induced embryos at stage 24. Embryos induced at NF stage 14 typically gave rise to a smaller expression area of *Rxl* (Bb) and *Six3* (Be), compared with the control side, while induction at NF stage 17 led to more embryos showing enlarged areas of *Rxl* (Bc) and *Six3* (Bf) expression in the injected sides. (C) Statistical analysis of RxL-GR injected embryos examined for the expression of *Rxl* (left) and *Six3* (right) two stages later after induced at NF stage 14 and 17 respectively. *n*, the total number of counted embryos. (D) Statistical analysis of RxL-GR injected embryos examined for the expression of *Rxl* and *Six3* at NF stage 24 when induced at NF stage 14 and 17 respectively.

Taken together, these results indicate that on one hand, retinal progenitor cells are not competent to respond to XRxL until late neurula stage, NF stage 17; on the other hand, premature activation of XRxL interfered with eye vesicle formation during further development. Thus, the induction of RxL-GR function by addition of Dex was performed at NF stage 16/17 for the rest of experiments.

4.11 XRxL overexpression induces additional photoreceptor formation

XRxL loss-of-function resulted in a reduced, sometimes even completely abolished expression of photoreceptor marker genes of the retina. This result led us to examine the expression of these genes after XRxL overexpression. Interestingly, injection of a small amount of *RxL-GR* RNA (25 pg at the 4-cell stage) could even robustly induce *Rho* expression in displaced photoreceptors, which often grew as dents or folds of the normal photoreceptor layer, invaginated into the INL (Figure 4.15B, white arrow). This happened with a quite high frequency in RxL-GR activated embryos (60.7% of analyzed embryos, *n*=17/28, Figure 4.15F), although the eye vesicles might be reduced in size compared to the control. In some cases, the ectopic photoreceptors induced by RxL-GR activation occurred in the inner nuclear layer (INL) posterior to the lens (as shown in an embryo injected with 50 pg *RxL-GR*, Figure 4.15C, arrows). When embryos were injected with a higher concentration of *RxL-GR* RNA (e.g. 150 pg), *Rho* expression invaded not only the INL (Figure 4.15D, white arrow), but also into the ganglion cell layer (GCL) (Figure 4.15D,E, black arrows). In some cases, ectopic *Rho* expression even appeared at discrete locations from the normal photoreceptor layer (ONL) (Figure 4.15C-E, black arrows). Nevertheless, ectopic *Rho* expression has never been observed outside of the eye. Therefore, induction of RxL-GR activity

caused the formation of ectopic photoreceptors at the expense of the INL, where amacrine and bipolar cells are located normally.

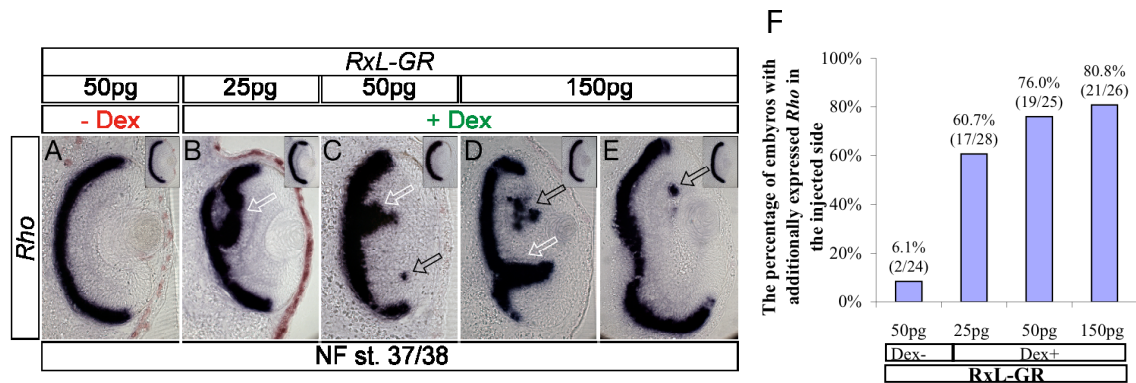


Figure 4.15 Additional photoreceptor formation induced by *XRxL* overexpression. (A-E) Transversal retinal sections of embryos injected with indicated concentrations of synthetic *RxL-GR* RNA into one of the dorsoanimal blastomeres at the 4-cell stage and analyzed for *Rho* expression with WMISH at NF stage 37/38. The non-injected retina of each embryo was shown in the insert. Embryos were not treated with Dex (A), or treated with Dex at NF stage 16/17 (B-E). Induction of *RxL-GR* function not only led to *Rho* expression in fold-like invagination from the ONL into the INL, or even the GCL (white arrows), but also to the discrete ectopic *Rho* expression spots in these layers (black arrows). (F) Statistic of *RxL-GR* injected embryos with ectopically expressed *Rho*.

The percentage of embryos with ectopically expressed *Rho* increased with the dosage of injected *RxL-GR* when treated with Dex at NF stage 16/17 (Figure 4.15F). A small proportion (6.1%) of *RxL-GR* injected embryos without Dex treatment also gave rise to ectopic *Rho* expression, which probably results from the lacking of GR-fusion protein as described in other studies (Gammill and Sive, 1997; Locker et al., 2006).

4.12 *XRxL* overexpression did not affect the proliferation of overall retinal progenitor cells

The ectopic photoreceptors caused by *XRxL* overexpression led us to question whether this results from an increased proliferation of a specific group of retinal progenitor cells which biased to become photoreceptors, or from an increased commitment of progenitor cells which would differentiate into photoreceptors. The number of proliferating cells was examined in the *XRxL* overexpressed embryos at NF stage 28/29 and 33/34 respectively, by means of detection of PH3 positive cells. At stage 28/29, the later-born cell types, including most of the photoreceptors are in a proliferative state, whereas in stage 33/34 embryos, the majority of photoreceptor cells exit the cell cycle, though most of the bipolar cells and Müller glia cells are still proliferating (Decembrini et al., 2006).

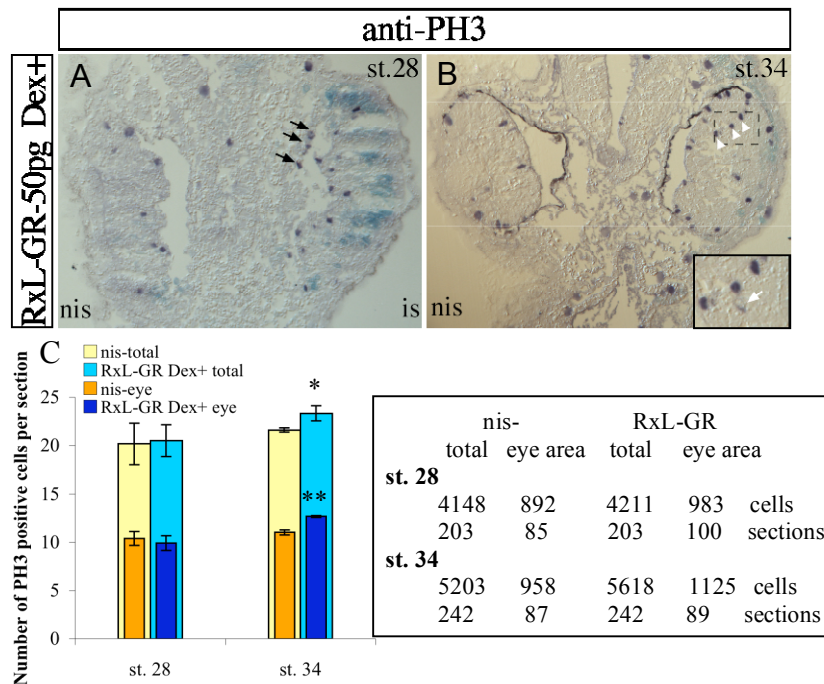


Figure 4.16 Slightly increased cells proliferation at tadpole stage caused by *RxL* gain-of-function. (A,B)

Transversal sections of PH3 immunostained NF stage 28 (A) or stage 34 (B) embryos injected with 50 pg *RxL-GR* in a dorsoanimal blastomere at the 4-cell stage and treated with Dex at stage 16/17, with dorsal sides upward and injected sides to the

right. Black arrows point to the proliferating cells in the presumptive RPE region in the injected side of an NF stage 28 embryo; white arrowheads show the proliferating cells located in the INL of the retina in the injected side of the NF stage 34 embryo; white arrow points to the ectopic RPE within NR. (C) Comparison of the numbers of PH3-positive cells in total or in the eye area between the non-injected side (yellow bars for total, orange bars for the eye area) and the RxL-GR activated side (light blue bars for total, dark blue bars for the eye area) of NF stage 28 and 34 embryos respectively. The average of PH3 positive cell number on per section was determined in each embryo. For stage 28 and stage 34 embryos, non-injected, $n=2$ embryos; RxL-GR activated, $n=2$ embryos respectively. Values are given as means \pm s.e.m. Quantification of counted PH3-positive cells and sections are shown in the frame. *, $p=0.25$; **, $p=0.07$ (student's *t*-test).

Comparison of the injected side with the control side of the RxL-GR activated (50 pg) embryos at NF stages 28/29 showed that the total numbers of PH3 positive cells were equal in both sides (20.5 per section in the injected side vs. 20.2 per section in the control side, Figure 4.16A,C). In addition, the number of proliferating cells in the eye area of the injected side was also similar to that of eye area in the control side (9.9 per retina section vs. 10.4 per retina section, Figure 4.16A,C). At this stage, we observed somewhat increased proliferative cells in the presumptive RPE region (black arrows in Figure 4.16A) in the injected side. However, at stage 33/34, the total number of proliferating cells in the injected side was slightly, but significantly higher than that in the control side (23.3 per section vs. 21.6 per section) and this difference was due to more proliferating cells of the eye area in the injected side (Figure 4.16B,C, 12.6 per injected-retina section for vs. 11.0 per control-retina section). At this stage, proliferating cells were often detected in the presumptive INL of the retina in the injected side (Figure 4.16B, frame and white arrowheads), and in some cases, accompanied with the ectopic RPE mingled in the INL (Figure

4.16B, insert, white arrow). Most of the proliferating cells at this stage should differentiate into bipolar cells or Müller cells. However, the overgrowth of photoreceptors in the INL caused by *RxL* gain-of-function suggested that these cells could also be the precursors of photoreceptors. If this is the case, overexpression of *XRxL* seems to provide an extra bias which led more RPCs to adopt photoreceptor fate instead of other cell fates.

We further analysed whether extra *XRxL* function increased apoptosis. The *RxL-GR* (50 pg) injected embryos were induced by addition of Dex at NF stage 16/17 and collected at stage 33/34 for TUNEL assay. Meanwhile, injected-embryos without Dex treatment were also analysed at the same stage as a control. Compared to the retina in the non-injected side, a slightly increased number of apoptotic cells were detected in the retina of *RxL-GR* induced side (3.0 per retina section vs. 4.0 per retina section, Figure 4.17A,C,D), whereas when the *RxL-GR* injected embryos were not induced, the numbers of apoptotic cells in the eye area were equal in both sides (2.9 per retina section of injected side vs. 3.0 per retina section of non-injected side, Figure 4.17A,B,D). In line with these results, overexpression of the chicken homolog, *cRaxL* in chicken retina also led to slightly increased apoptotic retinal cells in the GCL and the INL (Sakagami et al., 2003).

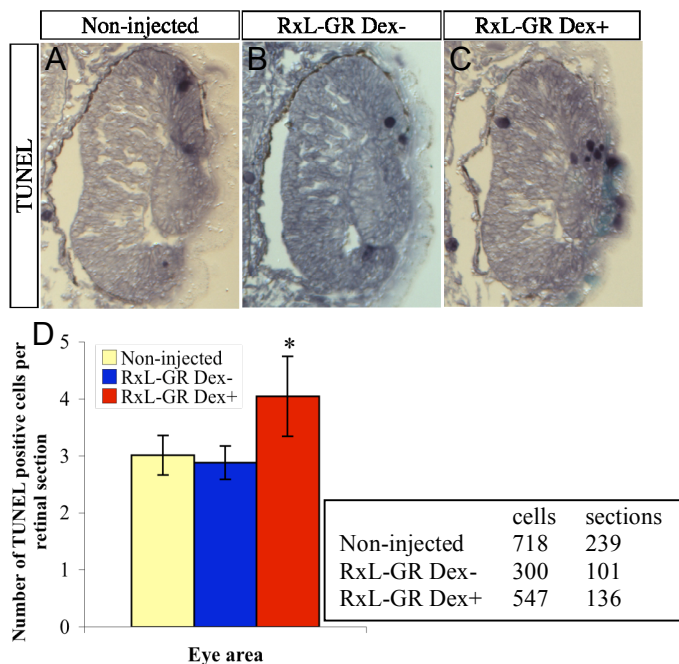


Figure 4.17 RxL-GR activation caused slightly increased number of apoptotic cells in retinas. Embryos injected with 50 pg synthetic *RxL-GR* RNA into a dorsoanimal blastomere at the 4-cell stage and then grown in a medium without Dex (Dex-) (B), or with addition of Dex (Dex+) at NF stage 16/17 (A,C). These embryos were subjected to TUNEL assay at NF stage 33/34. (A-C) Transversal sections of retinas in the non-injected side (A), or *RxL-GR* injected side with (C) or without (B) Dex induction. The dark blue dots represent the TUNEL positive

cells. (D) Comparison of the number of TUNEL positive cells in eye areas of non-injected side (yellow bar), or *RxL-GR* injected side with (red bars) or without (blue bars) Dex induction of NF stage 34 embryos. The average of TUNEL positive cell number on per section was determined in each retina. For non-injected, $n=5$ retinas; for *RxL-GR* injected, without induction, $n=2$ retinas; for *RxL-GR* injected and induced, $n=3$ retinas. Values are given as means \pm s.e.m. Quantification of counted TUNEL positive cells and section are given in the frame. *, compared to the non-injected retinas, $p=0.20$, (student's *t-test*).

As shown above, overexpression of *XRxL* induced the photoreceptor marker *Rho* expressed ectopically in the INL and the GCL, and also led to a slightly increased number of apoptotic cells. Taken together, it is likely that *XRxL* promotes photoreceptor cell differentiation at the expense of other retinal cell types.

4.13 XRxL functions as a transcriptional activator

As a DNA-binding transcription factor, XRxL could function as a transcriptional activator or repressor. To address this question, we generated two chimeric constructs: *RxL-EngR*, in which the *XRxL* complete ORF was in-frame fused to the repressor domain of *Drosophila engrailed*, and *RxL-VP16*, in which *XRxL* ORF was in-frame fused to the region coding the activator domain of virus protein VP16. If XRxL is a transcriptional repressor, *RxL-EngR* injected embryos are supposed to show a similar phenotype with wild-type *RxL* injected embryos, whereas if XRxL functions as a transcriptional activator, embryos injected with *RxL-VP16* should show a phenotype similar to wild-type *RxL* injected embryos.

We microinjected the synthetic *RxL-EngR* or *RxL-VP16* RNA into a dorsoanimal blastomere of the 4-cell stage embryos and compared the resulting eye phenotypes with wild-type *RxL* injected embryos. Most of the *RxL-EngR* injected embryos showed a reduced eye size on the injected side (66.7%, $n=14/21$ for the 25 pg injection; 71.7%, $n=33/46$ for the 100 pg injection, Figure 4.18J-Q), similar to embryos injected with RxL-MO (Figure 4.7). Injection of *RxL-EngR* RNA at a high dose (100 pg) even led to a complete loss of eye in some cases (8.7%), as revealed by the hematoxylin-eosin staining on transversal sections (Figure 4.18N-Q), differing from the eye phenotype caused by RxL-MO injection (Figure 4.7B-C''). Thus, *RxL-EngR* may even bring additional negative force into the Rx binding region of the corresponding Rx-target genes, which is not the case upon morpholino injection as a "loss-of-protein" function situation. Injection of even a very small dose of *RxL-VP16* RNA (2.5 pg) led to an eye phenotype (Figure 4.18F-I) resembling that caused by injection of 25 pg wide-type *RxL* (Figure 4.18B-E). Within the eye of *RxL-VP16* injected side, the ONL invaginated into the INL (Figure 4.18H, black arrows) and sometimes the RPE mingled in the NR (Figure 4.18H, green arrowheads), just similar to overexpression of wild-type *RxL* (Figure 4.18D black arrow, green arrowhead). When embryos were injected with 5 pg *RxL-VP16* at the 4-cell stage, most of them died from gastrulation defects, like embryos injected with 100 pg of the wild-type *RxL* RNA (Data not shown).

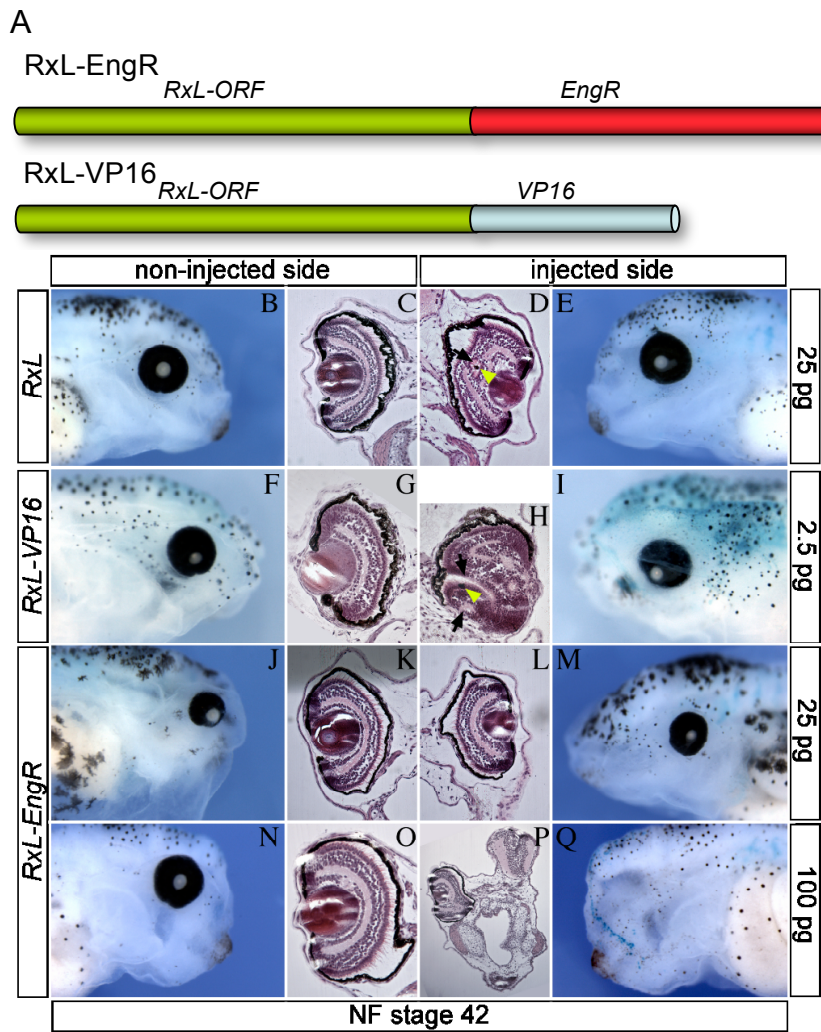


Figure 4.18
Microinjection of *RxL-VP16*, instead of *RxL-EngR*, induced an eye phenotype similar to that of overexpression of wild-type *RxL*. (A) Schematic diagrams of *Xenopus RxL* chimeric constructs, *RxL-EngR* and *RxL-VP16*. (B-Q) Embryos co-injected with indicated amount of synthetic wild-type *RxL* (B-E), *RxL-VP16* (E-I) or *RxL-EngR* (J-Q) RNA and β -gal RNA in a dorsoanimal blastomere at the 4-cell stage and analyzed at NF stage 42. (B, F, J, N) Lateral views of non-injected sides, anterior to the right. (E, I, M, Q) Lateral views of

injected sides, anterior to the left. (C, G, K, O, D, H, L, P) Transversal sections of eyes in the non-injected side (C, G, K, O) and injected side (D, H, L, P) of respective embryos were stained with hematoxylin-eosin and displayed with dorsal sides upward. Green arrowheads indicate the RPE mingled in the NR; black arrows point to the ONL invaginated into the INL or the GCL.

In order to confirm the function of *RxL-EngR* and *RxL-VP16* on a molecular level, the expression of the photoreceptor marker, *Rho* was further examined in embryos injected with either *RxL-EngR* or *RxL-VP16* RNA. It turned out that injection of *RxL-EngR* led to a reduced *Rho* expression accompanied with the impaired eye vesicle formation on the injected side (Figure 4.19C-C''), similar to *RxL-MO* microinjection (Figure 4.10A-B'). However, injection of *RxL-VP16* RNA led to ectopic expression of *Rho* at the expense of cells in the INL and the GCL and impaired lens formation (Figure 4.19B-B''), which resembled the overexpression of wild-type *RxL* (Figure 4.19A-A'').

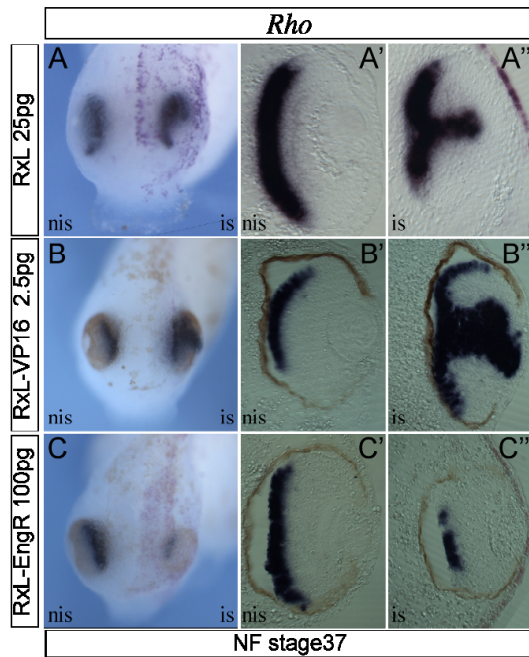


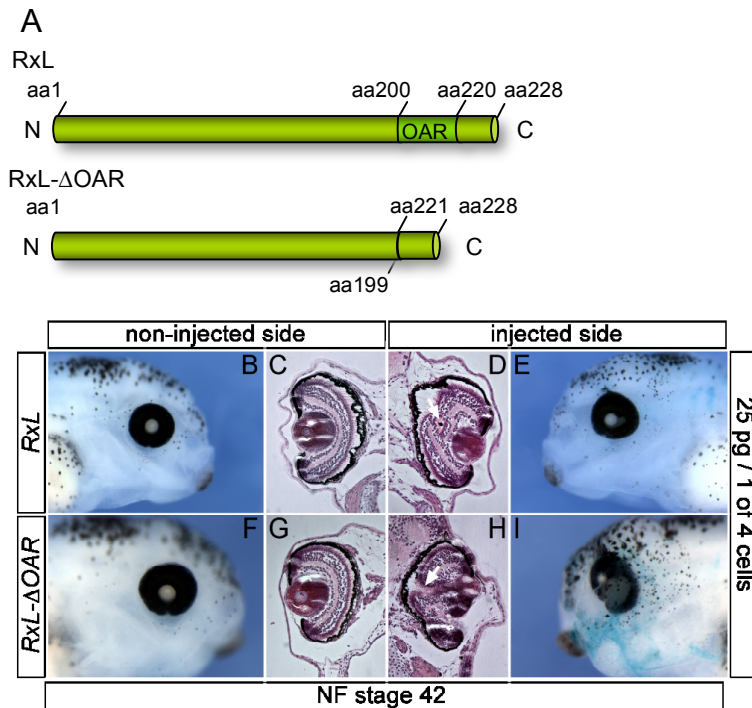
Figure 4.19 Effects of microinjection of *RxL-VP16* and *RxL-EngR* on the expression of photoreceptor-specific gene *Rho*. (A-C'') Embryos injected with indicated dosages of synthetic wild-type *RxL* (A-A''), *RxL-VP16* (B-B'') or *RxL-EngR* (C-C'') RNA in one of the dorsoanimal blastomeres at the 4-cell stage and analyzed for *Rho* expression by WMISH at NF stage 37/38. (A,B,C) Dorsal views of injected embryos with injected sides (red color) to the right. (A',A'',B',B'',C',C'') Transversal sections of eyes in the control side (A',B',C') and the injected side (A'',B'',C'') of respective embryos shown in A, B and C, with dorsal side upward. nis, non-injected side; is, injected side.

Judged from the phenotypes and the *Rho* expression patterns of embryos injected with these chimeric constructs, it could be concluded that RxL-VP16, instead of RxL-EngR, functions similar to wild-type XRxL, indicating that XRxL is a transcriptional activator rather than a repressor, which is in line with the results of *in vitro* experiments (Pan et al., 2006b).

4.14 OAR domain does not function as the activation domain of XRxL

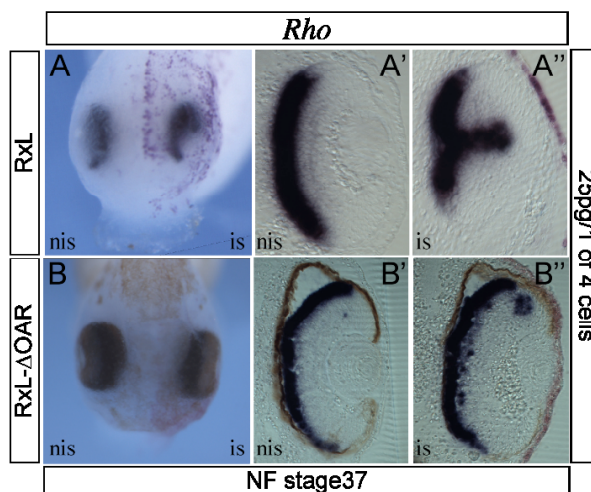
If XRxL functions as a transcriptional activator, then which motif does play the role as the activation domain in XRxL protein? The OAR domain is a transcriptional activator in *orthopedia* (Simeone et al., 1994). In the paralogous gene of *RxL*, *Xenopus Rx1*, the OAR seems also to function as a transcriptional activation domain, since microinjection of the *Rx1* lacking the OAR domain led to a phenotype similar to overexpression of the dominant negative construct of *Rx1* (Andreazzoli et al., 1999). However, in zebrafish *Rx2* and another *paired*-class homeodomain gene, *Alx-4*, the OAR domain is not required for the activity (Chuang and Raymond, 2001; Hudson et al., 1998). Thus, an *RxL* chimera was generated, in which only the OAR domain was deleted from *RxL* ORF, referred to as *RxL-ΔOAR*. In this construct, we carefully remained the part C-terminal to the OAR domain (aa221-228) (Figure 4.20A).

The synthetic *RxL-ΔOAR* RNA was injected into a dorsoanimal blastomere of embryos at the 4-cell stage. Unexpectedly, two thirds of the *RxL-ΔOAR* injected embryos showed an eye phenotype closely resembling that injected with wild-type *RxL* (Figure 4.20B-I). The overgrown ONL invaginated into the INL was also observed in the retina of *RxL-ΔOAR* injected side (Figure 4.20H white arrows).



(B,F) Lateral views of non-injected sides, anterior to the right. (E,I) Lateral views of injected sides, anterior to the left. (C,D,G,H) Transversal sections of eyes on the non-injected side (C,G) and injected side (D,H) of each embryos were stained with hematoxylin-eosin and displayed with dorsal sides upward. White arrows point out the ONL invaginated into the INL or even the GCL.

We further analyzed the expression of *Rho* in *RxL-ΔOAR* injected embryos. Ectopic expression of *Rho* in the INL was also detected in the eye of injected side (Figure 4.21B-B''), similar to the effects of wild-type *RxL* overexpression. These results indicate that the OAR domain does not play a critical role for the activity of XRxL.



(A'',B'') of embryos shown in A and B respectively, dorsal sides upward.

Figure 4.20 Microinjection of *RxL-ΔOAR* led to an eye phenotype similar to that caused by microinjection of wild-type *RxL*. (A) Schematic drawing of the construct of *RxL-ΔOAR*, which is *Xenopus* *RxL* lacking the OAR domain. Numbers indicate the positions according to amino acids (aa) sequence of XRxL. (B-I) Embryos co-injected with indicated amount of synthetic wild-type *RxL* (B-E) or *RxL-ΔOAR* (F-I) RNA and β -gal RNA into a dorsoanimal blastomere at the 4-cell stage and analyzed at NF stage 42. (B,F) Lateral views of non-injected

Figure 4.21 Microinjection of *RxL-ΔOAR* RNA caused additional expression of *Rho* in the INL. (A-B'') Embryos injected with indicated concentrations of synthetic wild-type *RxL* (A-A'') or *RxL-ΔOAR* (B-B'') RNA into one of the dorsoanimal blastomeres at the 4-cell stage and analyzed for *Rho* expression at stage 37/38 by WMISH. (A,B) Dorsal views of embryos with the injected sides (red color) to the right. (A',B',A'',B'') Transversal sections of the eye on the non-injected side (A',B') or injected side

4.15 Targeted overexpression of *XRxL* in retinal progenitor cells biased the photoreceptor fate

It has been known that the different types of retinal cells are generated from the same pool of multipotential retinal progenitor cells (RPCs) (reviewed by Cepko et al., 1996; Harris, 1997). Under the influence of extrinsic and intrinsic clues, RPCs differentiate into seven basic retinal cell types sequentially (reviewed by Livesey and Cepko, 2001).

Our results have showed that the RPCs do not properly respond to *XRxL* until late neurula stage, when the retinal progenitor cells are all in a proliferative state (Zaghloul et al., 2005). Moreover, overexpression of *XRxL* led to the ectopic expression of photoreceptor marker gene *Rho* at the expense of the INL, but never outside of the eye area. These evidences led us to the hypothesis that *XRxL* might play a role in retinal cell fate determination.

Stage 17/18 retinoblasts were lipofected *in vivo* with *XRxL* DNA expression plasmids (Figure 4.22A) and some of RPCs thereby gain extra copy of *RxL*. *eGFP* DNA was co-transfected with the experimental constructs to identify the lipofected cells, which allows to examine the proportions of different retinal cell types (Figure 4.22B). *eGFP* DNA normalized to the total amount of DNA used in the experimental group was lipofected as the control (Ohnuma et al., 2002b). The different retinal cell types of the eGFP positive cells were counted individually and the ratios were compared between control and experimental groups.

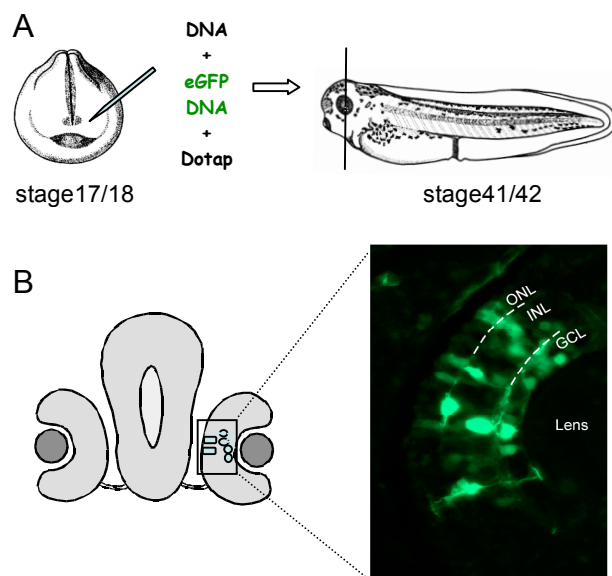


Figure 4.22 Schematic diagram of the procedure to analyze the lipofected retinas. (A) The presumptive eye area of embryos at NF stage 17/18 was lipofected with the mixture of *eGFP* and the desired DNA construct in the presence of the lipofection reagent, DOTAP. Lipofected embryos were collected at NF stage 41/42 and cryostat sectioned transversally. (B) Different types of retina cells with eGFP signal were counted according to their shape and location.

Compared with the retinas lipofected with *eGFP* alone, lipofection of *XRxL* in retinoblasts significantly increased ($p < 0.0001$) the proportion of photoreceptor cells by approximate 50% (Figure 4.23B compared with Figure 4.23A; quantified in Figure 4.23E). Moreover, the significant decrease in the proportions of amacrine ($p < 0.0001$) and bipolar cells ($p < 0.0001$) were

also observed in *RxL* lipofected retinas, while the proportion of ganglion, horizontal and Müller cells was not changed. These results indicated that targeted overexpression of *XRxL* in RPCs increases the number of cells which acquired a photoreceptor cell fate at the expense of amacrine and bipolar fates.

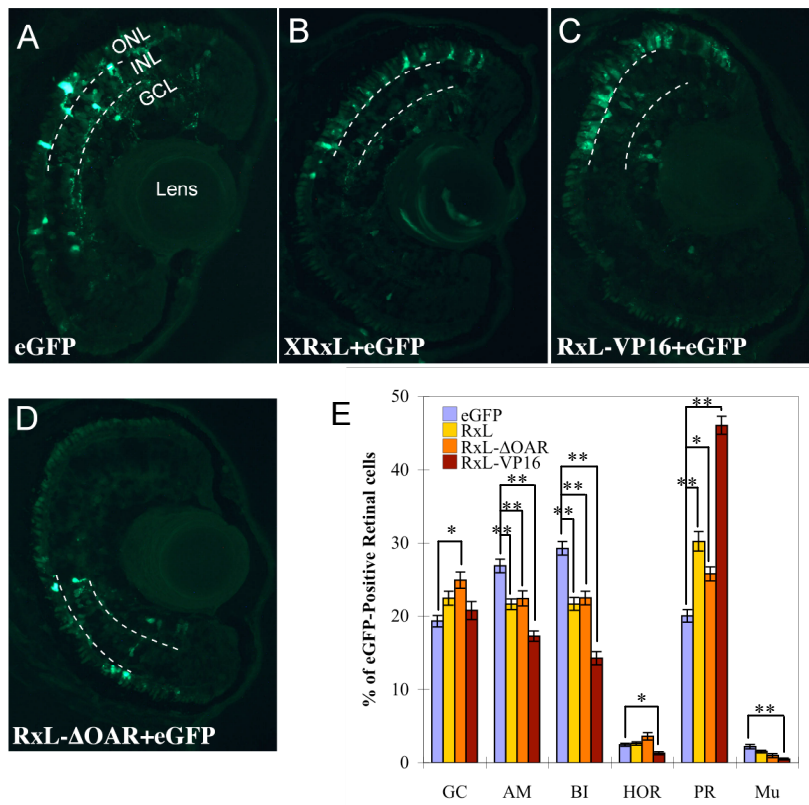


Figure 4.23 Overexpression of wild-type *RxL*, *RxL-VP16* and *RxL-ΔOAR* in retinoblasts increased the proportion of photoreceptors. (A-D) Transversal sections of NF stage 41/42 retinas lipofected with *eGFP* (A), or co-lipofected with *eGFP* and wild-type *RxL* (B), *RxL-VP16* (C) or *RxL-ΔOAR* (D) at NF stage 17/18. A diversity of retinal cell types express the fluorescence marker. White lines are drawn over the inner and outer plexiform

layers to better identify the ONL, INL and GCL. Lipofection of wild-type *RxL* (B), *RxL-VP16* (C) or *RxL-ΔOAR* significantly increased photoreceptor proportion in the lipofected retinal cells, compared to that lipofected with *eGFP* alone (A, in the ONL). (E) Each of the retina cell types (GC, ganglion cells; AM, amacrine cells; BI, bipolar cells; HOR, horizontal cells; PR, photoreceptor cells, Mu, Müller cells) was counted per retina (n) and the percentage for each was determined and is given in the mean value. *eGFP*, $n=40$; *RxL*+*eGFP*, $n=56$; *RxL-VP16*+*eGFP*, $n=29$ and *RxL-ΔOAR*+*eGFP*, $n=12$. The error bars represent the s.e.m. *, $p<0.001$; **, $p<0.0001$ (student's *t*-test).

4.16 *RxL-VP16* and *RxL-ΔOAR* also promote photoreceptor cell fate

As shown above, microinjection of *RxL-VP16* RNA in a dorsoanimal blastomere of 4-cell stage embryos affected *Xenopus* eye development in a way similar to overexpression of wild-type *RxL*, suggesting that *XRxL* functions most likely as a transcriptional activator. If this is true, targeted overexpression of *RxL-VP16* in RPCs should lead to similar effects on the retinal cell specification as lipofection of wild-type *XRxL*.

NF stage 17/18 retinoblasts were lipofected with an *RxL-VPI6* DNA expression plasmids, and the resulting proportion of photoreceptor cells indeed increased by approximate 100% ($p < 0.0001$), compared to retinas lipofected with *eGFP* alone (Figure 4.23C; quantified in Figure 4.23E). Similarly, the proportions of amacrine cells and bipolar cells were also decreased ($p < 0.0001$) but to a greater extent than wild-type *RxL* lipofected retinas. Additionally, lipofection of *RxL-VPI6* also led to a decreased proportion of horizontal ($p < 0.001$) and Müller cells ($p < 0.0001$). However, the proportion of ganglion cells was still not affected, like lipofection of wild-type *XRxL*.

Lipofection of *RxL-ΔOAR* also significantly increased the proportion of photoreceptor cells ($p < 0.001$) at the expense of amacrine ($p < 0.0001$) and bipolar cells ($p < 0.0001$; Figure 4.23D compared with Figure 4.23A; quantified in Figure 4.23E), though less efficiently than lipofection of wild-type *XRxL*. In addition, lipofection of *RxL-ΔOAR* led to an increase in the proportion of ganglion cells by 29% ($p < 0.001$), which is different from lipofection of wild-type *XRxL* or *RxL-VPI6*.

Taken together, *RxL* functions as a transcriptional activator in *Xenopus* retinal cell differentiation by means of promoting photoreceptor cell fate. However, the OAR domain of *XRxL* seems not essential for its activity. On the other hand, the chimeric protein *RxL-ΔOAR* does not function completely resembling the wild-type *RxL*, since *RxL-ΔOAR* also promoted the ganglion cell fate in addition to the photoreceptor cell fate.

4.17 Targeted repression of *XRxL* function in RPC inhibits photoreceptor fate

If additional *XRxL* promotes photoreceptor differentiation, does suppression of *XRxL* function interfere with photoreceptor development? To test this, NF stage 17/18 retinoblasts were lipofected with *RxL-MO*. The *RxL-MO* lipofected retinas did not show fewer *eGFP* positive colonies than those lipofected with *eGFP* alone (the numbers of *eGFP* positive cells/retina for retinas lipofected with *eGFP* alone, or co-lipofected with *eGFP* and Cont-MO or *RxL-MO* are 125, 119 and 148 respectively), suggesting that proliferation of retinal precursor cells was not impaired. However, compared to the retinas lipofected with *eGFP* alone, lipofection of *RxL-MO* led to a significant decrease of 33% ($p < 0.001$) in the proportion of photoreceptor cells (Figure 4.24A,C; quantified in Figure 4.24D), along with an increase in the proportion of ganglion cells by 27%, while the Cont-MO lipofected retinas did not show a significant difference in ratios of retina cell types with the control retinas (Figure 4.24A,B,D).

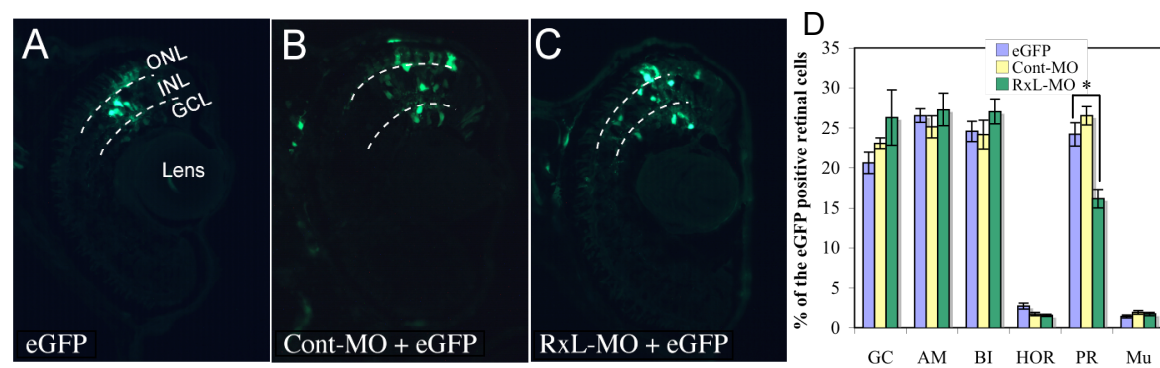


Figure 4.24 Lipofection of RxL-MO in retinoblasts decreased the proportion of photoreceptors. (A-C) Transversal sections of NF stage 41/42 retinas lipofected with *eGFP* (A) or co-lipofected with *eGFP* and Cont-MO (B) or RxL-MO (C) at NF stage 17/18. (D) Each of the retina cell types (GC, ganglion cells; AM, amacrine cells; BI, bipolar cells; HOR, horizontal cells; PR, photoreceptor cells, Mu, Müller cells) was counted in the eGFP positive population per lipofected retina (n). Percentage for each cell type was determined in each retina and is given in the mean value. eGFP, $n=16$; Cont-MO+eGFP, $n=12$; RxL-MO+eGFP, $n=12$. The error bars represent the s.e.m. *, $p<0.001$ (student's *t*-test).

In line with the results of the targeted overexpression of *XRxL* in RPCs (see 4.15), targeted suppression of *XRxL* function in RPCs led to inhibition of the photoreceptor fate.

4.18 *XRxL* lipofected photoreceptors are both rods and cones

We further wondered if overexpression of *XRxL* increased the proportion of rods, cones, or both. To answer this question, a cone photoreceptor-specific antibody against calbindin was used to identify cones in the lipofected retinas. The eGFP-positive photoreceptors were counted as calbindin-labeled cones or -unlabeled rods. To increase the number of photoreceptors in this analysis, *RxL-VP16* was used in these experiments. The retinas lipofected with *eGFP* alone gave rise to almost equal ratios of calbindin-labeled and -unlabeled photoreceptor cells (Figure 4.25A,C), consistent with previous reports (Chang and Harris, 1998; Viczian et al., 2003). However, lipofection of *RxL-VP16* slightly nevertheless significantly increased the proportion of rod by 10% ($p<0.005$) at the expense of cone photoreceptor cells ($p<0.005$) (Figure 4.25B,C). Therefore, RxL-VP16 promotes both rods and cones, with a preference for the rods, although our experiment did not exclude the possibility that a single *RxL-VP16* lipofected photoreceptor cell might express both cones and rods character genes.

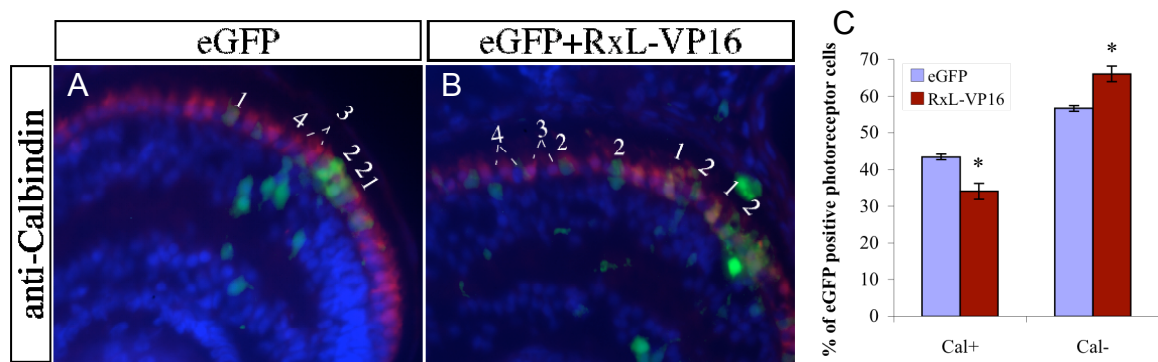


Figure 4.25 Lipofection of *RxL-VP16* in retinoblasts increased the proportion of rods at the expense of cone photoreceptor cells. (A,B) Cryostat sections (10 μm) of retinas lipofected with *eGFP* alone (A) or *RxL-VP16* and *eGFP* (B) then stained with anti-cone photoreceptor antibody (anti-Calbindin, in red) and DAPI (in blue). Untransfected cones appear red (3), and transfected cones appear orange (1). The photoreceptor cells in the intervals of cones with only DAPI-staining (4) are the untransfected rods, while cells appearing green in the ONL are transfected rods (2). (C) Graph showing the ratios of calbindin-labelled (Cal+, cones) and -unlabelled (Cal-, rods) eGFP positive photoreceptor cells (n) in *eGFP* ($n=86$) or *eGFP* and *RxL-VP16* ($n=392$) lipofected retinas. The numbers of each type of eGFP positive photoreceptor cells were counted and the percentages were determined in each retina. Values are given in mean. The error bars represent the s.e.m. *, $p<0.005$ (student's *t*-test).

Thus, *XRxL* promotes retinal precursor cells to acquire a photoreceptor fate, mainly at the expense of amacrine and bipolar cells, probably by means of providing bias for generation of rod photoreceptors.

5 Discussion

In this study, we have identified a new *Rx*-type gene in *Xenopus*, *XRxL*. A phylogenetic analysis, based on the deduced amino acid sequences of the most conserved homeobox and OAR domain of all reported *Rx*-type genes, revealed that all vertebrates with the exception of murinae (mouse and rat) possess two different *Rx* genes. *XRxL* belongs to the group of “*Rx-like*” genes in lower vertebrates, which corresponds to the “*Rx-Q50*” group of mammals (Figure 4.3). Loss- and gain-of-function experiments demonstrated that *Xenopus RxL* is not involved in eye development until late neurula stage. Unlike its paralog, *XRx1*, *XRxL* does not promote the proliferation of retinal progenitor cells. Instead, *XRxL* promotes generation of both rod and cone photoreceptors with a preference for rods, at the expense of amacrine and bipolar cells.

5.1 *Xenopus RxL* is a new member of the group of vertebrate “*Rx-like*” genes

In 1997, the first description of *Rx* genes showed that *Rx* genes are indispensable for proper eye formation (Mathers et al., 1997). Up to now, 34 complete Genbank entries of *Rx*-type genes from 27 species have been identified, which we grouped into four different categories, including one group of invertebrate *Rx*-type genes and three groups of *Rx*-type genes from vertebrates (Figure 4.2, Figure 4.3). Invertebrates seem to possess only one type of *Rx* genes, while vertebrates seem to possess two types of *Rx* genes normally. One is from the “classical vertebrate *Rx*” group, and another from the “*Rx-Q50*” group or the “*Rx-like*” group in mammals or lower vertebrates, respectively.

5.1.1 Vertebrate *Rx* genes of different groups are expressed in different patterns

During vertebrates (except rodents) eye development, an *Rx* gene belonging to the “classical vertebrate *Rx*” group is first required to specify a presumptive eye area within the anterior neural plate, while a second *Rx*-type gene, of the “*Rx-Q50*” group in mammals or the “*Rx-like*” group in lower vertebrates is required for the developing retina. The second *Rx*-type gene is usually expressed later than its paralog in the “classical vertebrate *Rx*” group. In *Xenopus*, *Rx1* (*x1_rx1a* or *x1_rx2a*) transcripts are first detected by *in situ* hybridization in late gastrula/early neurula embryos. Its expression demarcates a uniform field in the anterior neural plate, which gives rise to structures of the future eye field and forebrain. During neurulation, in addition to the retina as the primary site of *XRx1* expression, the pineal gland and the ventral hypothalamus also express this gene (Mathers et al., 1997). Similar to *Xenopus Rx1*, murine *Rx1* (*mm_rax*) is first activated in the anterior neural plate of E7.5 embryos. At E10.5, expression of murine *Rx1* is confined to the

developing retina and ventral brain (Furukawa et al., 1997a; Mathers et al., 1997). In zebrafish (*Danio rerio*), the three *Rx* genes display slightly different expression patterns. The onset of *zRx3* (*dr_rx3*) expression is earlier than that of *zRx1* and *zRx2* (*dr_rx1* and *dr_rx2* respectively), although their initial patterns, which are restricted to the anterior neural plate, appear identical. Later in development, *zRx3* is continuously expressed in the retina and the ventral hypothalamus, while *zRx1* and *zRx2* remain expressed exclusively in the retina (Chuang et al., 1999). Similar to *zRx3*, medaka fish (*Oryzias latipes*) *Rx3* (*ol_rx3*) also belongs to the “classical vertebrate *Rx*” group based on our findings. It is initially expressed at late gastrula stage as well, and its transcripts continuously remain in the retina and part of the forebrain. Although its expression progressively weakens down in the retina during somitogenesis and remains strong only in the ventral diencephalon, the adult fish does express this gene in the inner nuclear layer (INL) of retina as well as the hypothalamus (Deschet et al., 1999). However, medaka fish *Rx2* (*ol_rx2*) is expressed several hours later than *Rx3* in the developing optic vesicle and then remains in the neuroretina, but not in the hypothalamus (Loosli et al., 2001). Consistently, chicken (*Gallus gallus*) *Rax* (*gg_rax1*), which belongs to the “classical vertebrate *Rx*” group, is expressed in the anterior neural fold during neurulation and is continuously expressed in the retina and ventral forebrain until later stages (Chen and Cepko, 2002; Ohuchi et al., 1999). *cRaxL* (*gg_rax2*), a member of the “*Rx-like*” group, is expressed in the anterior neural ectoderm later than *cRax*, and its weak expression in the presumptive ventral brain soon vanishes to the undetectable level, while the expression in the optic vesicle remains strong during embryogenesis (Chen and Cepko, 2002). A review of expression patterns of *Rx* genes in different vertebrate species reveals conserved aspects of *Rx* genes. Members of the “classical vertebrate *Rx*” group are expressed in the anterior neural plate at early neurula stages, then in the eye and the ventral forebrain at subsequent stages. On the other hand, *Rx-type* genes of the “*Rx-like*” group are expressed later and their transcripts are confined to the eye area from eye vesicle stage onward.

5.1.2 Vertebrate *Rx* genes of different groups play different roles in eye development

The different expression patterns of *Rx* genes implicate divergent functions among different groups of *Rx* genes. The *Rx1*^{-/-} mice fail to form the optic sulci, which give rise to optic cups, and the ventral neuroectoderm is much thinner in mutants than in normal siblings (Mathers et al., 1997; Zhang et al., 2000). In *Xenopus*, injection of a putative dominant negative construct of *Rx1*, *XRx1-EnR*, or an *Rx1* specific antisense oligonucleotide led to a reduction or loss of eyes, accompanied with an anterior head phenotype similar to that of *Rx1*^{-/-} mice (Andreazzoli et al., 1999; Andreazzoli et al., 2003). In *Rx3* mutants of medaka *eyeless* and zebrafish *chokh* (*chk*), the failed optic sulci evagination and blocked optic vesicle cell proliferation lead to the complete absence of eyes (Loosli et al., 2001). In addition, the forebrain morphogenesis is also affected in this mutant (Loosli et al., 2003; Winkler et al., 2000). These results support the idea that those *Rx*

genes defined as members of the “classical vertebrate *Rx*” group are required for the initiation of early eye development. Recently, the visualization of early eye morphogenesis at single-cell resolution in medaka fish revealed that before optic vesicle evagination, medaka *Rx3* determines the fate-specific convergence and migration behaviors of RPCs (Rembold et al., 2006). In addition, evidence from overexpression of *Xenopus Rx1* indicated that genes of this group promote the proliferation of the RPCs (Mathers et al., 1997; Andreatzoli et al., 1999). In contrast, genes of the “*Rx-like*” group seem to be involved in eye development later than their paralogs of the “classical *Rx*” group. In the *Rx3* mutant zebrafish, *chokk*, *zRx1* expression is absent from the optic vesicle and *zRx2* expression is completely abolished at all stages, suggesting that these two genes are downstream *zRx3*. The study on medaka *eyeless* mutants indicates that *Rx2* (*ol_rx2*) is expressed independent of *Rx3* and functions in later aspects of retinogenesis (Loosli et al., 2001). In *Xenopus*, our study also showed that inhibition of *XRxL* function did not affect the specification of eye field (Figure 4.8A-C), indicating that *XRxL* acts downstream or in parallel to *XRx1*. On the other hand, genes of the “*Rx-like*” group show a conserved function in the photoreceptor specification. In the differentiated retina, zebrafish *Rx1* and *Rx2* expression seem to be restricted to cone photoreceptors (Chuang and Raymond, 2001), while medaka *Rx2* is confined to the outer nuclear layer where photoreceptor cells are localized, and the ciliary margin (Loosli et al., 2001). In chicken, *cRaxL* was also demonstrated to play a role in the initiation of photoreceptor differentiation, and a dominant negative *cRax* (belongs to the “classical vertebrate *Rx*” group) does not affect photoreceptor differentiation (Chen and Cepko, 2001). In this study, we have demonstrated that lipofection of *XRxL* in retinal progenitor cells led to an overproduction of photoreceptor cells at the expense of amacrine and bipolar cells. On the contrary, lipofection of *XRx1* did not change the proportions of the retinal cell types, suggesting its role to maintain the multipotency of retinal progenitors (Casarosa et al., 2003). Taken together, members of the “classical vertebrate *Rx*” group are indispensable for the initiation of eye formation and the maintenance of retinal stem cell characters of RPCs, while genes of the “*RxL-like*” group function during the retinal cell differentiation.

5.1.3 The “*Rx-Q50*” group genes might be orthologs of the “*Rx-like*” group genes

Up to now, no “*Rx-like*” gene has been identified in mammals (Figure 4.2 and Figure 4.3). However, the role of the “*Rx-like*” genes seems to be substituted by genes of the “*Rx-Q50*” group, which defines the second group of *Rx*-type genes in higher vertebrates. The best-studied member of the “*Rx-Q50*” group is *QRx*, which is conserved in human and bovine. *QRx* was obtained by a yeast one-hybrid screen using the bovine *Rhodopsin* promoter Ret-1 DNA regulatory element as bait (Wang et al., 2004). *In situ* hybridization analysis showed that *QRx* is expressed in the ONL and the INL, with stronger expression in the ONL. Interestingly, this gene appears to be absent from the mouse genome. However, the upstream region of human *QRx* is capable of directing

expression in presumptive photoreceptor precursor cells in transgenic mice, indicating that the regulatory network still exists, although the gene has been deleted (Wang et al., 2004). On the other hand, all identified genes of the “*Rx-Q50*” group lack the conserved OP domain, similar to members of the “*Rx-like*” group, like *XRxL* and *cRaxL* (Figure 4.2). In another gene of the “*Rx-like*” group, zebrafish *Rx2*, the OP domain seems to be dispensable for its function, since microinjection of the OP-truncated *zRx2* led to eye phenotypes similar to that caused by microinjection of wild-type *zRx2* (Chuang and Raymond, 2001). These results also suggest that genes of the “*Rx-Q50*” group and those of the “*Rx-like*” group may share a similar function in higher and lower vertebrates respectively.

Taken together, our categorization of the vertebrate *Rx* genes is supported by the evidence that *Rx* genes are conserved concerning their expression and functions within one group, but are divergent between the groups. This suggests that the genetic sharing and divergence among *Rx* genes provide hints for the shared and distinct function, which they fulfill most likely by the recruitment of particular transcriptional cofactors to their diverged domains (Chuang and Raymond, 2001).

5.1.4 The invertebrate *Rx* genes

Interestingly, invertebrate *Rx* genes seem not to be involved in eye development, but have conserved function in brain development (Davis et al., 2003). *Drosophila* (*Drosophila melanogaster*) *Rx* (*dm_rx*) and vertebrate *Rx* share 95% of the amino acids identity within their predicted homeodomains (Eggert et al., 1998; Mathers et al., 1997; Ohuchi et al., 1999). *DRx* is expressed in the procephalon, a region that gives rise to eye imaginal primordia and brain hemispheres (Chang et al., 2001). This pattern partially resembles vertebrate *Rx* expression in the anterior neural plate (Eggert et al., 1998; Mathers et al., 1997; Andreazzoli et al., 1999). However, *DRx* expression could not be detected in eye imaginal primordia or larval imaginal discs, but only remains in the embryonic brain (Eggert et al., 1998). In a *DRx* null allele mutant, the compound eye and larval visual system is normal, but the central brain structure is severely defected (Davis et al., 2003). This indicates that *DRx* is not required for the establishment of the visual system, but is required for brain development. Planarian *Rx* homologs from *Dugesia japonica* and *Girardia tigrina* were also isolated, but they are not expressed in the eye (Salo et al., 2002). In *Saccoglossus kowalevskii*, *Rx* is expressed in the anterior neuroectoderm. Since this acorn worm does not have eyes, *Rx* expression in these species cannot be associated with eye development either (Lowe et al., 2003). Although insects and vertebrates do share a band wide of homologous genes conserved in eye development, like *Pax6*, *tll*, *Six3/Six6*, *eya* and so on (Zuber et al., 2003), this differential dependence of eye formation on *Rx* in insects and vertebrates may reflect different evolutionary origin of these two types of eyes, or *vice versa*, the distinct function of *Rx* genes caused the formation of different types of eye (Bailey et al., 2004).

5.2 *XRxL* directs the retinal cell fate determination

The suppression of *RxL* function in *Xenopus* by antisense morpholino oligonucleotide (RxL-MO) injection did not affect the expression of genes involved in early eye development, like *Rx1*, *Pax6* and *Six3*, before the end of neurulation stages (Figure 4.8), indicating that *RxL* is not required for the specification of the eye field. This result is consistent with the observation that overexpression of *XRxL* has no effects on the expression of *Rx1*, *Pax6* and *Six3* before NF stage 18 (Figure 4.14). Therefore, the eye field cells are not competent to respond to *XRxL* before stage 18, when the cells in the presumptive eye area are still primary retinal stem cells (RSC) (reviewed by Zaghloul et al., 2005). *XRx1* is known to be involved in the proliferation of RSCs and RPCs (Zaghloul et al., 2005), while *XRxL* seems to function differently. Overexpression of *XRxL* led to only a slight increased number of proliferating retinal cells (Figure 4.16), which is similar to overexpression of its homologs, *zRx2* in zebrafish and *cRaxL* in chicken (Chuang and Raymond, 2001; Sakagami et al., 2003). Moreover, microinjection of synthetic *XRxL* RNA induced ectopic expression of the photoreceptor marker, *Rho*. Targeted overexpression of *XRxL* in retinoblasts led to a significantly increased proportion of photoreceptors at the expense of amacrine and bipolar cells (Figure 4.23), but did not significantly affect the fraction of ganglion cells. On the other hand, in RxL-MO lipofected retinas, the fraction of photoreceptor cells was significantly decreased. However, RxL-MO lipofection apparently increased the ganglion cells proportion instead of that of amacrine and bipolar cells (Figure 4.24). This discordant effect may be due to the involvement of the other cell fate determinants in distinct pathways. Sakagami and colleagues showed that transfection of chicken retinas with *cRaxL* led to a decreased number of ganglion cells, while expression of the dominant-negative *cRaxL* increased the number of ganglion cell (Sakagami et al., 2003). These results suggest that the presence of *XRxL* is indispensable for photoreceptor cell differentiation, while a decreased or lost *XRxL* expression is probably required for the generation of other retinal cell types.

Taken together, *XRxL* is involved in directing the differentiation of multipotential retinal progenitor cells, but not essential to promote their proliferation.

5.2.1 *XRxL* may cooperate with the cell cycle mechanism to coordinate retinal cell fate determination

The time at which a progenitor cell exists the cell cycles is called the “birth date” of the produced postmitotic cells. Accumulating evidence supports the idea that components of the cell cycle cooperate with cell fate determinant factors to coordinate retinogenesis. For instance, overexpression of *p27Xic1*, a cell cycle inhibitor, not only drives the progenitors out of the cycle early, but also turns most of them into Müller glial cell (Ohnuma et al., 1999). Moreover,

blocking the Hh pathway slowed down cell cycle kinetics and delayed cell cycle exit, which in turn led the RGCs to be born later (Locker et al., 2006). However, overexpression of *Xath5*, a determination factor for RGCs, could increase the RGCs proportion in retinal cells at the expense of the later born cell type, but did not drive the RGCs to be born earlier (Ohnuma et al., 2002a). In line with this result, in *ath5* mutants of mice and zebrafish, no RPCs exited the cell cycle at the time when RGCs are normally born (Brown et al., 2001; Kay et al., 2001). Interestingly, when *Xath5* and *p27Xic1* were co-lipofected into retinal progenitors, these cells exited cell cycle earlier, and the resulting progenies were almost all RGCs, instead of Müller cells (Ohnuma et al., 2002a). Thus, it seems that the cell fate determinative power of determinant factors can override that of the cell cycle factors. It is not clear how *RxL* affects the cell cycle, or *vice versa*, to convert retinal progenitor cells into photoreceptors. We did observe that *XRxL* microinjection led to a mild increase in the number of proliferative cells in the retina at NF stage 34, when the most proliferating cells are normally supposed to be born as bipolar cells or Müller cells. Since overexpression of *XRxL* did not lead to an increased number of either of these two cell types, it is most likely these proliferative cells observed in the NF stage 34 *RxL*-overexpressed retinas are precursors of photoreceptors, indicating that *RxL* may indeed affect the cell cycle of these photoreceptor precursors.

In respect to the timing of cell differentiation and cell cycle exit, Notch signals are well known to promote gliogenesis at the expense of neurogenesis (Gaiano and Fishell, 2002; Lundkvist and Lendahl, 2001). Recently, it was revealed that Notch activity permits progenitor cells to remain proliferative and undifferentiated, whereas diminished Notch activity releases these progenitors from cell cycle and leads to their differentiation (Hatakeyama and Kageyama, 2004; Jadhav et al., 2006a). Indeed, the expression of *Math3*, *NeuroD1* and *Otx2* is significantly upregulated in *Notch1* deficient retina, indicating that the inhibition of Notch signaling is essential for the activation of these genes that can further induce the retinal cell differentiation (Jadhav et al., 2006b). It was further proposed that low Notch activity promotes photoreceptor fate rather than the other non-photoreceptor retinal cell fates (Jadhav et al., 2006b). Particularly, conditional knock-out of Notch signaling at early stage led to the majority of photoreceptors born as cones, while when Notch signaling is knocked-out at later stage, photoreceptors are formed exclusively as rods (Jadhav et al., 2006b). These results indicate that the timing of Notch signaling is correlated with retinal cell type determination. Therefore, the regulatory properties of Notch signaling in retinogenesis point to a potential relation with the role of *XRxL* in respect to photoreceptor differentiation.

However, to better understand the correlation between *XRxL* and the machinery regulating cell cycle of RPCs, more precise experiments, including the birth-dating analysis are further required.

5.2.2 *XRxL* is involved in the cell fate determination at very early stage

A largely accepted model suggests that the retinal cell determination passes through a series of “step-wise” specification events (Zaghloul et al., 2005). First, retinal stem cells (RSCs) are specified from the DRPs (definitive embryonic retina-producing precursors), which are defined by 9 animal blastomeres at the 32-cell stage in the *Xenopus* embryo (Huang and Moody, 1993). This is followed by the specification of RPCs from RSCs. After RPCs exit their last cell cycle, the postmitotic daughter cells are influenced by intrinsic and extrinsic cues and finally specified to a certain type of retinal cells. Moody and colleagues showed that even at cleavage stages, blastomeres are biased to form certain neurotransmitter subtypes among amacrine cells (Moody et al., 2000). Moreover, soon after induction, the early eye field already appears as a combination of the overlapping but not identical expression subfields of a set of genes, which indicates that the diversity of progenitors might already exist at this early time point of development (Zuber et al., 2003). In this study, the earliest expression of *XRxL* was detected at a very weak level at NF stage 12.5 and 14 by RT-PCR (Figure 4.5). Though this faint expression could not be localized by WMISH, it is possible that *XRxL* transcripts reside in a small population of RSCs at these stages. This kind of “precocious” expression has been mentioned by Livesey and Cepko for several other genes expressed in retinal progenitor cells. These genes are characteristic of their postmitotic progeny, although they seem not to have a specific function already in progenitors (Livesey and Cepko, 2001). WMISH analysis showed that *XRxL* expression labels a subset of *XRxI* expressing cells in the optic vesicles from NF stage 19 onward and throughout tailbud stages (Figure 4.4). Since the expression area of *XRxI* is thought to mark the whole population of RPCs during this period (Mathers et al., 1997), it is possible that *XRxL* expression gives an intrinsic bias to a subset of RPCs and makes them competent to acquire a specific cell fate. *XRxL* could be a new member of such genes whose precocious expression in retina characterizes an intrinsic bias of the retinal progenitor cells, or even the retinal stem cells. It may already play a role to guide the fate choice before or during the commitment of the early-progenitor cells.

5.2.3 *XRxL* promotes both rod and cone fates

XRxL expression shows a burst at early tadpole stage (NF stage 31), when photoreceptors start to differentiate (Chang and Harris, 1998). At NF stage 34, when most photoreceptor cells are differentiated, *XRxL* expression reaches the highest level, and sharply demarcates the ONL where photoreceptor cells are localized (Figure 4.4). Our loss- and gain-of-function experiments provided further evidence that *XRxL* promotes the cell fate of both cone and rod photoreceptors, with a preference for rods (Figure 4.23, Figure 4.24, Figure 4.25). This result differs from the lipofection of a related homeobox gene, *XOtx5b*, which increases the proportion of both cones and rods in equal numbers (Vicizian et al., 2003). It has been suggested that cones share the same progenitors with ganglion cells and amacrine cells, belonging to the first-born retinal cell types

(Belliveau and Cepko, 1999; Casarosa et al., 2003; Chang and Harris, 1998), while the first rods are born several hours later than cones in *Xenopus* (Chang and Harris, 1998) and few days later in the rodent (Belliveau and Cepko, 1999; Rapaport et al., 2004). There are two possible models for the sequential genesis of cones and rods. In one model, cones and rods are generated from distinct progenitors independently. Rods differentiate from late-progenitors, which are less plastic than the early-progenitors giving rise to cones. In the second model as proposed by Raymond, cones are a default state of general photoreceptor determination, and that the same cells may become rods through a later, secondary induction (Raymond, 1991). However, the common point of both models is that the determination of rods requires the precursor cells to interpret more intrinsic and extrinsic cues than that of cones. How does *XRxL* make more photoreceptor progenitors to choose the rod fate instead of cone fate? It is possible that *XRxL* is such an intrinsic cue to promote photoreceptor cell fate, and its lasting expression in differentiating photoreceptor cells gives them the extra cue to differentiate to rods. In support of this idea, our WMISH analysis shows that strong *XRxL* expression starts at early tadpole stage (NF stage 31), when photoreceptors start to differentiate (Chang and Harris, 1998), and reaches highest levels when most photoreceptor cells are differentiated (NF stage 34) (Figure 4.4). Chang and Harris demonstrated that although the first cones are born earlier than rods, rods are generated faster than cones during the overlapping period of their generation (Chang and Harris, 1998). Thus, we hypothesize that *XRxL* drives a subset of RPCs competent to generate photoreceptors and pushes them out of the cell cycle during the period when rods are generated faster than cones.

Taken together, *XRxL* may be involved in the very early stage of the retinal cell fate determination, allowing multipotent mitotic progenitors competent to become photoreceptor-progenitors. In the case of *XRxL* overexpression, more RPCs gain this property and differentiate to photoreceptors during the period when rods are generated faster than cones.

It is worth to mention that the majority of photoreceptor cell in avian retina are cones and 97% of mouse photoreceptors are rods, while the *Xenopus* retina contains almost an equal number of cones and rods (Chen and Cepko, 2002; Chang and Harris, 1998). Therefore, *Xenopus* would be an ideal animal model to study the association between cone and rod photoreceptors fate determination.

5.3 *XRxL* functions as a transcriptional activator

Our experiments with *XRxL* dominant-negative and -positive acting chimeras demonstrated that *XRxL* functions as a transcriptional activator rather than a repressor (4.13, 4.15), which is in agreement with the results from *in vitro* studies of this gene (Pan et al., 2006b). Similarly, *XRxI* was also demonstrated to function as a transcriptional activator, in which the OAR domain was

proposed to act as the activation domain (Andreazzoli et al., 1999, Kimura et al., 2000). However, our findings seemed to be discordant with their proposal. Overexpression of OAR domain-deleted *XRxL* (*RxL-ΔOAR*) gave rise to a phenotype comparable to that caused by overexpression of wild-type *XRxL*. Lipofection of the *RxL-ΔOAR* DNA expression plasmid into retinoblasts also increased the number of photoreceptor cells, similar to, though to a less extent than lipofection with wild-type *XRxL* (Figure 4.23). These results suggest that the OAR domain is not essential for the activity of *XRxL*.

Recent studies on other members of the *aristaleless*-related gene family shed a light on the function of the OAR domain (Brouwer et al., 2003). The authors suggested that OAR domain could serve as an intramolecular switch to tune the binding of homeodomain to the target DNA, which in turn affected the activity of these transcription factors (Brouwer et al., 2003). Their results also suggest that the OAR domain may diverge during evolution and thereby functions inconsistently. Interestingly, members of the “Rx-Q50” group possess a largely truncated OAR domain (Figure 4.2, Figure 4.3), indicating that the OAR domain of members of this group might be dispensable. Overexpression of the OAR domain-truncated *zRx2* in zebrafish led to a phenotype similar to that caused by overexpression of wide-type *zRx2*. This suggests that the OAR domain is not essential for the activity of *zRx2* as well (Chuang and Raymond, 2001). These results together with our findings for *Xenopus RxL* suggest that the OAR domain is not so essential for the activity of the “vertebrate Rx-like” or “vertebrate Rx-Q50” group members. However, microinjection of the OAR-truncated *XRx1* chimera left more than half of injected embryos unaffected, and caused one third showing a phenotype opposite to that induced by overexpression of the wild-type *XRx1* (Andreazzoli et al., 1999). Although this consequence was previously attributed to the activator role of OAR domain (Andreazzoli et al., 1999), it is also possible that the OAR domain is important for *XRx1* to bind to the target DNA.

In addition, *XRxL* lacks the conserved N-terminal octapeptide (OP), which functions as a repressor in other homeobox proteins and is present in *XRx1* (Mailhos et al., 1998; Mathers et al., 1997; Smith and Jaynes, 1996). Interestingly, the OP domain is also absent in the closest homolog of *XRxL*, *cRxL* and its higher vertebrate homolog, *QRx*, (Figure 4.2, Figure 4.3). The function of OP domain in *Rx* genes was also investigated by the overexpression of an OP-deleted *zRx2* in zebrafish, which led to an eye phenotype comparable to the overexpression of the wild-type *zRx2*. This result further suggests that the function of the OP is not essential for *zRx2* as well (Chuang and Raymond, 2001). Modification of N- and C- termini of some *aristaleless*-related proteins, like, *Pitx2*, *Prx2* and *Cart1*, led to similar effects on the activity of these proteins (Amendt et al., 1999; Brouwer et al., 2003; Norris and Kern, 2001), suggesting the correlated roles of these two parts in regulating the function of these proteins. It was proposed that intramolecular interactions between the N- and C- termini may lead to a protein conformation associated with a relative inactive state

of these transcription factors (Amendt et al., 1999), and the truncation of either terminus may lead to an unfolded conformation of these proteins, which mimics the structure required for their activity *in vivo*. In consistence with this proposal, the truncation of either of the two termini of *zRx2* had similar effects on eye development in zebrafish (Chuang and Raymond, 2001). Interestingly, we found that a conserved motif “RxxSIxAL” resides in both the OP and the OAR domain of Rx-type proteins (Figure 4.2), also indicating a potential correlated function between the OP and the OAR domain in Rx-type proteins.

Taken together, it is possible that the OAR domain functions to modify the DNA binding properties of Rx-type proteins, and the OAR domain may be of different importance for the activity of the related proteins. In addition, the N-terminally located OP may cooperate with the C-terminally located OAR domain to regulate the transcriptional activity of Rx-type proteins.

5.4 The role of XRxL in the cascade of regulating photoreceptor cell specification

Several transcription factors involved in photoreceptor cell specification have been identified to date, including NeuroD, Ath, Nr1, Nr2e3, Otx family members and Rx family members (Chen and Cepko, 2002; Kobayashi et al., 1999; Mears et al., 2001; Nishida et al., 2003; Viczian et al., 2003; Yan et al., 2005). However, how the network among these genes is coordinated remains largely obscure.

5.4.1 XRxL acts downstream XRx1 during eye development

In this study, *XRxL* loss-of-function experiments show that the inhibition of XRxL activity does not affect the initial expression of *Rx1* in *Xenopus*, indicating that XRxL functions downstream or parallel to *Rx1*. In the zebrafish *Rx3* mutant *chokh*, *zRx2* expression is missing, which suggests that the *zRx2* acts downstream *zRx3* (Loosi et al., 2003). As shown in Figure 4.3, zebrafish *Rx3* and *Rx2* are orthologs of *Xenopus Rx1* and *RxL* respectively. Therefore, it is likely that *XRxL* is downstream its paralogous gene, *XRx1*.

5.4.2 XRxL may cooperate with Otx family members during the photoreceptor differentiation

Several members of the *Otx* family were reported to play a role in photoreceptor differentiation. For instance, *Crx*, which was recently defined as a divergent member of *Otx5* family (Plouhinec et al., 2003), has been identified in mouse, human and zebrafish and demonstrated to be important for generation or maintenance of photoreceptors (Freund et al., 1997; Liu et al., 2001). In *Crx*-null mice, both rods and cones, albeit lacking the outer segment structures, are formed, suggesting that *Crx* is not required for the initiation of photoreceptor specification (Furukawa et al., 1997b). Unlike mammalian *Crx*, which is expressed in photoreceptor cells just after they are born (Chen

et al., 1997; Furukawa et al., 1997b; Morrow et al., 1998), zebrafish *Crx* is expressed in mitotic cells presumably committed to generate photoreceptor cells (Liu et al., 2001). *XOtx5b*, a gene highly related to *Crx*, has been identified in *Xenopus*. *XOtx5b* transcripts are localized in bipolar and photoreceptor cells of the developing retina, though only the transcripts in the ONL get translated (Decembrini et al., 2006; Viczian et al., 2003). In chicken, overexpression of *Crx* failed to rescue the phenotype induced by a dominant-negative allele of *cRaxL*, indicating that *cRaxL* may play an earlier role than *Crx* (Chen and Cepko, 2002). In our study, microinjection of RxL-MO did not result in a reduced intensity of *XOtx5b* expression at tadpole stage (NF stage 34, Figure 4.9), indicating that *XOtx5b* is not a direct downstream target of *XRxL*. Assuming that *XOtx5b* and chicken *Crx* are orthologs of each other, these results apparently suggest that these two *Otx5* family members may have a function parallel to that of “*Rx-like*” genes. However, the function of *XOtx5b* and *Crx* may not be completely identical, since *XOtx5b* also plays a role in early embryogenesis before the onset of eye formation (Vignali et al., 2000). Nonetheless, factors of the *Otx5* family and “*Rx-like*” family probably work together to determine the photoreceptor cell fate, since QRx was demonstrated to interact physically with *Crx* to transactivate a *Rhodopsin* promoter (Wang et al., 2004). In mouse, another *Otx* family gene, *Otx2* is expressed in the developing retina and is a direct regulator of *Crx* (Nishida et al., 2003). However, in *Xenopus*, *Otx2* promotes bipolar cell fate rather than photoreceptor fate (Decembrini et al., 2006; Viczian et al., 2003). Viczian and colleagues revealed that *XOtx2* inhibited the activity of *XOtx5b* in bipolar cells and helped to determine the bipolar cells instead of photoreceptors. A recent study showed that *XOtx2* protein was first translated in differentiating bipolar cells later than *XOtx5b* in differentiating photoreceptor cells (Decembrini et al., 2006). It will be interesting to understand how *XRxL* cooperates with members of *Otx* family to determine the retinal cell fate.

5.4.3 *XRxL* and *NeuroD* may reside in the same pathway to generate photoreceptor cells

NeuroD, a bHLH containing transcription factor, is thought to promote the generation of amacrine cells and photoreceptors. Targeted overexpression of *NeuroD* in *Xenopus* as well as in rat retinal progenitor cells both led to an increased number of photoreceptors and amacrine cells (Wang and Harris, 2005), and *NeuroD* loss-of-function severely depleted photoreceptors in retina (Yan and Wang, 2004). In cultured RPE cells from chicken, the viral transfection of *Ngn2* and *ath5* induced the expression of *NeuroD* and afterward, *RaxL*, but not *vice versa*. Therefore, the authors proposed two possible pathways for photoreceptor cell generation, one is *Ngn2*→*NeuroD*→*RaxL*, and the second is *ath5*→*NeuroD*→*RaxL* (Yan et al., 2005). The growing evidence shows that *neurogenin* plays a major role in photoreceptor generation in vertebrates (Marquardt et al., 2001; Perron et al., 1999; Wang and Harris, 2005). Moreover, *Xenopus neurogenin* has been shown to function upstream *NeuroD* during primary neurogenesis of the

neural plate (Ma et al., 1996). Thus, it will be interesting to address the question if the proposed pathway $\text{Ngn} \rightarrow \text{NeuroD} \rightarrow \text{RxL}$ is also true in *Xenopus*, since the second contradicts findings from *Xenopus*, in which Kanekar and colleagues showed that *Xath5* is expressed later than *NeuroD* and *NeuroD* overexpression activates expression of *Xath5*, but not *vice versa* (Kanekar et al., 1997 Neuron and Erratum, 1998).

Interestingly, the formation of additional photoreceptors and of rosette-like structures assembled of photoreceptors (Figure 4.15) was also reported when *Pax6* was inactivated specifically in the eye surface ectoderm or by genetic or mechanical ablation of the lens. In all these cases signals emanating from the lens or surface ectoderm were missing, which are thought to guide the proper formation of a regular stratified retina. Here, massive hyperproliferation and/or transdetermination of prospective retinal and/or forebrain tissue were reasoned for the respective phenotypes (Ashery-Padan and Gruss, 2001; Breitman et al., 1989; Harrington et al., 1991; Kaur et al., 1989). At stage 33/34, when most photoreceptors have become postmitotic, an apparent change of *Pax6* expression in retina is the downregulation of *Pax6* in photoreceptors (Hirsch and Harris, 1997). At this stage, expression of *Pax6* and *XRxL* seems to be mutually exclusive. The premature induction of *XRxL* led to a reduction of *Pax6* expression and a reduced eye size (Figure 4.8, Figure 4.9). This resembles the result of the microinjection of *NeuroD* in *Xenopus* embryos, which reduced *Pax6* expression and led to a reduction or loss of retinal tissue (Hirsch and Harris, 1997). Therefore, taking the advantage of a temporally inducible *Pax6* and *XRxL* might help to study the related function of *Pax6* and *XRxL* in the regulation of photoreceptor differentiation. It is also interesting to explore whether *NeuroD* and *XRxL* repel *Pax6* expression though the same mechanism.

5.4.4 Other genes specifically promoting the rod photoreceptor cell fate

The identified factors, which specifically promote the rod photoreceptor cell fate, include the neural retinal leucine zipper protein, *Nrl*, and the retina-specific orphan nuclear receptor, *Nr2e3*. *Nrl* is a transcription factor of the large Maf (L-Maf) superfamily and is essential to regulate photoreceptor differentiation, especially to activate rod-specific gene expression (Mears et al., 2001; Swain et al., 2001). In *Nrl*-null (*Nrl*^{-/-}) mice, the formation of rod photoreceptors is abolished, but the total number of photoreceptor is not changed (Mears et al., 2001), suggesting its role to direct photoreceptors toward the rod fate. In a recent study, lipofection of *XNrl*, originally *XL-Maf*, in *Xenopus* retinoblasts led to an increased fraction of rod photoreceptors at the expense of cones, accompanied by a reduction of the total number of amacrine and bipolar cells. However, the total number of photoreceptors apparently remains unaffected (McIlvain and Knox, 2007). The expression *XNrl* is first detected at NF stage 24 by RT-PCR and WMISH (Ishibashi and Yasuda, 2001; McIlvain and Knox, 2007), which is later than the initial expression

of *XRxL*. *XNr2e3* transcripts are first visualized by *in situ* hybridization at NF stage 34, when 90% of photoreceptor precursors have already left the cell cycle (Holt et al., 1988). Microinjection of the human homolog of *XNr2e3*, *hNr2e3*, led to the overproduction of rods at the expense of cones, without changing the proportion of the main retinal cell types. This result suggests that *Nr2e3* overexpression in non-photoreceptor progenitors is not sufficient to override their final fate. Consistently, the *Nr2e3* mutant mice, *Nr2e3^{rd7}* shows a similar morphology to that of *Nrl^{-/-}* retinas, with an excessive numbers of cones at the expense of rods (Haider et al., 2001; Mears et al., 2001). Interestingly, *Nrl^{-/-}* retinas do not express the rod-specific gene transcripts, while *Nr2e3^{rd7}* photoreceptors abnormally express both rod and cone genes within the same cell (Chen et al., 2005; Corbo and Cepko, 2005). In *Nrl^{-/-}* mice, *Nr2e3* transcripts are absent, suggesting that *Nr2e3* functions downstream *Nrl*, which is probably also the case in *Xenopus*. Taken together, *XNr2e3* and *XNrl* seem to direct the differentiated photoreceptors toward rod fate at the expense of cone, while *XRxL*, which plays an earlier role than *XNrl* and *XNr2e3*, promotes both rod and cone fates, with a preference for rods, at the expense of amacrine and bipolar cell fates.

5.5 Photoreceptor degeneration and *XRxL*

The majority of inherited retinal degenerations are caused by the mutation in photoreceptor-specific genes (www.sph.uth.tmc.edu/Retnet/). A mutation of *QRx*, the human ortholog of *XRxL*, has been identified in several retinal disease patients, which is consistent with the role of this gene in photoreceptor function and/or survival (Wang et al., 2004). In teleost *Astyanax mexicanus*, the blind cave dwelling (cavefish) forms eye primordia, which later arrest in development, degenerate and sink into the orbit. In the blind cave dwelling, *As-Rx1* (*am_rx1*), the ortholog of *XRxL*, was expressed more weakly, transiently and restricted to the central zone of the ONL, comparing with the surface dwelling (surface fish) during development. This suggests that the degeneration of cavefish retina may be caused by the suppression of the genes involved in photoreceptor differentiation. The reduced expression of *As-Rx1* could be a reason of eye degeneration (Strickler et al., 2002). In our study, when *XRxL* function is specifically suppressed by microinjection of RxL-MO, photoreceptor cells were arrayed in a very loose way with the outer segments being significantly reduced (Figure 4.7). This phenotype is similar to, but less severe than that caused in a retinal degeneration model (LaVail et al., 1998), in which mutations are present in the *Rhodopsin* gene, resembling the autosomal-dominant form of retinitis pigmentosa in human. Since the mouse ortholog of *RxL* (*QRx*) is absent from the mouse genome and the chicken retina contains a majority of cone, which is largely different from human retina, *Xenopus* could still be an ideal model for understanding the mechanisms of diseases related to the human ortholog of *RxL*.

6 Summary

Genes of the *Rx* family play critical roles in vertebrate eye formation. Various *Rx* paralogs have been identified in many vertebrate species including human, chick, zebrafish and medakafish. In this thesis, a new *Rx*-type gene, *Rx-like (RxL)*, was newly isolated from *Xenopus*. A phylogenetic tree was constructed based on the predicted amino acid sequences of the most conserved homeodomain and the OAR domain of all known *Rx*-type genes. According to the phylogenetic analysis results, all-known *Rx*-type genes could be divided into four groups, including the “invertebrate *Rx*” group, which contains all *Rx* genes from invertebrates, the “classical vertebrate *Rx*” group, the “vertebrate *Rx-Q50*” group, and the “vertebrate *Rx-like*” group. It seems that each examined vertebrate, except rodent, possesses two *Rx*-type genes from distinct groups, with one always from the “classical vertebrate *Rx*” group, and another from the “*Rx-like*” group or the “*Rx-Q50*” group depending on lower or higher vertebrates. *XRxL* belongs to the “vertebrate *Rx-like*” group.

The earliest expression of *XRxL* in the presumptive eye area is detected at late neurula stage, much later than *XRx1*, whose expression already demarcates the presumptive eye area within the anterior neural plate during gastrulation. Suppression of *XRxL* function *in vivo* leads to an impaired formation of photoreceptors, without interferences on the specification of the early eye field. Gain-of-function experiments further demonstrate that retinal progenitor cells do not respond to *XRxL* until late neurulation, indicating that *XRxL* functions later than *XRx1* during development. Overexpression of *XRxL* leads to ectopic expression of photoreceptor-specific *Rhodopsin* in the retina, but only slightly increased the number of proliferating cells at later stage. This is different from overexpression of its paralogous gene, *XRx1*, which markedly increased the number of proliferating cells in the presumptive eye area even at late gastrula stage.

Targeted overexpression of *XRxL* in retinoblasts increased the fraction of photoreceptor cells at the expense of amacrine and bipolar cells. *XRxL* promotes both subtypes of photoreceptor cells, rods and cones, with a preference for rods. This again differs from *XRx1*, which promotes the Müller cell fate during retinal cell differentiation. Furthermore, our *in vivo* experiments revealed that *XRxL* functions as a transcriptional activator. However, the OAR domain, which acts as the activation domain in *XRx1*, is not essential for the activity of *XRxL*.

In conclusion, this study investigated the function of a newly identified *Rx*-type gene, *XRxL*, during eye development in *Xenopus*. *XRxL* promotes photoreceptor differentiation, but does not promote the proliferation of retinal progenitor cells. *XRxL* function is more similar to that of members in the “vertebrate *Rx-like*” group or the “vertebrate *Rx-Q50*” group, compared to the function of members in the “classical vertebrate *Rx*” group. These results supports the idea that

the two groups of *Rx*-type genes in vertebrates have different function during eye development, which is in line with our categorization for the *Rx*-type gene family based on sequences alignment. Along with findings from other species, we propose that during vertebrate eye development, the *Rx*-type gene from the “classical vertebrate *Rx*” group is involved in the early eye field specification within the anterior neural plate and continuously provides the retinal identity and multipotency of retinal progenitor cells, whereas the second *Rx*-type gene from the “vertebrate *Rx-like*” group or the “vertebrate *Rx-Q50*” group mainly regulates the differentiation of retinal cell types, especially photoreceptors.

7 Bibliography

- Amato, M. A., Arnault, E. and Perron, M. (2004) Retinal stem cells in vertebrates: parallels and divergences. *Int J Dev Biol* **48**, 993-1001.
- Amendt, B. A., Sutherland, L. B. and Russo, A. F. (1999) Multifunctional role of the Pitx2 homeodomain protein C-terminal tail. *Mol Cell Biol* **19**, 7001-10.
- Andreazzoli, M., Gestri, G., Angeloni, D., Menna, E. and Barsacchi, G. (1999) Role of Xrx1 in *Xenopus* eye and anterior brain development. *Development* **126**, 2451-60.
- Andreazzoli, M., Gestri, G., Cremisi, F., Casarosa, S., Dawid, I. B. and Barsacchi, G. (2003) Xrx1 controls proliferation and neurogenesis in *Xenopus* anterior neural plate. *Development* **130**, 5143-54.
- Ashery-Padan, R. and Gruss, P. (2001) Pax6 lights-up the way for eye development. *Curr Opin Cell Biol* **13**, 706-14.
- Ashery-Padan, R., Marquardt, T., Andrejewski, N., and Gruss, P. (2001) Unraveling the multiple functions of Pax6 in eye development by conditional mutagenesis. *MPIbpc News* **7**, 1-6.
- Bailey, T. J., El-Hodiri, H., Zhang, L., Shah, R., Mathers, P. H. and Jamrich, M. (2004) Regulation of vertebrate eye development by Rx genes. *Int J Dev Biol* **48**, 761-70.
- Belliveau, M. J. and Cepko, C. L. (1999) Extrinsic and intrinsic factors control the genesis of amacrine and cone cells in the rat retina. *Development* **126**, 555-66.
- Bernier, G., Panitz, F., Zhou, X., Hollemann, T., Gruss, P. and Pieler, T. (2000) Expanded retina territory by midbrain transformation upon overexpression of Six6 (*Optx2*) in *Xenopus* embryos. *Mech Dev* **93**, 59-69.
- Blitz, I. L. and Cho, K. W. (1995) Anterior neurectoderm is progressively induced during gastrulation: the role of the *Xenopus* homeobox gene orthodenticle. *Development* **121**, 993-1004.
- Bopp, D., Burri, M., Baumgartner, S., Frigerio, G. and Noll, M. (1986) Conservation of a large protein domain in the segmentation gene paired and in functionally related genes of *Drosophila*. *Cell* **47**, 1033-40.
- Bouwmeester, T., Kim, S., Sasai, Y., Lu, B. and De Robertis, E. M. (1996) Cerberus is a head-inducing secreted factor expressed in the anterior endoderm of Spemann's organizer. *Nature* **382**, 595-601.
- Breitman, M. L., Bryce, D. M., Giddens, E., Clapoff, S., Goring, D., Tsui, L. C., Klintworth, G. K. and Bernstein, A. (1989) Analysis of lens cell fate and eye morphogenesis in transgenic mice ablated for cells of the lens lineage. *Development* **106**, 457-63.

- Brouwer, A., ten Berge, D., Wiegerinck, R. and Meijlink, F. (2003) The OAR/aristaless domain of the homeodomain protein *Cart1* has an attenuating role in vivo. *Mech Dev* **120**, 241-52.
- Brown, N. L., Patel, S., Brzezinski, J. and Glaser, T. (2001) *Math5* is required for retinal ganglion cell and optic nerve formation. *Development* **128**, 2497-508.
- Burmeister, M., Novak, J., Liang, M. Y., Basu, S., Ploder, L., Hawes, N. L., Vidgen, D., Hoover, F., Goldman, D., Kalnins, V. I., Roderick, T. H., Taylor, B. A., Hankin, M. H. and McInnes, R. R. (1996) Ocular retardation mouse caused by *Chx10* homeobox null allele: impaired retinal progenitor proliferation and bipolar cell differentiation. *Nat Genet* **12**, 376-84.
- Casarosa, S., Amato, M. A., Andreazzoli, M., Gestri, G., Barsacchi, G. and Cremisi, F. (2003) *Xrx1* controls proliferation and multipotency of retinal progenitors. *Mol Cell Neurosci* **22**, 25-36.
- Casarosa, S., Andreazzoli, M., Simeone, A. and Barsacchi, G. (1997) *Xrx1*, a novel *Xenopus* homeobox gene expressed during eye and pineal gland development. *Mech Dev* **61**, 187-98.
- Cayouette, M., Poggi, L. and Harris, W. A. (2006) Lineage in the vertebrate retina. *Trends Neurosci* **29**, 563-70.
- Cepko, C. L., Austin, C. P., Yang, X., Alexiades, M. and Ezzeddine, D. (1996) Cell fate determination in the vertebrate retina. *Proc Natl Acad Sci USA* **93**, 589-95.
- Chang, T., Mazotta, J., Dumstrei, K., Dumitrescu, A. and Hartenstein, V. (2001) Dpp and Hh signaling in the *Drosophila* embryonic eye field. *Development* **128**, 4691-704.
- Chang, W. S. and Harris, W. A. (1998) Sequential genesis and determination of cone and rod photoreceptors in *Xenopus*. *J Neurobiol* **35**, 227-44.
- Chen, C. M. and Cepko, C. L. (2002) The chicken *RaxL* gene plays a role in the initiation of photoreceptor differentiation. *Development* **129**, 5363-75.
- Chen, J., Rattner, A. and Nathans, J. (2005) The rod photoreceptor-specific nuclear receptor Nr2e3 represses transcription of multiple cone-specific genes. *J Neurosci* **25**, 118-29.
- Chen, S., Wang, Q. L., Nie, Z., Sun, H., Lennon, G., Copeland, N. G., Gilbert, D. J., Jenkins, N. A. and Zack, D. J. (1997) *Crx*, a novel Otx-like paired-homeodomain protein, binds to and transactivates photoreceptor cell-specific genes. *Neuron* **19**, 1017-30.
- Chow, R. L., Altmann, C. R., Lang, R. A. and Hemmati-Brivanlou, A. (1999) *Pax6* induces ectopic eyes in a vertebrate. *Development* **126**, 4213-22.
- Chow, R. L. and Lang, R. A. (2001) Early eye development in vertebrates. *Annu Rev Cell Dev Biol* **17**, 255-96.

- Chuang, J. C., Mathers, P. H. and Raymond, P. A. (1999) Expression of three *Rx* homeobox genes in embryonic and adult zebrafish. *Mech Dev* **84**, 195-8.
- Chuang, J. C. and Raymond, P. A. (2001) Zebrafish genes *rx1* and *rx2* help define the region of forebrain that gives rise to retina. *Dev Biol* **231**, 13-30.
- Corbo, J. C. and Cepko, C. L. (2005) A hybrid photoreceptor expressing both rod and cone genes in a mouse model of enhanced S-cone syndrome. *PLoS Genet* **1**, e11.
- Davis, A. A., Matzuk, M. M. and Reh, T. A. (2000) Activin A promotes progenitor differentiation into photoreceptors in rodent retina. *Mol Cell Neurosci* **15**, 11-21.
- Davis, R. J., Tavsanli, B. C., Dittrich, C., Walldorf, U. and Mardon, G. (2003) *Drosophila retinal homeobox (drx)* is not required for establishment of the visual system, but is required for brain and clypeus development. *Dev Biol* **259**, 272-87.
- De Robertis, E. M. and Kuroda, H. (2004) Dorsal-ventral patterning and neural induction in *Xenopus* embryos. *Annu Rev Cell Dev Biol* **20**, 285-308.
- Decembrini, S., Andreazzoli, M., Vignali, R., Barsacchi, G. and Cremisi, F. (2006) Timing the generation of distinct retinal cells by homeobox proteins. *PLoS Biol* **4**, e272.
- Delaune, E., Lemaire, P. and Kodjabachian, L. (2005) Neural induction in *Xenopus* requires early FGF signalling in addition to BMP inhibition. *Development* **132**, 299-310.
- Dent, J. A., Polson, A. G. and Klymkowsky, M. W. (1989) A whole-mount immunocytochemical analysis of the expression of the intermediate filament protein vimentin in *Xenopus*. *Development* **105**, 61-74.
- Deschet, K., Bourrat, F., Ristoratore, F., Chourrout, D. and Joly, J. S. (1999) Expression of the medaka (*Oryzias latipes*) *Ol-Rx3* paired-like gene in two diencephalic derivatives, the eye and the hypothalamus. *Mech Dev* **83**, 179-82.
- Domingos, P. M., Itasaki, N., Jones, C. M., Mercurio, S., Sargent, M. G., Smith, J. C. and Krumlauf, R. (2001) The Wnt/beta-catenin pathway posteriorizes neural tissue in *Xenopus* by an indirect mechanism requiring FGF signalling. *Dev Biol* **239**, 148-60.
- Drager, U. C., Li, H., Wagner, E. and McCaffery, P. (2001) Retinoic acid synthesis and breakdown in the developing mouse retina. *Prog Brain Res* **131**, 579-87.
- Eggert, T., Hauck, B., Hildebrandt, N., Gehring, W. J. and Walldorf, U. (1998) Isolation of a *Drosophila* homolog of the vertebrate homeobox gene *Rx* and its possible role in brain and eye development. *Proc Natl Acad Sci U S A* **95**, 2343-8.
- Ekker, S. C., Ungar, A. R., Greenstein, P., von Kessler, D. P., Porter, J. A., Moon, R. T. and Beachy, P. A. (1995) Patterning activities of vertebrate hedgehog proteins in the developing eye and brain. *Curr Biol* **5**, 944-55.

- Ezzeddine, Z. D., Yang, X., DeChiara, T., Yancopoulos, G. and Cepko, C. L. (1997) Postmitotic cells fated to become rod photoreceptors can be respecified by CNTF treatment of the retina. *Development* **124**, 1055-67.
- Freund, C. L., Gregory-Evans, C. Y., Furukawa, T., Papaioannou, M., Looser, J., Ploder, L., Bellingham, J., Ng, D., Herbrick, J. A., Duncan, A., Scherer, S. W., Tsui, L. C., Loutradis-Anagnostou, A., Jacobson, S. G., Cepko, C. L., Bhattacharya, S. S. and McInnes, R. R. (1997) Cone-rod dystrophy due to mutations in a novel photoreceptor-specific homeobox gene (CRX) essential for maintenance of the photoreceptor. *Cell* **91**, 543-53.
- Furukawa, T., Kozak, C. A. and Cepko, C. L. (1997a) *rax*, a novel paired-type homeobox gene, shows expression in the anterior neural fold and developing retina. *Proc Natl Acad Sci U S A* **94**, 3088-93.
- Furukawa, T., Morrow, E. M. and Cepko, C. L. (1997b) *Crx*, a novel *otx*-like homeobox gene, shows photoreceptor-specific expression and regulates photoreceptor differentiation. *Cell* **91**, 531-41.
- Furukawa, T., Mukherjee, S., Bao, Z. Z., Morrow, E. M. and Cepko, C. L. (2000) *rax*, *Hes1*, and *notch1* promote the formation of Müller glia by postnatal retinal progenitor cells. *Neuron* **26**, 383-94.
- Gaiano, N. and Fishell, G. (2002) The role of notch in promoting glial and neural stem cell fates. *Annu Rev Neurosci* **25**, 471-90.
- Gammill, L. S. and Sive, H. (1997) Identification of *otx2* target genes and restrictions in ectodermal competence during *Xenopus* cement gland formation. *Development* **124**, 471-81.
- Gilbert, S. F. (2003) *Developmental Biology*. Sinauer Associates, Inc.: Sunderland.
- Glinka, A., Wu, W., Delius, H., Monaghan, A. P., Blumenstock, C. and Niehrs, C. (1998) Dickkopf-1 is a member of a new family of secreted proteins and functions in head induction. *Nature* **391**, 357-62.
- Glinka, A., Wu, W., Onichtchouk, D., Blumenstock, C. and Niehrs, C. (1997) Head induction by simultaneous repression of Bmp and Wnt signalling in *Xenopus*. *Nature* **389**, 517-9.
- Grindley, J. C., Davidson, D. R. and Hill, R. E. (1995) The role of Pax-6 in eye and nasal development. *Development* **121**, 1433-42.
- Haider, N. B., Naggert, J. K. and Nishina, P. M. (2001) Excess cone cell proliferation due to lack of a functional NR2E3 causes retinal dysplasia and degeneration in rd7/rd7 mice. *Hum Mol Genet* **10**, 1619-26.

- Hammerschmidt, M., Bitgood, M. J. and McMahon, A. P. (1996) Protein kinase A is a common negative regulator of Hedgehog signaling in the vertebrate embryo. *Genes Dev* **10**, 647-58.
- Harrington, L., Klintworth, G. K., Secor, T. E. and Breitman, M. L. (1991) Developmental analysis of ocular morphogenesis in alpha A-crystallin/diphtheria toxin transgenic mice undergoing ablation of the lens. *Dev Biol* **148**, 508-16.
- Harris, W. A. (1997) Cellular diversification in the vertebrate retina. *Curr Opin Genet Dev* **7**, 651-8.
- Harris, W. A. and Perron, M. (1998) Molecular recapitulation: the growth of the vertebrate retina. *Int J Dev Biol* **42**, 299-304.
- Hatakeyama, J. and Kageyama, R. (2004) Retinal cell fate determination and bHLH factors. *Semin Cell Dev Biol* **15**, 83-9.
- Hatakeyama, J., Tomita, K., Inoue, T. and Kageyama, R. (2001) Roles of homeobox and bHLH genes in specification of a retinal cell type. *Development* **128**, 1313-22.
- Hatini, V., Tao, W. and Lai, E. (1994) Expression of winged helix genes, BF-1 and BF-2, define adjacent domains within the developing forebrain and retina. *J Neurobiol* **25**, 1293-309.
- Heasman, J. (2006) Patterning the early *Xenopus* embryo. *Development* **133**, 1205-17.
- Hemmati-Brivanlou, A. and Melton, D. A. (1994) Inhibition of activin receptor signaling promotes neuralization in *Xenopus*. *Cell* **77**, 273-81.
- Hensey, C. and Gautier, J. (1998) Programmed cell death during *Xenopus* development: a spatio-temporal analysis. *Dev Biol* **203**, 36-48.
- Hill, R. E., Favor, J., Hogan, B. L., Ton, C. C., Saunders, G. F., Hanson, I. M., Prosser, J., Jordan, T., Hastie, N. D. and van Heyningen, V. (1991) Mouse small eye results from mutations in a paired-like homeobox-containing gene. *Nature* **354**, 522-5.
- Hines, W. A., Thorburn, J. and Thorburn, A. (1999) A low-affinity serum response element allows other transcription factors to activate inducible gene expression in cardiac myocytes. *Mol Cell Biol* **19**, 1841-52.
- Hirsch, N. and Harris, W. A. (1997) *Xenopus* Pax-6 and retinal development. *J Neurobiol* **32**, 45-61.
- Hojo, M., Ohtsuka, T., Hashimoto, N., Gradwohl, G., Guillemot, F. and Kageyama, R. (2000) Glial cell fate specification modulated by the bHLH gene *Hes5* in mouse retina. *Development* **127**, 2515-22.
- Holleman, T., Bellefroid, E. and Pieler, T. (1998) The *Xenopus* homologue of the *Drosophila* gene *tailless* has a function in early eye development. *Development* **125**, 2425-32.
- Holleman, T., Panitz, F. and Pieler, T. (1999) *In situ hybridization techniques with Xenopus embryos*. Oxford Univ. Press: New York.

- Hollenberg, S. M., Cheng, P. F. and Weintraub, H. (1993) Use of a conditional MyoD transcription factor in studies of MyoD trans-activation and muscle determination. *Proc Natl Acad Sci U S A* **90**, 8028-32.
- Holt, C. E., Bertsch, T. W., Ellis, H. M. and Harris, W. A. (1988) Cellular determination in the *Xenopus* retina is independent of lineage and birth date. *Neuron* **1**, 15-26.
- Hu, M. and Easter, S. S. (1999) Retinal neurogenesis: the formation of the initial central patch of postmitotic cells. *Dev Biol* **207**, 309-21.
- Huang, S. and Moody, S. A. (1993) The retinal fate of *Xenopus* cleavage stage progenitors is dependent upon blastomere position and competence: studies of normal and regulated clones. *J Neurosci* **13**, 3193-210.
- Hudson, R., Taniguchi-Sidle, A., Boras, K., Wiggan, O. and Hamel, P. A. (1998) Alx-4, a transcriptional activator whose expression is restricted to sites of epithelial-mesenchymal interactions. *Dev Dyn* **213**, 159-69.
- Huh, S., Hatini, V., Marcus, R. C., Li, S. C. and Lai, E. (1999) Dorsal-ventral patterning defects in the eye of BF-1-deficient mice associated with a restricted loss of shh expression. *Dev Biol* **211**, 53-63.
- Hyatt, G. A., Schmitt, E. A., Fadool, J. M. and Dowling, J. E. (1996) Retinoic acid alters photoreceptor development *in vivo*. *Proc Natl Acad Sci U S A* **93**, 13298-303.
- Hyer, J., Mima, T. and Mikawa, T. (1998) FGF1 patterns the optic vesicle by directing the placement of the neural retina domain. *Development* **125**, 869-77.
- Iemura, S., Yamamoto, T. S., Takagi, C., Uchiyama, H., Natsume, T., Shimasaki, S., Sugino, H. and Ueno, N. (1998) Direct binding of follistatin to a complex of bone-morphogenetic protein and its receptor inhibits ventral and epidermal cell fates in early *Xenopus* embryo. *Proc Natl Acad Sci U S A* **95**, 9337-42.
- Inoue, T., Hojo, M., Bessho, Y., Tano, Y., Lee, J. E. and Kageyama, R. (2002) *Math3* and *NeuroD* regulate amacrine cell fate specification in the retina. *Development* **129**, 831-42.
- Ishibashi, S. and Yasuda, K. (2001) Distinct roles of *maf* genes during *Xenopus* lens development. *Mech Dev* **101**, 155-66.
- Jadhav, A. P., Cho, S. H. and Cepko, C. L. (2006a) Notch activity permits retinal cells to progress through multiple progenitor states and acquire a stem cell property. *Proc Natl Acad Sci U S A* **103**, 18998-9003.
- Jadhav, A. P., Mason, H. A. and Cepko, C. L. (2006b) Notch 1 inhibits photoreceptor production in the developing mammalian retina. *Development* **133**, 913-23.
- Kanekar, S., Perron, M., Dorsky, R., Harris, W. A., Jan, L. Y., Jan, Y. N. and Vetter, M. L. (1997) *Xath5* participates in a network of bHLH genes in the developing *Xenopus* retina. *Neuron* **19**, 981-94.

- Kanekar, S., Perron, M., Dorsky, R., Harris, W. A., Jan, L. Y., Jan, Y. N. and Vetter, M. L. (1998) Erratum. *Neuron* **21**, 1223.
- Kaur, S., Key, B., Stock, J., McNeish, J. D., Akesson, R. and Potter, S. S. (1989) Targeted ablation of alpha-crystallin-synthesizing cells produces lens-deficient eyes in transgenic mice. *Development* **105**, 613-9.
- Kay, J. N., Finger-Baier, K. C., Roeser, T., Staub, W. and Baier, H. (2001) Retinal ganglion cell genesis requires *lakritz*, a Zebrafish atonal Homolog. *Neuron* **30**, 725-36.
- Kimura, A., Singh, D., Wawrousek, E. F., Kikuchi, M., Nakamura, M. and Shinohara, T. (2000) Both PCE-1/RX and OTX/CRX interactions are necessary for photoreceptor-specific gene expression. *J Biol Chem* **275**, 1152-60.
- Kobayashi, M., Takezawa, S., Hara, K., Yu, R. T., Umesono, Y., Agata, K., Taniwaki, M., Yasuda, K. and Umesono, K. (1999) Identification of a photoreceptor cell-specific nuclear receptor. *Proc Natl Acad Sci U S A* **96**, 4814-9.
- Kolm, P. J. and Sive, H. L. (1995) Efficient hormone-inducible protein function in *Xenopus laevis*. *Dev Biol* **171**, 267-72.
- Korf, B., Rollag, M. D. and Korf, H. W. (1989) Ontogenetic development of S-antigen- and rod-opsin immunoreactions in retinal and pineal photoreceptors of *Xenopus laevis* in relation to the onset of melatonin-dependent color-change mechanisms. *Cell Tissue Res* **258**, 319-29.
- Koshiba-Takeuchi, K., Takeuchi, J. K., Matsumoto, K., Momose, T., Uno, K., Hoepker, V., Ogura, K., Takahashi, N., Nakamura, H., Yasuda, K. and Ogura, T. (2000) Tbx5 and the retinotectum projection. *Science* **287**, 134-7.
- Kroll, K. L. and Amaya, E. (1996) Transgenic *Xenopus* embryos from sperm nuclear transplantations reveal FGF signaling requirements during gastrulation. *Development* **122**, 3173-83.
- Ku, M. and Melton, D. A. (1993) Xwnt-11: a maternally expressed *Xenopus* wnt gene. *Development* **119**, 1161-73.
- Kumasaka, M., Sato, H., Sato, S., Yajima, I. and Yamamoto, H. (2004) Isolation and developmental expression of *Mitf* in *Xenopus laevis*. *Dev Dyn* **230**, 107-13.
- Kuroda, H., Fuentealba, L., Ikeda, A., Reversade, B. and De Robertis, E. M. (2005) Default neural induction: neuralization of dissociated *Xenopus* cells is mediated by Ras/MAPK activation. *Genes Dev* **19**, 1022-7.
- Kuroda, H., Wessely, O. and De Robertis, E. M. (2004) Neural induction in *Xenopus*: requirement for ectodermal and endomesodermal signals via Chordin, Noggin, beta-Catenin, and Cerberus. *PLoS Biol* **2**, E92.

- Lagutin, O. V., Zhu, C. C., Kobayashi, D., Topczewski, J., Shimamura, K., Puelles, L., Russell, H. R., McKinnon, P. J., Solnica-Krezel, L. and Oliver, G. (2003) Six3 repression of Wnt signaling in the anterior neuroectoderm is essential for vertebrate forebrain development. *Genes Dev* **17**, 368-79.
- LaVail, M. M., Yasumura, D., Matthes, M. T., Lau-Villacorta, C., Unoki, K., Sung, C. H. and Steinberg, R. H. (1998) Protection of mouse photoreceptors by survival factors in retinal degenerations. *Invest Ophthalmol Vis Sci* **39**, 592-602.
- Lee, J. E., Hollenberg, S. M., Snider, L., Turner, D. L., Lipnick, N. and Weintraub, H. (1995) Conversion of *Xenopus* ectoderm into neurons by NeuroD, a basic helix-loop-helix protein. *Science* **268**, 836-44.
- Levine, E. M., Fuhrmann, S. and Reh, T. A. (2000) Soluble factors and the development of rod photoreceptors. *Cell Mol Life Sci* **57**, 224-34.
- Li, X., Perissi, V., Liu, F., Rose, D. W. and Rosenfeld, M. G. (2002) Tissue-specific regulation of retinal and pituitary precursor cell proliferation. *Science* **297**, 1180-3.
- Liu, Y., Shen, Y., Rest, J. S., Raymond, P. A. and Zack, D. J. (2001) Isolation and characterization of a zebrafish homologue of the cone rod homeobox gene. *Invest Ophthalmol Vis Sci* **42**, 481-7.
- Livesey, F. J. and Cepko, C. L. (2001) Vertebrate neural cell-fate determination: lessons from the retina. *Nat Rev Neurosci* **2**, 109-18.
- Livesey, F. J., Furukawa, T., Steffen, M. A., Church, G. M. and Cepko, C. L. (2000) Microarray analysis of the transcriptional network controlled by the photoreceptor homeobox gene *Crx*. *Curr Biol* **10**, 301-10.
- Locker, M., Agathocleous, M., Amato, M. A., Parain, K., Harris, W. A. and Perron, M. (2006) Hedgehog signaling and the retina: insights into the mechanisms controlling the proliferative properties of neural precursors. *Genes Dev* **20**, 3036-48.
- Logan, C. Y. and Nusse, R. (2004) The Wnt signaling pathway in development and disease. *Annu Rev Cell Dev Biol* **20**, 781-810.
- Loosli, F., Staub, W., Finger-Baier, K. C., Ober, E. A., Verkade, H., Wittbrodt, J. and Baier, H. (2003) Loss of eyes in zebrafish caused by mutation of *chokh/rx3*. *EMBO Rep* **4**, 894-9.
- Loosli, F., Winkler, S., Burgtorf, C., Wurmbach, E., Ansorge, W., Henrich, T., Grabher, C., Arendt, D., Carl, M., Krone, A., Grzebisz, E. and Wittbrodt, J. (2001) Medaka eyeless is the key factor linking retinal determination and eye growth. *Development* **128**, 4035-44.
- Loosli, F., Winkler, S. and Wittbrodt, J. (1999) *Six3* overexpression initiates the formation of ectopic retina. *Genes Dev* **13**, 649-54.

- Lowe, C. J., Wu, M., Salic, A., Evans, L., Lander, E., Stange-Thomann, N., Gruber, C. E., Gerhart, J. and Kirschner, M. (2003) Anteroposterior patterning in hemichordates and the origins of the chordate nervous system. *Cell* **113**, 853-65.
- Lundkvist, J. and Lendahl, U. (2001) Notch and the birth of glial cells. *Trends Neurosci* **24**, 492-4.
- Lupo, G., Liu, Y., Qiu, R., Chandraratna, R. A., Barsacchi, G., He, R. Q. and Harris, W. A. (2005) Dorsoventral patterning of the *Xenopus* eye: a collaboration of Retinoid, Hedgehog and FGF receptor signaling. *Development* **132**, 1737-48.
- Ma, Q., Kintner, C. and Anderson, D. J. (1996) Identification of neurogenin, a vertebrate neuronal determination gene. *Cell* **87**, 43-52.
- Macdonald, R., Barth, K. A., Xu, Q., Holder, N., Mikkola, I. and Wilson, S. W. (1995) Midline signalling is required for *Pax* gene regulation and patterning of the eyes. *Development* **121**, 3267-78.
- Maden, M. (2002) Retinoid signalling in the development of the central nervous system. *Nat Rev Neurosci* **3**, 843-53.
- Mailhos, C., Andre, S., Mollereau, B., Goriely, A., Hemmati-Brivanlou, A. and Desplan, C. (1998) *Drosophila* Goosecoid requires a conserved heptapeptide for repression of paired-class homeoprotein activators. *Development* **125**, 937-47.
- Marcus, R. C., Gale, N. W., Morrison, M. E., Mason, C. A. and Yancopoulos, G. D. (1996) Eph family receptors and their ligands distribute in opposing gradients in the developing mouse retina. *Dev Biol* **180**, 786-9.
- Mariani, F. V. and Harland, R. M. (1998) XBF-2 is a transcriptional repressor that converts ectoderm into neural tissue. *Development* **125**, 5019-31.
- Marquardt, T., Ashery-Padan, R., Andrejewski, N., Scardigli, R., Guillemot, F. and Gruss, P. (2001) Pax6 is required for the multipotent state of retinal progenitor cells. *Cell* **105**, 43-55.
- Marquardt, T. and Gruss, P. (2002) Generating neuronal diversity in the retina: one for nearly all. *Trends Neurosci* **25**, 32-8.
- Mathers, P. H., Grinberg, A., Mahon, K. A. and Jamrich, M. (1997) The *Rx* homeobox gene is essential for vertebrate eye development. *Nature* **387**, 603-7.
- Mathers, P. H. and Jamrich, M. (2000) Regulation of eye formation by the *Rx* and *pax6* homeobox genes. *Cell Mol Life Sci* **57**, 186-94.
- Maurus, D., Heligon, C., Burger-Schwarzler, A., Brandli, A. W. and Kuhl, M. (2005) Noncanonical Wnt-4 signaling and EAF2 are required for eye development in *Xenopus laevis*. *Embo J* **24**, 1181-91.

- McCabe, K. L., Gunther, E. C. and Reh, T. A. (1999) The development of the pattern of retinal ganglion cells in the chick retina: mechanisms that control differentiation. *Development* **126**, 5713-24.
- McFarlane, S., Zuber, M. E. and Holt, C. E. (1998) A role for the fibroblast growth factor receptor in cell fate decisions in the developing vertebrate retina. *Development* **125**, 3967-75.
- McIlvain, V. A. and Knox, B. E. (2007) Nr2e3 and Nrl can reprogram retinal precursors to the rod fate in *Xenopus* retina. *Dev Dyn* **236**, 1970-9.
- Mears, A. J., Kondo, M., Swain, P. K., Takada, Y., Bush, R. A., Saunders, T. L., Sieving, P. A. and Swaroop, A. (2001) *Nrl* is required for rod photoreceptor development. *Nat Genet* **29**, 447-52.
- Meijlink, F., Beverdam, A., Brouwer, A., Oosterveen, T. C. and Berge, D. T. (1999) Vertebrate aristaless-related genes. *Int J Dev Biol* **43**, 651-63.
- Miller, J. R., Rowing, B. A., Larabell, C. A., Yang-Snyder, J. A., Bates, R. L. and Moon, R. T. (1999) Establishment of the dorsal-ventral axis in *Xenopus* embryos coincides with the dorsal enrichment of dishevelled that is dependent on cortical rotation. *J Cell Biol* **146**, 427-37.
- Moody, S. A., Chow, I. and Huang, S. (2000) Intrinsic bias and lineage restriction in the phenotype determination of dopamine and neuropeptide Y amacrine cells. *J Neurosci* **20**, 3244-53.
- Morrow, E. M., Furukawa, T. and Cepko, C. L. (1998) Vertebrate photoreceptor cell development and disease. *Trends Cell Biol* **8**, 353-8.
- Nguyen, M. and Arnheiter, H. (2000) Signaling and transcriptional regulation in early mammalian eye development: a link between FGF and MITF. *Development* **127**, 3581-91.
- Nieuwkoop, P. D. (1963) Pattern formation in artificially activated ectoderm (*Rana pipiens* and *Ambystoma punctatum*). *Dev Biol* **7**, 255-79.
- Nieuwkoop, P. D. and Faber, J. (1967) *Normal Table of Xenopus laevis (Daudin)*. North-Holland Pub. Co.: Amsterdam.
- Nishida, A., Furukawa, A., Koike, C., Tano, Y., Aizawa, S., Matsuo, I. and Furukawa, T. (2003) *Otx2* homeobox gene controls retinal photoreceptor cell fate and pineal gland development. *Nat Neurosci* **6**, 1255-63.
- Norris, R. A. and Kern, M. J. (2001) Identification of domains mediating transcription activation, repression, and inhibition in the paired-related homeobox protein, Prx2 (S8). *DNA Cell Biol* **20**, 89-99.

- Ohnuma, S., Hopper, S., Wang, K. C., Philpott, A. and Harris, W. A. (2002a) Co-ordinating retinal histogenesis: early cell cycle exit enhances early cell fate determination in the *Xenopus* retina. *Development* **129**, 2435-46.
- Ohnuma, S., Mann, F., Boy, S., Perron, M. and Harris, W. A. (2002b) Lipofection strategy for the study of *Xenopus* retinal development. *Methods* **28**, 411-9.
- Ohnuma, S., Philpott, A., Wang, K., Holt, C. E. and Harris, W. A. (1999) p27Xic1, a Cdk inhibitor, promotes the determination of glial cells in *Xenopus* retina. *Cell* **99**, 499-510.
- Ohuchi, H., Tomonari, S., Itoh, H., Mikawa, T. and Noji, S. (1999) Identification of chick *rax/rx* genes with overlapping patterns of expression during early eye and brain development. *Mech Dev* **85**, 193-5.
- Oliver, G., Loosli, F., Koster, R., Wittbrodt, J. and Gruss, P. (1996) Ectopic lens induction in fish in response to the murine homeobox gene *Six3*. *Mech Dev* **60**, 233-9.
- Otani, A., Dorrell, M. I., Kinder, K., Moreno, S. K., Nusinowitz, S., Banin, E., Heckenlively, J. and Friedlander, M. (2004) Rescue of retinal degeneration by intravitreally injected adult bone marrow-derived lineage-negative hematopoietic stem cells. *J Clin Invest* **114**, 765-74.
- Pan, F. C., Chen, Y., Loeber, J., Henningfeld, K. and Pieler, T. (2006a) I-SceI meganuclease-mediated transgenesis in *Xenopus*. *Dev Dyn* **235**, 247-52.
- Pan, Y., Nekkhalapudi, S., Kelly, L. E. and El-Hodiri, H. M. (2006b) The *Rx-like* homeobox gene (*Rx-L*) is necessary for normal photoreceptor development. *Invest Ophthalmol Vis Sci* **47**, 4245-53.
- Perron, M., Kanekar, S., Vetter, M. L. and Harris, W. A. (1998) The genetic sequence of retinal development in the ciliary margin of the *Xenopus* eye. *Dev Biol* **199**, 185-200.
- Perron, M., Opdecamp, K., Butler, K., Harris, W. A. and Bellefroid, E. J. (1999) *X-ngnr-1* and *Xath3* promote ectopic expression of sensory neuron markers in the neurula ectoderm and have distinct inducing properties in the retina. *Proc Natl Acad Sci U S A* **96**, 14996-5001.
- Piccolo, S., Agius, E., Leyns, L., Bhattacharyya, S., Grunz, H., Bouwmeester, T. and De Robertis, E. M. (1999) The head inducer Cerberus is a multifunctional antagonist of Nodal, BMP and Wnt signals. *Nature* **397**, 707-10.
- Piccolo, S., Sasai, Y., Lu, B. and De Robertis, E. M. (1996) Dorsoventral patterning in *Xenopus*: inhibition of ventral signals by direct binding of chordin to BMP-4. *Cell* **86**, 589-98.
- Plouhinec, J. L., Sauka-Spengler, T., Germot, A., Le Mentec, C., Cabana, T., Harrison, G., Pieau, C., Sire, J. Y., Veron, G. and Mazan, S. (2003) The mammalian *Crx* genes are highly divergent representatives of the *Otx5* gene family, a gnathostome orthology class of orthodenticle-related homeogenes involved in the differentiation of retinal photoreceptors and circadian entrainment. *Mol Biol Evol* **20**, 513-21.

- Porter, F. D., Drago, J., Xu, Y., Cheema, S. S., Wassif, C., Huang, S. P., Lee, E., Grinberg, A., Massalas, J. S., Bodine, D., Alt, F. and Westphal, H. (1997) *Lhx2*, a LIM homeobox gene, is required for eye, forebrain, and definitive erythrocyte development. *Development* **124**, 2935-44.
- Prada, C., Puga, J., Perez-Mendez, L., Lopez, R. and Ramirez, G. (1991) Spatial and Temporal Patterns of Neurogenesis in the Chick Retina. *Eur J Neurosci* **3**, 559-569.
- Quiring, R., Walldorf, U., Kloter, U. and Gehring, W. J. (1994) Homology of the *eyeless* gene of *Drosophila* to the *Small eye* gene in mice and *Aniridia* in humans. *Science* **265**, 785-9.
- Rapaport, D. H., Wong, L. L., Wood, E. D., Yasumura, D. and LaVail, M. M. (2004) Timing and topography of cell genesis in the rat retina. *J Comp Neurol* **474**, 304-24.
- Rasmussen, J. T., Deardorff, M. A., Tan, C., Rao, M. S., Klein, P. S. and Vetter, M. L. (2001) Regulation of eye development by frizzled signaling in *Xenopus*. *Proc Natl Acad Sci U S A* **98**, 3861-6.
- Raymond, P. A. (1991) Cell determination and positional cues in the teleost retina: development of photoreceptors and horizontal cells. In: *Development of the visual system*. D. M.-K. Lam and C. J. Shatz, Eds. MIT Press: Cambridge.
- Rembold, M., Loosli, F., Adams, R. J. and Wittbrodt, J. (2006) Individual cell migration serves as the driving force for optic vesicle evagination. *Science* **313**, 1130-4.
- Rojas-Muñoz, A., Dahm, R. and Nusslein-Volhard, C. (2005) *chokh/rx3* specifies the retinal pigment epithelium fate independently of eye morphogenesis. *Dev Biol* **288**, 348-62.
- Saha, M. S. and Grainger, R. M. (1993) Early opsin expression in *Xenopus* embryos precedes photoreceptor differentiation. *Brain Res Mol Brain Res* **17**, 307-18.
- Sakagami, K., Ishii, A., Shimada, N. and Yasuda, K. (2003) *RaxL* regulates chick ganglion cell development. *Mech Dev* **120**, 881-95.
- Salo, E., Pineda, D., Marsal, M., Gonzalez, J., Gremigni, V. and Batistoni, R. (2002) Genetic network of the eye in Platyhelminthes: expression and functional analysis of some players during planarian regeneration. *Gene* **287**, 67-74.
- Schneider, S., Steinbeisser, H., Warga, R. M. and Hausen, P. (1996) Beta-catenin translocation into nuclei demarcates the dorsalizing centers in frog and fish embryos. *Mech Dev* **57**, 191-8.
- Schohl, A. and Fagotto, F. (2002) Beta-catenin, MAPK and Smad signaling during early *Xenopus* development. *Development* **129**, 37-52.
- Schwarz, M., Cecconi, F., Bernier, G., Andrejewski, N., Kammandel, B., Wagner, M. and Gruss, P. (2000) Spatial specification of mammalian eye territories by reciprocal transcriptional repression of *Pax2* and *Pax6*. *Development* **127**, 4325-34.

- Simeone, A., D'Apice, M. R., Nigro, V., Casanova, J., Graziani, F., Acampora, D. and Avantsgiato, V. (1994) *Orthopedia*, a novel homeobox-containing gene expressed in the developing CNS of both mouse and *Drosophila*. *Neuron* **13**, 83-101.
- Smith, L. E. (2004) Bone marrow-derived stem cells preserve cone vision in retinitis pigmentosa. *J Clin Invest* **114**, 755-7.
- Smith, S. T. and Jaynes, J. B. (1996) A conserved region of engrailed, shared among all en-, gsc-, Nk1-, Nk2- and msh-class homeoproteins, mediates active transcriptional repression in vivo. *Development* **122**, 3141-50.
- Stenkamp, D. L., Frey, R. A., Prabhudesai, S. N. and Raymond, P. A. (2000) Function for *Hedgehog* genes in zebrafish retinal development. *Dev Biol* **220**, 238-52.
- Strickler, A. G., Famuditi, K. and Jeffery, W. R. (2002) Retinal homeobox genes and the role of cell proliferation in cavefish eye degeneration. *Int J Dev Biol* **46**, 285-94.
- Swain, P. K., Hicks, D., Mears, A. J., Apel, I. J., Smith, J. E., John, S. K., Hendrickson, A., Milam, A. H. and Swaroop, A. (2001) Multiple phosphorylated isoforms of NRL are expressed in rod photoreceptors. *J Biol Chem* **276**, 36824-30.
- Tao, Q., Yokota, C., Puck, H., Kofron, M., Birsoy, B., Yan, D., Asashima, M., Wylie, C. C., Lin, X. and Heasman, J. (2005) Maternal wnt11 activates the canonical wnt signaling pathway required for axis formation in *Xenopus* embryos. *Cell* **120**, 857-71.
- Tucker, P., Laemle, L., Munson, A., Kanekar, S., Oliver, E. R., Brown, N., Schlecht, H., Vetter, M. and Glaser, T. (2001) The *eyeless* mouse mutation (*ey1*) removes an alternative start codon from the *Rx/rax* homeobox gene. *Genesis* **31**, 43-53.
- Turner, D. L. and Weintraub, H. (1994) Expression of *achaete-scute* homolog 3 in *Xenopus* embryos converts ectodermal cells to a neural fate. *Genes Dev* **8**, 1434-47.
- Viczian, A. S., Vignali, R., Zuber, M. E., Barsacchi, G. and Harris, W. A. (2003) *XOtx5b* and *XOtx2* regulate photoreceptor and bipolar fates in the *Xenopus* retina. *Development* **130**, 1281-94.
- Vignali, R., Colombetti, S., Lupo, G., Zhang, W., Stachel, S., Harland, R. M. and Barsacchi, G. (2000) *Xotx5b*, a new member of the *Otx* gene family, may be involved in anterior and eye development in *Xenopus laevis*. *Mech Dev* **96**, 3-13.
- Wang, J. C. and Harris, W. A. (2005) The role of combinational coding by homeodomain and bHLH transcription factors in retinal cell fate specification. *Dev Biol* **285**, 101-15.
- Wang, Q. L., Chen, S., Esumi, N., Swain, P. K., Haines, H. S., Peng, G., Melia, B. M., McIntosh, I., Heckenlively, J. R., Jacobson, S. G., Stone, E. M., Swaroop, A. and Zack, D. J. (2004) *QRX*, a novel homeobox gene, modulates photoreceptor gene expression. *Hum Mol Genet* **13**, 1025-40.

- Wang, S., Krinks, M., Lin, K., Luyten, F. P. and Moos, M., Jr. (1997) Frzb, a secreted protein expressed in the Spemann organizer, binds and inhibits Wnt-8. *Cell* **88**, 757-66.
- Wessely, O., Agius, E., Oelgeschlager, M., Pera, E. M. and De Robertis, E. M. (2001) Neural induction in the absence of mesoderm: beta-catenin-dependent expression of secreted BMP antagonists at the blastula stage in *Xenopus*. *Dev Biol* **234**, 161-73.
- Winkler, S., Loosli, F., Henrich, T., Wakamatsu, Y. and Wittbrodt, J. (2000) The conditional medaka mutation *eyeless* uncouples patterning and morphogenesis of the eye. *Development* **127**, 1911-9.
- Yan, R. T., Ma, W., Liang, L. and Wang, S. Z. (2005) bHLH genes and retinal cell fate specification. *Mol Neurobiol* **32**, 157-71.
- Yan, R. T. and Wang, S. Z. (1998) NeuroD induces photoreceptor cell overproduction *in vivo* and de novo generation *in vitro*. *J Neurobiol* **36**, 485-96.
- Yan, R. T. and Wang, S. Z. (2004) Requirement of *NeuroD* for photoreceptor formation in the chick retina. *Invest Ophthalmol Vis Sci* **45**, 48-58.
- Yang, X. J. (2004) Roles of cell-extrinsic growth factors in vertebrate eye pattern formation and retinogenesis. *Semin Cell Dev Biol* **15**, 91-103.
- Young, R. W. (1985) Cell differentiation in the retina of the mouse. *Anat Rec* **212**, 199-205.
- Yu, R. T., Chiang, M. Y., Tanabe, T., Kobayashi, M., Yasuda, K., Evans, R. M. and Umesono, K. (2000) The orphan nuclear receptor Tlx regulates Pax2 and is essential for vision. *Proc Natl Acad Sci U S A* **97**, 2621-5.
- Zaghloul, N. A., Yan, B. and Moody, S. A. (2005) Step-wise specification of retinal stem cells during normal embryogenesis. *Biol Cell* **97**, 321-37.
- Zhang, L., Mathers, P. H. and Jamrich, M. (2000) Function of Rx, but not Pax6, is essential for the formation of retinal progenitor cells in mice. *Genesis* **28**, 135-42.
- Zhang, X. M. and Yang, X. J. (2001) Temporal and spatial effects of Sonic hedgehog signaling in chick eye morphogenesis. *Dev Biol* **233**, 271-90.
- Zhou, X., Hollemann, T., Pieler, T. and Gruss, P. (2000) Cloning and expression of *xSix3*, the *Xenopus* homologue of murine *Six3*. *Mech Dev* **91**, 327-30.
- Zimmerman, L. B., De Jesus-Escobar, J. M. and Harland, R. M. (1996) The Spemann organizer signal noggin binds and inactivates bone morphogenetic protein 4. *Cell* **86**, 599-606.
- Zuber, M. E., Gestri, G., Viczian, A. S., Barsacchi, G. and Harris, W. A. (2003) Specification of the vertebrate eye by a network of eye field transcription factors. *Development* **130**, 5155-67.
- Zuber, M. E., Perron, M., Philpott, A., Bang, A. and Harris, W. A. (1999) Giant eyes in *Xenopus laevis* by overexpression of *XOptx2*. *Cell* **98**, 341-52.

8 Appendix

The Genbank accession numbers of *Rx*-type genes represented in Figure 4.2 and Figure 4.3, as well as their species names and common species names are given in the following table.

Table 8.1 The Genbank accession numbers of nucleotide sequences of all known *Rx*-type gene from different species

Abbrev.	Accession-No	Organism (Species)	Common name
aa_rx	XM_001659914	<i>Aedes aegypti</i>	yellow fever mosquito
am_rx1	AF264703	<i>Astyanax mexicanus</i>	Mexican tetra
bt_qrx	NM_182653	<i>Bos taurus</i>	cow
cf_rx1	XM_849723	<i>Canis familiaris</i>	dog
ci_rx	NM_001032511	<i>Ciona intestinalis</i>	sea squirt
dm_rx	NM_166413	<i>Drosophila melanogaster</i>	fruit fly
Dp_rx	XM_001360934	<i>Drosophila pseudoobscura</i>	Fruit fly
dr_rx1	AF001907	<i>Danio rerio</i>	zebrafish
dr_rx2	AF001908	<i>Danio rerio</i>	zebrafish
dr_rx3	NM_131227	<i>Danio rerio</i>	zebrafish
gg_rax1	AF420600	<i>Gallus gallus</i>	chick
gg_rax2	AF420601	<i>Gallus gallus</i>	chick
hb_rx	XM_001119966	<i>Apis mellifera</i>	Western honey bee
hs_rax	NM_013435	<i>Homo sapiens</i>	human
hs_raxL	NM_032753	<i>Homo sapiens</i>	human
jw_rx	XM_001603887	<i>Nasonia vitripennis</i>	jewel wasp
md_rx	XM_001365988	<i>Monodelphis domestica</i>	gray short-tailed opossum
md_rxL	XM_001373844	<i>Monodelphis domestica</i>	gray short-tailed opossum
mm_rax	NM_013833	<i>Mus musculus</i>	house mouse
nv_rx	XM_001634160	<i>Nematostella vectensis</i>	sea anemone
oa_rx	XM_001516307	<i>Ornithorhynchus anatinus</i>	platypus
ol_rx2	OLA250405	<i>Oryzias latipes</i>	Medaka killifish
ol_rx3	OLA298300	<i>Oryzias latipes</i>	Medaka killifish
pt_rax	XM_001142510	<i>Pan troglodytes</i>	common chimpanzee
pt_raxL	NM_001081487	<i>Pan troglodytes</i>	common chimpanzee
rm_rax	XM_001087324	<i>Macaca mulatta</i>	rhesus monkey
rm_raxL	XM_001100945	<i>Macaca mulatta</i>	rhesus monkey
rn_rax	NM_053678	<i>Rattus norvegicus</i>	brown rat
sk_rx	AY313142	<i>Saccoglossus kowalevskii</i>	acorn worm
sp_rx	XM_001177341	<i>Strongylocentrotus purpuratus</i>	purple sea urchin
tc_rc	XM_968375	<i>Tribolium castaneum</i>	flour beetles
x1_rx1a	NM_001088218	<i>Xenopus laevis</i>	African clawed frog
x1_rx2a	NM_001088220	<i>Xenopus laevis</i>	African clawed frog
x1_rxL	DQ360108	<i>Xenopus laevis</i>	African clawed frog

Acknowledgments

Special thanks are given to my supervisor Prof. Thomas Hollemann for offering me the opportunity to work on this project, which allowed me to start in the very interesting field of developmental biology. I am very grateful to him for giving patient guidance when I was a beginner, encouraging me to face the challenges, and providing constructive discussion and suggestions throughout this thesis work.

I express my gratitude to Prof. Tomas Pieler for allowing me to start my PhD work in the department of developmental biochemistry at Georg August University, Göttingen.

I would like to thank Dr. Muriel Perron in University Paris XI, France, for accepting me to learn lipofection technique in her lab and keeping discussion on the results. I also thank her group members for helping me with solving my experimental and living problems there.

I very appreciate that Dr. Herbert Neuhaus and Dr. Frank Müller carefully checked the manuscript of my thesis, and gave critically correction and helpful suggestions.

I am very grateful to Juliane Herfurth, Annett Thate, and Undine Ziese for their technical assistance. I appreciate their technical expertise and readiness to help. I give my gratitude to Jia Xu for her hard work on TUNEL assay and PH3 immunostaining as parts of this thesis.

I am grateful to my colleague Marlen Metzsig for her generously exchanging our working computers, providing me a big convenience of writing with a laptop. I would like to thank sweet Anne Corsing for lending me her chair, which really relieved my back pain during the thesis writing. I also want to say thanks to Dörte Adolph for helping with managing the submission of the thesis.

I express my gratitude to Dr. Dagobert Glanz for always being nice to help with finding chemicals and take care of the microinjection instruments. I would also like to thank members of Prof. Mechthild Hatzfeld's lab for discussing protocols and giving instruction for using fluorescence microscopes.

As this thesis is ending, I cannot forget those nice colleagues who gave me a lot of help when I started this project. I am very much thankful to Dr. Yonglong Chen, Emmanuel Tadjuidje, Martin Kriebel, Marco Winkler, Shirui Hou and Fongcheng Pan for teaching me fundamental techniques in the *Xenopus* field and giving technical advises. I also thank Andreas Notle for always hurrying up with my samples for sequencing at that time.

I am very grateful to my parents and the rest of my family for their love, constant support and understanding throughout my PhD study.

Affidavit

Herewith I declare, that I prepared the PhD thesis
“The function of a newly identified retinal homeobox-containing gene, *Xenopus RxL*
in retinal development”
on my own and with no other sources and aids than quoted.

Halle (Saale), Germany

04.04.2008

Curriculum Vitae

Name: Huiyuan Wu
Date of Birth: 06.04.1973
Palace of Birth: Xiwuzhumuqin Banner, Inner Mongolia, China
Nationality: Chinese
Address: Institute of Physiological Chemistry, Martin-Luther University,
Hollystr. 1, Halle (Saale), 06108, Germany

Education

09.1980 – 07.1985 Primary school, Xiwuzhumuqin Banner, China
09.1985 – 07.1988 Junior high school, Xiwuzhumuqin Banner, China
09.1988 – 07.1991 Senior high school, Xilinhaote, P.R.China
07.1995 B.Sc. Shenyang Pharmaceutical University, Shenyang, China
07.1998 M.Sc. Shenyang Pharmaceutical University, Shenyang, China
07.2004 – 10.2004 PhD candidate, Dept. of Developmental Biochemistry, Georg-August
University, Göttingen, Germany
10.2004 – 04.2008 PhD candidate, Institute of Physiological Chemistry, Martin-Luther
University, Halle (Saale), Germany

Working Experience

07.1998 – 11.2001 Assistant Reseacher, the Biocatalysis Laboratory of State Key Lab of
Bioreactor Engineering of ECUST, China
11.2001– 09.2002 Researcher Associate, the Biocatalysis Laboratory of State Key Lab of
Bioreactor Engineering of ECUST, China
10.2002 – 09.2003 Participant of the 30th UNESCO Course in Microbiology, Osaka
University and Kyoto University, Japan
12.2003 – 03.2004 Visiting Scientist, Laboratory of Molecular Microbial Science, Institute
for Chemical Research, Kyoto University, Japan

List of Publications

Hui-Yuan Wu, Muriel Perron and Thomas Hollemann, *XRxL*, a novel intrinsic cue of directing photoreceptor fate determination, *Prepared*

Hui-Yuan Wu, Jian-He Xu, Suk-Fong Tsang and Jianyong Wu Efficient resolution of a chiral alcohol (R, S)-HMPC by enzymatic transesterification with vinyl acetate using surfactant-modified lipase *Enzyme Microb. Technol.*, **2004**, 34: 523-8

Hui-Yuan Wu, Jian-He Xu, and Qi Xin, Improved production of (S)-ketoprofen ester hydrolase by a mutant of *Trichosporon brassicae* CGMCC 0574 *Journal of Industrial Microbiology & Biotechnology*, **2003**, 30: 357-61

Peng-Fei Gong, Jian-He Xu, Yan-Fa Tang, and Hui-Yuan Wu, Catalytic Performance of an Isolated Epoxide Hydrolase from *Bacillus megaterium* in Kinetic Resolution of Aryloxy Epoxides, *Biotechnol. Prog.* **2003**, 19: 652-4

Peng-Fei Gong, Hui-Yuan Wu, Jian-He Xu *et al*, Biocatalytic preparation of enantiopure (R)-Ketoprofen from its racemic ester by a new yeast isolate *Citeromyces matriensis* CGMCC 0573 *Appl. Microbiol. Biotech.* **2002**, 58: 728-34

Duan Shen, Jian-He Xu, Hui-Yuan Wu and You-Yan Liu, Significantly improved esterase activity of *Trichosporon brassicae* cells for ketoprofen resolution by 2-propanol permeabilization *J. Mol. Catal B: Enzymatic* **2002**, 18: 219-24

Duan Shen, Jianhe Xu, Pengfei Gong and Huiyuan Wu *et al* Isolation of an esterase-producing *Trichosporon brassicae* and its catalytic performance in kinetic resolution of Ketoprofen *Can.J.Microbiol.*, **2002**, 47: 1111-6

Yu-Qiao Zhao, Hui-Yuan Wu and Jian-He Xu, Isolation and application of *Acinetobacter* sp. YQ231 producing highly enantioselective esterases, *Chin. J. Appl. Environ. Biol.* **2002**, 8: 640- 3

Hui-Yuan Wu, Jian-He Xu, You-Yan Liu, A Practical Enzyme Method for Preparation of (S)-ketoprofen with a Crude *Candida Rugosa* Lipase *Synthetic Communication*, **2001**, 31: 91-6

Jian-He Xu, Hui-Yuan Wu and Duan Shen *et al*, Preparation of the optically pure 2-arylpropionic acids by two newly isolated yeast strains. **Invention Patent, Appl, No. 01126617.1**

Peng-Fei Gong, Jian-He Xu and Hui-Yuan Wu, Mathematical analysis for the sensitivity of parameters to determine the enantiomeric ratio (*E*) in enantioselective biocatalysis, *Hua Gong Xue Bao* (in Chinese), **2001**, 52: 54-8

Yan-Fa Tang, Jian-He Xu, Hui-Yuan Wu, Qin Ye, Birgit Schulze, Isolation and characterization of an epoxide hydrolase producer for enantioselective hydrolysis of (R,S)-phenyl glycidyl ether, *Wei Sheng Wu Tong Bao* (in Chinese), **2001**, 28: 14-5